5. RESULTS AND DISCUSSION

5.1 Functional antagonism assay of standards and synthesized multitargeted ligands

5.1.1 Establishing baseline values for agonists and studies with standard antagonists of α_1 and AT_1 receptor

The primary aim of the studies was to identify a potential candidate that showed balanced inhibition of the α_1 and the AT_1 receptors. This was brought about by studying the antagonistic ability of different test compounds against phenylephrine(246) and Ang II mediated contractions of the rat thoracic aorta(247). Similar studies were also performed with the standard compounds for the purpose of direct comparison. The studies were initiated with the evaluation of terazosin against phenylephrine mediated contractions. Phenylephrine initiated contractions in the rat aortic strips at concentrations ranging from 5 nM or higher. It was observed that addition of 10 µM terazosin caused a rightward parallel shift in the concentration response curve of phenylephrine. pA_2 calculations revealed a value of **8.97 ± 0.14** which was in line with previously reported value on rat aorta(248, 249), (250). Hence, this value was considered as the standard value for further studies and reported accordingly. This study allowed establishment of baseline values for phenylephrine and simultaneously permitted calculation of pA_2 value of NCEs against α_1 receptors (251).

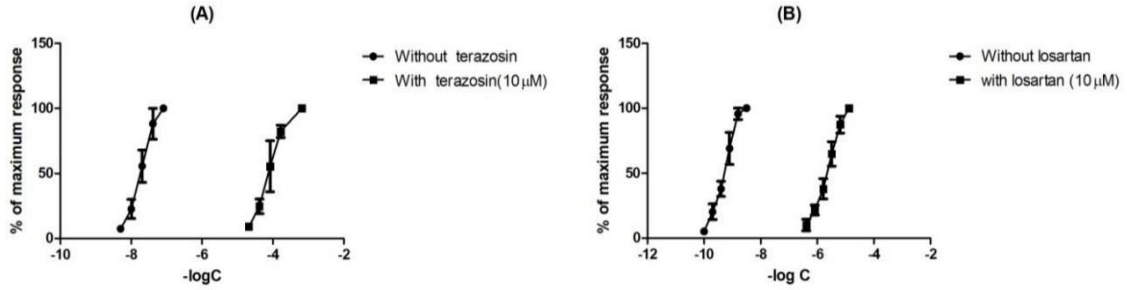

Figure 5.1: Concentration response curves (pA_2 values) of standard drugs **(A)** phenylephrine and **(B)** angiotensin II in presence of standard drugs at 10 µM (n=3).

Similar studies were performed on separate set of aortic strips using angiotensin II as the agonist where losartan was used as the standard antagonist (252),(253). Concentration response curve (CRC) was obtained with Ang II at concentrations ranging from 1 nM and higher. Incubation of losartan (0.1 µM) or higher concentrations (10 µM) resulted in a rightward parallel shift of the CRC of Ang II with pA_2 value being **8.63 ± 0.08** as per the previous reports (254).

5.1.2 Screening of potential compounds for dual antagonism of α_1 and AT_1 receptors

After establishing the pA_2 value for standard drugs against their respective agonists, it was decided to evaluate the potency of newly synthesized NCEs for their balanced antagonistic potential against α_1 and AT_1 receptors. Various novel compounds bearing 6,7-dimethoxyquinazoline and 7,8-dimethoxyquinazoline as parent scaffolds were screened by functional antagonism assay using rat aorta. The resulting pA_2 of NCEs are mentioned in tables 5.1-5.9 according to their scaffold, linker moiety and substitutions.

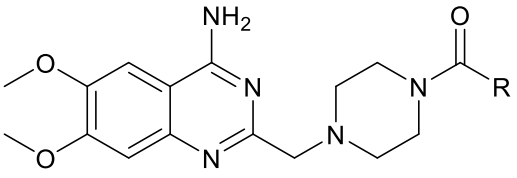

Series I

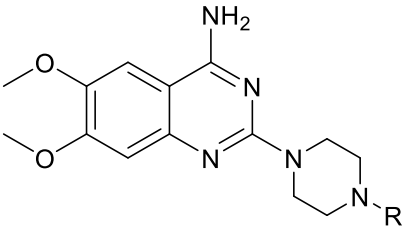

Series II

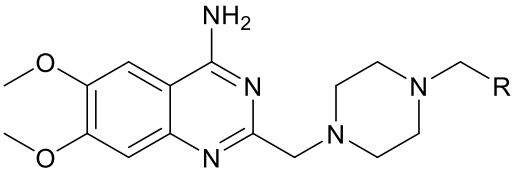

Series III

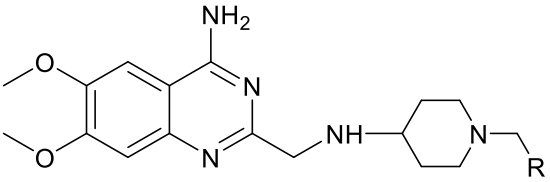

Series IV

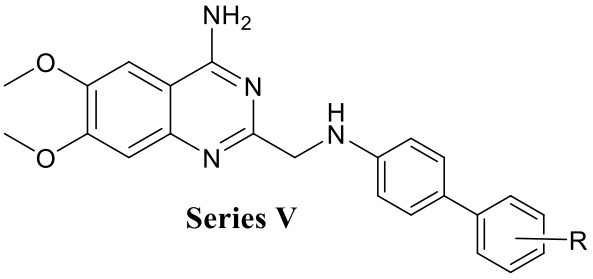

Series V

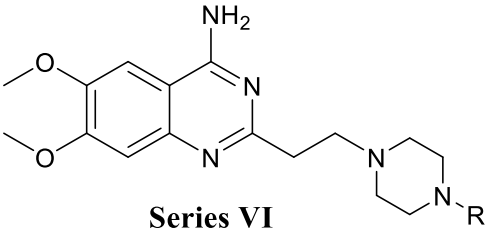

Series VI

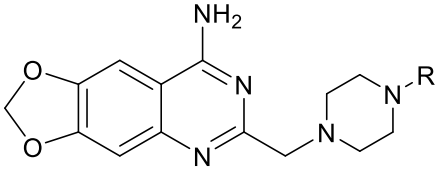

Series VII

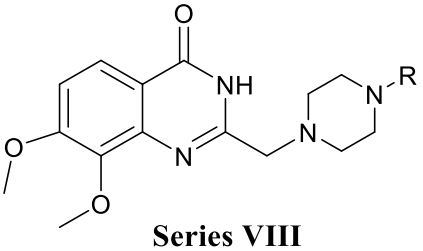

Series VIII

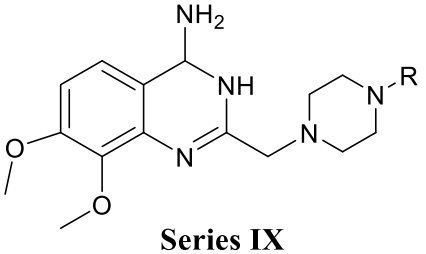

Series IX

Series I

Table 5.1: pA_2 value of compounds of series I

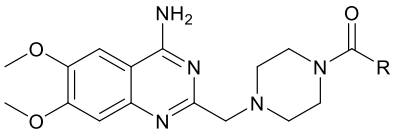

Series I

Compound	*Where –R is*	*p*A_2 values	
		α_1	AT_1
1	-C_6H_5	5.95 ± 0.83	4.75 ± 0.72
2	-C_6H_4F (o)	5.66±1.06	**7.75±0.49**
3	-C_6H_4OMe(o)	6.46±0.19	5.37±0.94
4	-C_6H_4OMe(m)	-	-
5	-C_6H_4Cl(m)	2.14±0.22	4.36±0.35
6	C_6H_4Br(m)	3.45±0.12	4.67±0.2
7	-$C_6H_3Cl_2$(o,m)	-	6.61±1.12
8	-$C_6H_3OMe_2$(o,m)	-	6.34±1.07
9	-C_6H_4Me(m)	-	-
10	-C_6H_4F(p)	3.28±0.87	2.15±0.21
11	-C_6H_4CN(p)	**6.93±0.47**	**6.87±0.60**
12	-CH_2-C_6H_5	1.98±0.34	3.03±0.45
13	-CH_2-C_6H_4Cl(m)	4.05±0.43	5.41±0.52
14	-CH_2-C_6H_4OMe(p)	-	-

(-) = Did not show any activity

Compounds **(1-14)** were designed and synthesized by inserting a methylene spacer between the 4-amino-6,7-dimethoxyquinazoline scaffold and the piperazine ring. Phenyl derivatives were attached with piperazine ring by carbonyl linker (-C=O). Test compounds were evaluated for functional antagonism assay. pA_2 values did not revealed comparable potency with standard drugs. Compound **(2)** showed considerable activity for AT_1 receptor while compound **(11)** displayed balanced modulation at both receptors but having sub level potency compared to standard drugs. Conversion of phenyl(piperazinyl)methanone moiety **(12)** to phenyl(piperazinyl)ethenone **(14)** as in compounds (**12-14**) also failed to produce significant inhibition on both the receptors as compared to standard drugs.

Series II

Table 5.2: pA_2 value of compounds of series II

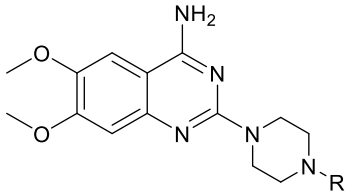

Series II

Compound	*Where –R is*	*p*A_2 values	
		α_1	AT_1
15	$-CH_3$	**9.23 ± 0.12**	5.75 ± 0.07
16	$-CH_2CH_3$	**10.41 ± 0.12**	5.08 ± 0.08
17	$-C_6H_5$	8.74 ± 0.08	3.31 ± 0.13
18	$-C_6H_4CN$ (*o*)	**9.47 ± 0.06**	**8.54 ± 0.07**
19	$-C_6H_4OCH_3$ (*o*)	7.26 ± 0.12	6.54 ± 0.51
20	$-C_5H_4N$	6.95 ± 0.08	5.09 ± 0.12
21	$-CH(C_6H_5)_2$	**7.09 ± 0.15**	**7.59 ± 0.58**

Series II designed by substituted phenyl derivatives attached directly to piperazine linker resulted into improved activity especially at α_1 receptor. Compound **(15-21)** showed good to excellent inhibition for α_1 receptor, with similar to higher activity when compared to terazosin (**15-21)**. However, compound **(15-17)** failed to exhibit significant AT_1 receptor antagonism. From the results it was speculated that absence of aromatic moiety is responsible for absence of AT_1 receptor antagonism. Substitution with benzene moiety in **(16)** resulted into compound **(17)** and substitution with different phenyl derivatives in **(16)** resulted into compound **(18-21).** As suspected, replacement with aromatic moiety resulted into improvement in AT_1 receptor blocking potency **(18-21).** Compound **(18)** showed excellent potency for α_1 and AT_1 receptor (pA_2 for **α_1=9.47±0.06, AT_1= 8.54±0.07**) (table 5.2). Compound **(21)** also showed balance modulation at both the receptors compared to standard drugs.

Series III

Table 5.3: pA_2 value of compounds of series III

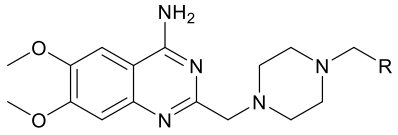

Series III

Compound	*Where –R is*	***p*A$_2$ values**	
		α_1	**AT_1**
22	-C_6H_5	4.55±0.43	5.41±0.52
23	-$C_6H_4CF_3$(o)	-	6.10±0.97
24	-C_6H_4Me(o)	**8.34±0.14**	**8.73 ±0.10**
25	-C_6H_4Br(o)	5.08±0.84	-
27	-C_6H_4CN (o)	5.89±0.90	-
28	-C_6H_4Br(p)	5.91±0.81	6.49±0.77
29	-C_6H_4Me(p)	5.91±0.35	6.12±0.72
30	-C_6H_4OMe(p)	**7.19±0.56**	-
31	-C_6H_4-t-butyl(p)	**7.50±0.69**	6.58±0.84
32	-C_6H_4-C-C_6H_4CN(o)	4.64±0.56	-
33	-naphtyl	6.32±0.62	6.95±0.37
34	-benzhydryl	**7.44±1.10**	**7.26±1.03**
35	-cyclohexyl	-	6.95±0.37

(-) = Did not show any activity

Series III was designed by reducing phenyl(piperazinyl) methanone of series I to benzylpiperazine. Further compounds were synthesized by different aromatic ring substitution at 2nd and 4th positions resulted into compounds **(22-35).** Compounds (**22, 23, 25-29**) reflected poor antagonism at both the targeted receptors. Compound **(24)** exhibited excellent antagonism at the target sites reflected by its superior pA_2 values. (pA_2 for **α_1=8.34±0.14, AT_1= 8.73 ±0.10)**. Replacement of substituted benzyl with benzhydryl in **(34)** also revealed balance modulation with comparable potency (table 5.3). Loss of aromaticity in compound **(35)** having cyclohexyl substitution resulted into diminished inhibition at both the target site.

Series IV

Table 5.4: pA_2 value of compounds of series IV

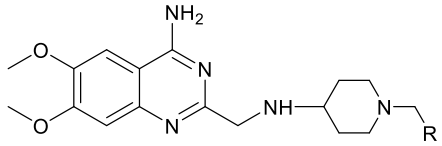

Series IV

Compound	*Where –R is*	***p*A$_2$ values**	
		α_1	**AT_1**
36	-C_6H_5	4.95±0.42	5.51±1.01
37	-C_6H_4Br(o)	6.43±0.05	-
38	-C_6H_4CN(o)	6.55±1.01	5.78±0.78
39	-C_6H_4Me(o)	6.79±0.20	5.66±0.25
40	-C_6H_4OMe(m)	6.75±0.22	5.96±0.12
41	-C_6H_4Me (p)	6.79±0.14	6.52±0.08

(-) = Did not show any activity

Series IV was explored with a view to study the effect of heterocyclic substitution on biological activity. To achieve the same, piperazine linker was replaced with piperadine ring. However, this attempt resulted into loss of potency as depicted in table 5.4. Compound **(36-41)** showed loss of activity compared to series III. Compound **(36-41)** showed mild activity at α_1 receptor (pA_2= 6-6.8) but resulted into absence of AT_1 antagonism.

Series V

Table 5.5: pA_2 value of compounds of series V

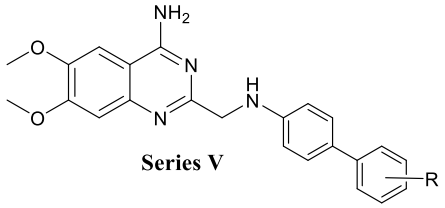

Series V

Compound	*Where –R is*	*p*A_2 values	
		α_1	AT_1
42	-C_6H_5	**7.82±0.06**	**7.99±0.10**
43	-C_6H_4Cl(o)	6.39±0.06	**7.20±0.20**
44	-C_6H_4Me(o)	**6.92±0.16**	**6.90±0.12**
45	-C_6H_4CN(p)	6.37±0.19	6.92±0.20
46	-C_6H_4SMe(p)	6.10±0.14	**7.71±0.08**
47	-$C_6H_4C(CH_3)_3$ (p)	6.32±0.1	5.31±0.22

Series V constituted by substituted biphenyl at 2nd or 4th position resulted into compound **(42-47)** with comparable potency exhibited at both the receptor. Compound **(42)** (pA_2 α_1=**7.82±0.06,** AT_1= **7.99±0.10**) displayed excellent blockade of α_1 and AT_1 receptor. Compound **(43-47)** showed mild to considerable antagonistic activity at both the target with pA_2 value ranging from 6-7.7 Compound **(44)** also showed balance antagonism by substitution at 2nd position with methyl group in compound **(42).** The results were encouraging as substitution with biphenyl derivatives offered balance modulation which support the notion of impact of aromaticity on AT_1 antagonism.

Series VI

Table 5.6: pA_2 value of compounds of series VI

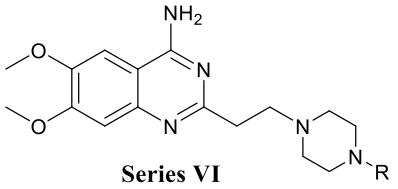

Series VI

Compound	***Where –R is***	***p*A$_2$ values**	
		α_1	**AT_1**
48	-C_6H_4Cl(o)	**9.24±0.07**	**7.00±0.09**
49	-C_6H_4CN(o)	**8.81±0.18**	**7.13±0.21**
50	-C_6H_4OMe(o)	**9.29±0.18**	4.99±0.04
51	-C_6H_4Me(o)	**9.27±0.09**	6.02±0.12
52	-pyridyl	-	-
53	-benzhydryl	**6.81±0.21**	**8.71±0.09**

(-) = Did not show any activity

Compound **(48-53)** synthesized by linking 6,7 dimethoxyquinazoline and substituted phenylpiperazine with ethyl linker which resulted into excellent antagonist activity at both the receptors. Compounds **(48)** and **(49)** possessed superior α_1 antagonism **9.24±0.07, 8.81±0.18** respectively with considerable activity at AT_1 receptor (**7.00±0.09, 7.13±0.21)**. Substitution at 2nd position with methoxy **(50)** and methyl group **(51)** resulted in suppression of AT_1 receptor antagonism but α_1 antagonistic activity was retained as shown in table 5.6. Heterocyclic ring substitution with pyridyl in **(48)** resulted into **(52)** which revealed the loss of activity at both the receptors. The novel synthesized compounds superior antagonism compared to terazosin with noteworthy antagonism of AT_1 receptor. These results also provide leads for future development of similar multitargeted ligands.

Series VII

Table 5.7: pA_2 value of compounds of series VII

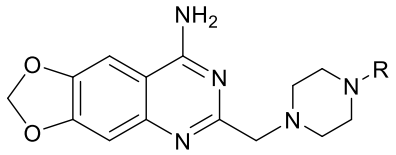

Series VII

Compound	*Where –R is*	***p*A$_2$ values**	
		α_1	**AT_1**
54	-C_6H_5	5.82±0.12	6.7±0.11
55	-C_6H_4F(o)	6.16±0.07	-
56	-C_6H_4CN(o)	**8.33±0.16**	5.80±0.06
57	-C_6H_4OMe(o)	6.37±0.05	4.70±0.19
58	-$C_6H_4NO_2$(p)	6.06±0.32	5.95±0.12
59	-C_6H_4Me(p)	6.07±0.23	5.96±0.27
60	-C_6H_4-butyl	6.06±0.28	5.42±0.28
61	-pyridine	6.59±0.23	5.31±0.21
62	-pyrimidine	5.68±0.11	-
63	-Napthyl	**7.57±0.21**	5.25±0.10
64	-Benzhydryl	6.22±0.28	6.08
65	-Cyclohexane	4.51±0.08	5.43±0.11
66	-CH_2-C_6H_4Br(o)	6.17± 0.15	6.07±0.21
67	-CH_2-C_6H_4Me(o)	6.23±0.24	6.21±0.09
68	-CH_2-C_6H_4OMe(p)	5.06±0.06	-
69	-CH_2-C_6H_4-t-butyl	6.52±0.30	**6.80±0.14**
70	-CH_2-Napthyl	6.69±0.14	5.66±0.10

(-) = Did not show any activity

In order to evaluate the effect parent scaffold on biological activity, 6,7-dimethoxy group on quinazoline scaffold linked to form cyclic diether resulting into compound **(54-70)**. As mentioned in table 5.7, changing in the parent scaffold resulted into decreased potency of compounds where only compound **(56)** and **(63)** showed considerable α_1 receptor blocking potential, however they failed to display considerable AT_1 receptor blocking action. pA_2 value for other NCEs were only between 5-6.80 suggesting inferiority of developed NCE.

Series VIII

Table 5.8: pA_2 value of compounds of series VIII

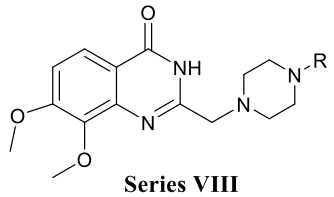

Series VIII

Compound	*Where –R is*	***p*A₂ values**	
		α_1	**AT_1**
71	-C_6H_5	6.23±0.01	4.46±0.31
72	-C_6H_4Cl(o)	7.05±0.05	5.62±0.2
73	-C_6H_4CN(o)	**6.93±0.06**	**6.82±0.05**
74	-C_6H_4OMe(o)	6.61±0.17	5.46±0.13
75	-$C_6H_4NO_2$(p)	5.28±0.09	6.1±0.02
76	-t-butyl	5.56±0.15	6.02±0.09
77	-pyridine	6.00±0.28	5.80±0.11

Series IX

Table 5.9: pA_2 value of compounds of series IX

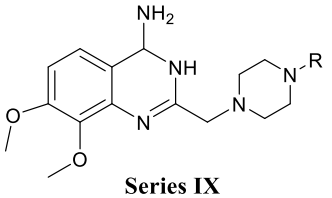

Series IX

Compound	*Where –R is*	***p*A₂ values**	
		α_1	**AT_1**
78	-C_6H_5	6.42±0.12	4.46±0.31
79	-C_6H_4Cl(o)	**7.05±0.27**	5.26±0.30
80	-C_6H_4CN(o)	**7.04±0.15**	**6.92±0.07**
81	-C_6H_4OMe(o)	6.8±0.12	5.67±0.09
82	-C_6H_4Me(o)	**7.87±0.05**	**7.35±0.2**
83	-$C_6H_4NO_2$(p)	**8.08±0.66**	6.25±0.24
84	-pyridine	5.44±0.12	5.97±0.1
85	-pyrimidine	5.68±0.24	6.00±0.21
86	-Napthyl	**7.07±0.04**	5.42±0.14
87	-benzhydryl	**7.37±0.30**	5.83±0.14
88	-CH_2-C_6H_5	6.39±0.31	5.82±0.20
89	-CH_2-C_6H_4CN(o)	5.38±0.21	-
90	-CH_2-C_6H_4Me(o)	**8.34±0.21**	**6.63±0.09**

Series VIII and IX were designed by using 7,8-dimethoxyquinazoline as a parent scaffold with different substitutions made at 2nd and 4th positions. Compound with carbonyl (C=O) group in parent moiety resulted into mild to moderate potency of developed NCE where compound **(71-77)** revealed pA_2 value ranging from 5.5 – 7 (Table 5.8). These results emphasized the role of 4-NH_2 in the parent scaffold which provides important interactions site within the target site of the receptor. While in series IX with 4 –amino 7,8 – dimethoxyquinazoline derivatives **(78-90)** produced compounds with significant improvement in potency compared to series VIII (Table 5.9). Compound **(82)** possessed balance modulation with good pA_2 value. Substitution with a more aromatic group resulted into loss of AT_1 receptor blocking action however α_1 antagonism was still preserved in compound **(86), (87)**. The addition of one carbon spacer to compound **(82)** resulted into **(90)** with enhanced α_1 blocking activity however activity towards AT_1 receptor was slightly compromised.

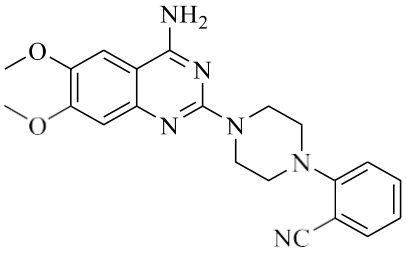

Compound (18)

2-(4-(4-amino-6,7-dimethoxyquinazolin-2-yl)piperazin-1-yl)benzonitrile

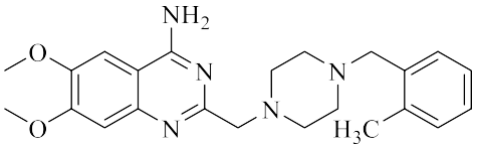

Compound (24)

6,7-dimethoxy-2-((4-(2-methylbenzyl)piperazin-1-yl)methyl)quinazolin-4-amine

After the extensive screening of developed NCEs, it was concluded that 6,7 dimethoxyquinazoline scaffolds with appropriate aromatic substitution with piperazine as linker can provide balance blocking activity at α_1 and AT_1 receptor.

From the above results, it was concluded that compound **(18) (pA_2 for α_1= 9.47±0.06, AT_1= 8.54±0.07)** and compound **(24) (pA_2 for α_1=8.55±0.13, AT_1= 8.68 ±0.02)** displayed

potent and balance inhibition at both target sites and hence, were explored for further study of activity, toxicity and *in-vivo* model of rat hypertension and cardiometabolic disorders.

5.1.3 Elaborated functional antagonism assay of potent compound (18) and (24)

The antagonism afforded by compound **(18)** and **(24)** on rat aortic strips was evaluated at 3 different concentrations (0.1, 1, 10 µM) to find that each higher concentration resulted in a further rightward parallel shift in the CRC of phenylephrine as well as Ang II. Schild et al. suggested that if series of antagonist concentrations when plotted against dose ratio gives the slope of unity, it indicates that obtained pA_2 value can be considered as actual affinity of ligands for the target (255). The pA_2 value calculated at different concentrations for compound **(18)** remained the same as that observed in preliminary studies. Accordingly, the pA_2 value of compound **(18)** against phenylephrine mediated contractions were 8.52±0.08 at 0.1 µM, 8.81±0.06 at 1 µM, 8.34±0.14 at 10 µM with mean value of **8.55±0.13** for **α_1** and **8.68±0.02** for **AT_1** (8.67±0.09 at 0.1 µM, 8.64±0.17 at 1 µM, 8.73±0.10 at 10 µM).

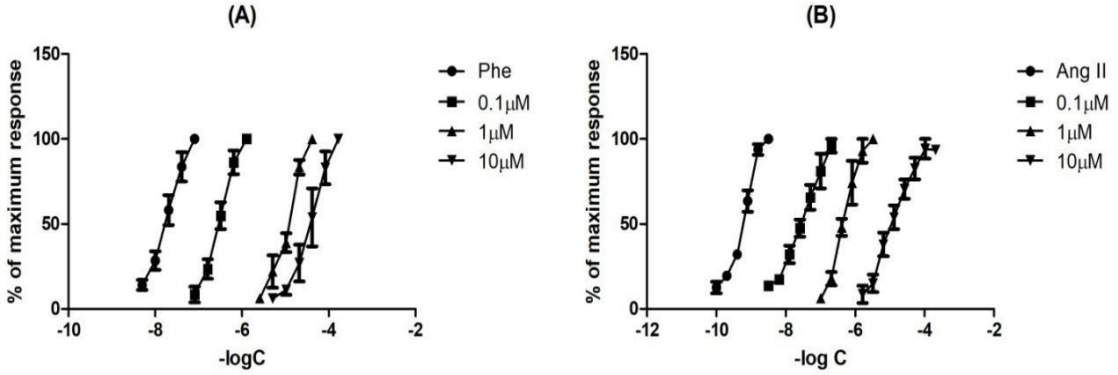

Figure 5.2: Concentration response curves (pA_2 value) of compound **(18)** at different concentrations.
(A) phenylephrine and **(B)** angiotensin II in presence of different concentrations of compound **(18)** at 0.1, 1, 10 µM.

Similar experiments were also performed for compound **(24)** and results showed rightward parallel shifts were observed at each concentration and with no significant deviation in pA_2 value at different concentration ranging from 0.1 µM to 10 µM. For α_1 receptor, mean pA_2 value was found to be **9.47±0.06** (9.35±0.04 at 0.1 µM, 9.50±0.07 at 1 µM, 9.57±0.06 at 10 µM) while at AT_1 receptor, pA_2 value is **8.54±0.07** (8.44±0.08 at 0.1 µM, 8.69±0.05 at 1 µM, 8.48±0.01 at 10 µM). These results also suggest competitive antagonism as similar pA_2 values were obtained at different concentrations (256).

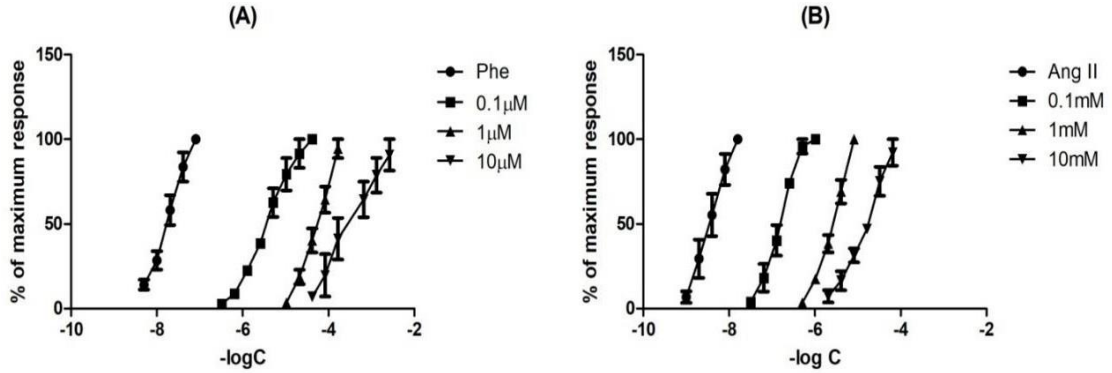

Figure 5.3: Concentration response curves (pA_2 value) of compound **(24)** at different concentrations. Concentration response curves of **(A)** phenylephrine and **(B)** angiotensin II in presence of different concentrations of compound **(24)** (0.1, 1, 10 μM).

5.2 Molecular docking study of compound (18) and (24) with α_1 and AT_1 Receptor

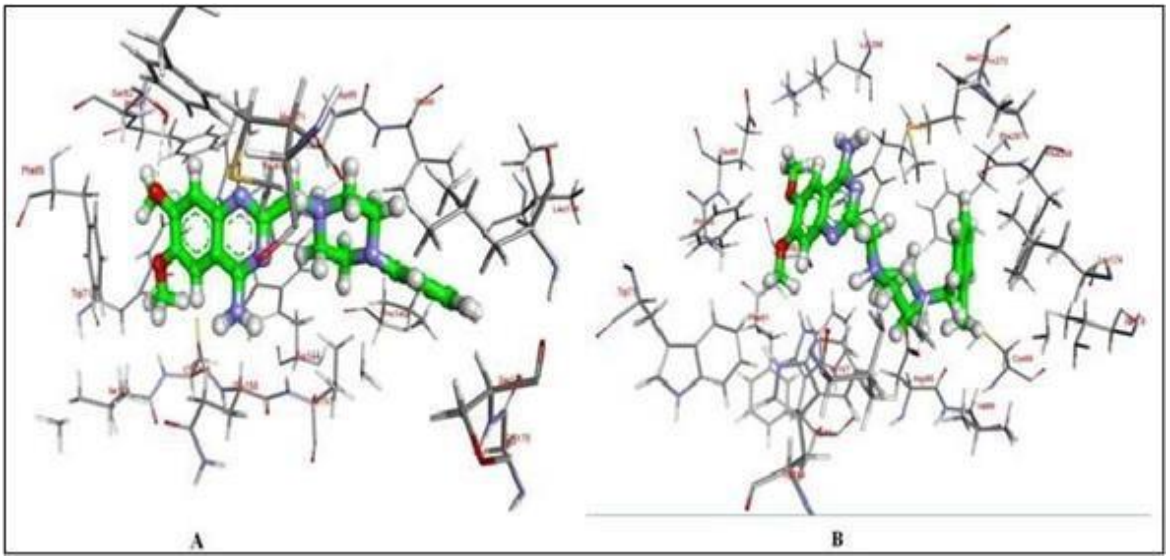

Figure 5.4: Docking interactions of compound **(18)** and **(24)** with α_1-receptor. Docking pose of **(A) (18)** and **(B) (24)** in the ligand binding site of α_1-receptor.

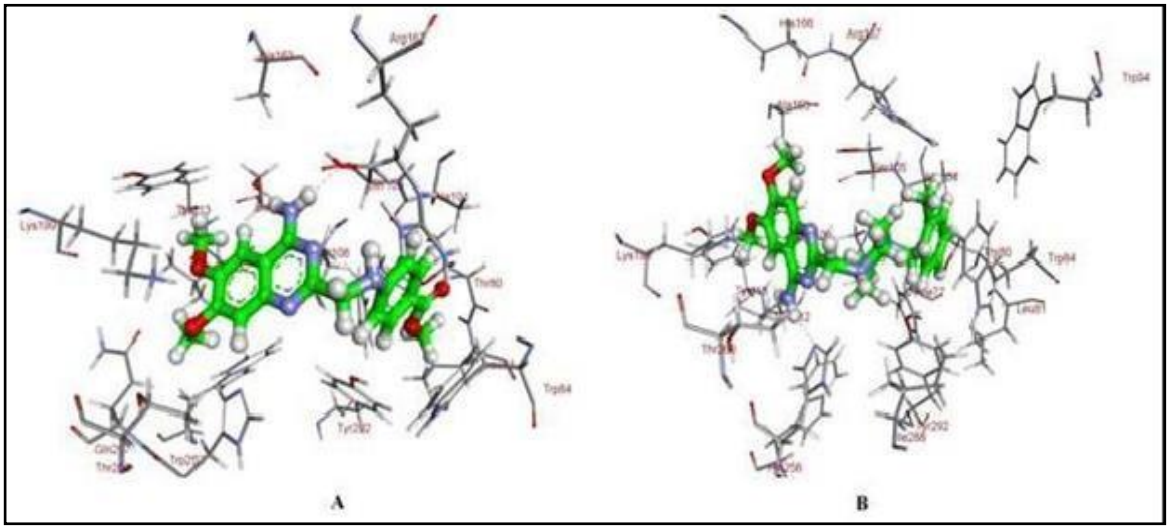

Figure 5.5: Docking interactions of compound **(18)** and **(24)** with AT_1-receptor. Docking pose of **(A) (18)** and **(B) (24)** in the ligand binding site of AT_1-receptor.

After performing *in-vitro* and *in-vivo* experiments, two potential compounds **(18)** and **(24)** exhibited dual antagonism at both the target receptors. Using the available data of biological activity in hand for the synthesized compounds, highly predictive pharmacophore and 3D-QSAR models (257) were developed to support the findings obtained from animal experiments. Docking interactions of compounds **(18)** and **(24)** are displayed in figure 5.4 and 5.5.

- **Docking of compound (18) and (24) with α_1 receptor**

In case of compound **(18)**, the protonated -NH of piperazine forms a salt bridge with Asp85 residue. One of the methoxy groups on dimethoxyquinazoline ring formed H - bond with Ser62. The aromatic ring of quinazoline offered further stability to the receptor ligand complex by showing π-π stacking with Trp81 [Figure 5.4 (A)] (257). For compound **(24)**, a salt bridge was formation was formed with Asp85. Additionally, the *o*-methylbenzyl group was observed to be present into the hydrophobic pocket of Cys89, Phe267, Phe268, Met271 and Pro272. The quinazoline part was found to be stabilized by hydrophobic interactions with Phe65, Trp71 and Phe291 [Figure 5.4 (B)] (257).

- **Docking of compound (18) and (24) with AT_1 receptor**

Docking interactions of compounds **(18)** and **(24)** were studied similarly within the active site of AT1-receptor. The aromatic ring of quinazoline was found to be stabilized by hydrophobic interactions with Leu112, Tyr113 and Trp253. The anilino part of the ligand

lent stability to the receptor-ligand complex by forming π-π stacking interactions with Trp84. The amino group of quinazoline ring offered further stability by having H-bonding with Ser105 and Ser109 [Figure 5.5 (A)].

In the case of compound **(24)**, the π-cation interactions of the aromatic ring of quinazoline and H-bonding of the -NH_2 group with His256 provide stability to the complex. But the orientation of *o*-methylbenzyl group towards Arg167 may be causing non-favorable interactions at this end as one part is polar, and the other is hydrophobic in nature [Figure 5.5 (B)].

5.3 *In-vivo* pressor response evaluation of compound (18) and (24) in anesthetized rats

5.3.1 Unmasked pressor response

The effects of compound **(18)** and **(24)** in *in-vitro* study were so profound that it was decided to evaluate them against the *in-vivo* effects of phenylephrine(258),(259) and Ang II(260) on rat arterial blood pressure. Acute administration of vasoactive agents isa frequently utilized technique to study hemodynamic changes in animals. Different research groups have studied effects of Ang II(261),(262) and phenylephrine(263) on arterial blood pressure. This method involves measurement of arterial blood pressure via cannulation of the carotid artery which provides actual direct measurement of blood pressure. This method may also be utilized to study arterial reactivity of different vasoactive substances.

Accordingly, two dose levels were selected and the effects of compound **(18)** and **(24)** were evaluated against intravenous injections of phenylephrine and Ang II (5 µg/kg, i.v. each). The effects of test compounds were compared with similar doses of terazosin and losartan as standards. Phenylephrine, selective α_1 receptor agonist produced increase in BP (ΔP= 40.66±8.12 mmHg). At a lower dose of 10 µg/kg, terazosin exhibited near 50% inhibition (50.27±4.64%) of pressor response to phenylephrine whereas compound **(18)** showed 19.55±1.28% and compound **(24)** showed 22.75±2.32% inhibition of pressor response which was significantly less as compared to terazosin ($p<0.001$). It was found that terazosin-mediated effects were stronger as compared to compound **(18)** and **(24)** in inhibiting the pressor response to phenylephrine.

At higher doses (50 µg/kg), the effects were more pronounced, and terazosin almost completely blocked the pressor effects of phenylephrine. Similarly, compound **(18)** and **(24)** at dose of 50 µg/kg offered 46.19±5.47% and 55.74±4.93% inhibition against pressor effect of phenylephrine, respectively [Figure 5.6 (A)].

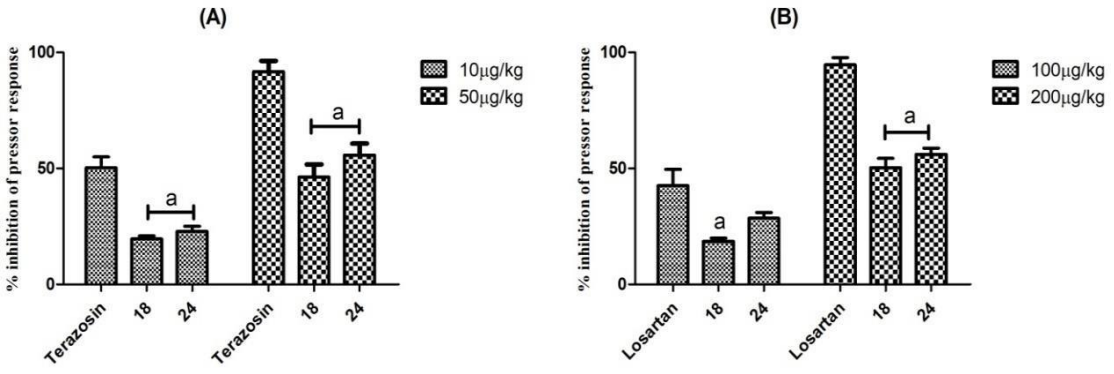

Figure 5.6: Effect of compound (18) and (24) against agonist induced pressor response (Unmasked condition) (A) Inhibition of mean arterial pressor response of phenylephrine in animals (n=3) previously dosed with compounds **(18)** and **(24)**, or terazosin. (**B**) Inhibition of mean arterial pressor response of Ang II in animals (n=4) previously dosed with compounds **(18)** and **(24)**, or losartan. Results are expressed as Mean±SEM values. Values were considered significant when $p<0.05$. a=compared to standard drug, b=compared to compound **(18)**.

Separate dose levels were employed for the evaluation of antagonistic effects against Ang II mediated vasoconstriction. Administration of i.v. bolus of Ang II (5 µg/kg) produced increase in MABP (ΔP=66.47±0.47 mmHg) (264). It was observed that increment in BP was more pronounced with Ang II compared to similar dose of phenylephrine (ΔP= 40.66±8.12 mmHg). Evaluation of mean arterial pressure revealed that losartan at a dose level of 100 µg/kg produced 42.55±6.99% inhibition of pressor response to Ang II. At similar dose level, the response of compounds **(18)** and **(24)** was found to be considerably feeble and produced only about 20% inhibition of Ang II pressor response. Administration of 200 µg/kg losartan prior to Ang II challenge resulted into almost complete inhibition of Ang II induced rise in blood pressure. However, compounds **(18)** and **(24)** were only able to inhibit 50.28±2.99% and 56.03±2.66%, respectively ($p<0.001$ vs. losartan) [Figure 5.6 (B)]. The results were unanticipated since there was a vast difference between the *in-vitro* data and preliminary *in-vivo* investigations.

In-vitro data showed quite encouraging potency of the test compound, however, *in-vivo* studies did not reflect the same. This disparity in the results could be due to differences in metabolism and pharmacokinetic profile of NCEs. However, it was unlikely as compounds were administered via i.v. route and effects were observed immediately as in the case of standard drugs.

While considering these alternatives, it was speculated that since developed NCEs are designed to exhibit dual antagonism, it is quite possible that the actual concentration of the

NCEs reaching at a particular receptor was lesser as compared to standard drugs at equal dose level. The reason for such inferior response may be because of distribution of the drug upon both the receptors in question, suggesting that only a fraction of dose is available at a given time to act upon a particular population of receptors when challenged against specific agonist.

5.3.2 Masked pressor response

To evaluate the above notion, it was planned to evaluate the pressor-inhibition potential of compound **(18)** and **(24)** under masked conditions. Here, masking of receptor was achieved by prior administration of selective antagonist of one receptor while evaluating the effect of the other receptor. Accordingly, *in-vivo* inhibition of phenylephrine mediated arterial pressor response was measured in those animals in which 200 µg/kg losartan was pre-administered. The idea behind such a protocol was to mask the effects of investigational NCEs on AT_1 receptor. Dose of losartan was selected on the basis of previous study [Figure 5.6 (B)] as 200 µg/kg showed more than 90% inhibition. Similarly, the other set involved measurement of inhibition of Ang II mediated arterial pressor response in those animals in which 50 µg/kg terazosin [dose selected as per figure 5.6 (A)] was pre-administered to mask the effects of compound **(18)** and **(24)** upon α_1 receptors.

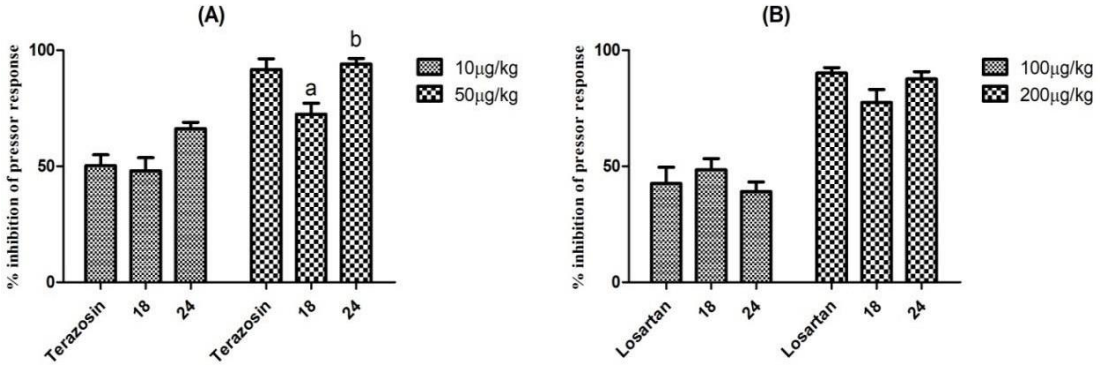

Figure 5.7: Effect of compound (18) and (24) against agonist induced pressor response (masked condition). **(A)** Effect of compound **(18)** and **(24)** against phenylephrine under losartan masking. **(B)** Ang II under terazosin masking. Results are expressed as Mean± SEM values (n=3). Values were considered significant when $p<0.05$. a= compared to terazosin, b=compared to compound **(18)**.

It can be observed through figure 5.7 (A) that previous administration of losartan (200 µg/kg) greatly increases the potential inhibition of compound **(18)** and **(24)** as there was no significant difference observed between terazosin and NCEs. At 10 µg/kg, compound **(18)**

and **(24)** exhibited inhibition of 48.00±5.58% and 66.13±2.84%, respectively, against phenylephrine mediated pressor response. At higher dose level of 50 µg/kg, terazosin was able to show around 90% inhibition while compound **(18)** showed around 70% (72.36±4.78%, $p<0.05$ vs. terazosin) and compound **(24)** exhibited 94.01±2.46% inhibition.

In the different set of experiments as depicted in figure 5.7 (B), pre-administration of terazosin 50 µg/kg, produced profound increase in inhibition offered by compound **(18)** and **(24)** against Ang II. At 100 µg/kg, compound **(18)** and **(24)** produced 43.37±5.32% while at 200 µg/kg, compound **(18)** and **(24)** produced 85.10±3.71% inhibition, against pressor effect of Ang II. There was no significant difference at both dose level compared to standard and investigational entities. These results are suggestive of the above-mentioned hypothesis regarding distribution of multitargeted ligands to two receptor system and it provides conclusive idea regarding the affinity of developed compounds **(18)** and **(24)** for both receptors in question. Simultaneously, it is also evident that it is possible to design ligands which have multiple targets for action. Such compounds may form the basis for favorable management of complex disorders like hypertension and other cardiovascular diseases.

5.4 Cytotoxicity assay of compound (18) and (24) in HEK293 cell

In-vitro cytotoxicity assays have been used extensively to study the effect of NCEs or drugs on cell viability (265),. It is necessary to evaluate the cytotoxic potential of developed NCE during preclinical studies, as it can become a cause of failure in the later stages, if not studied. After confirming *in-vitro* activity, developed NCEs were tested in HEK 293 kidney epithelial cell culture. Compound **(18)** and **(24)** did not produce cell death as survival was found to be >80% at most of the concentrations. Thus, it was concluded that both the compounds are safe to use, and it was decided to explore efficacy of developed compoundsin *in-vivo* models of hypertension and cardiometabolic disorder.

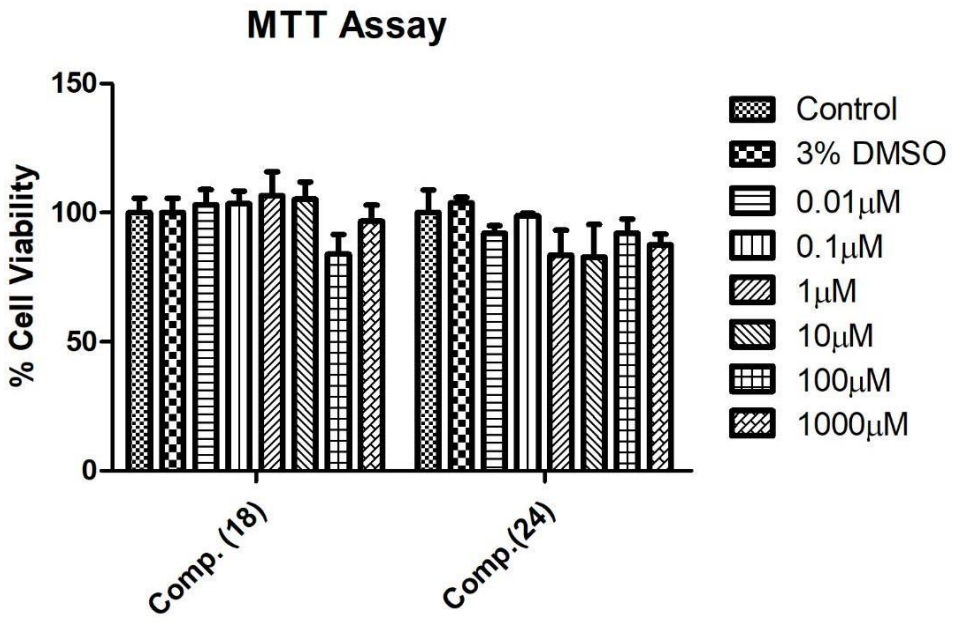

Figure 5.8: Survival of cells post-incubation with different concentrations of compounds **(18)** and **(24)**, 3% DMSO (vehicle) and control cells in HEK293 cells (n=3). Statistical analysis did not find any significant difference between the groups.

5.5 *In-silico* physicochemical properties of compound (18) and (24)

The biological, metabolic and toxicological effects of chemicals are in close concert with their physicochemical profile, which define the frequency and strength of molecular interactions of chemicals with target, and *in-vivo* penetration to cells and tissues which ultimately reflect its ADME properties(266),(267).

Poor physicochemical properties and ADME (absorption, distribution, metabolism, and excretion) profile is the leading cause of attrition in drug development process (267). According to data, major portion of drug candidates did not make through to clinical trials as a direct consequence of their unfavorable ADME profile (268). In recent times, development in field of computational chemistry and artificial intelligence enables the researcher to predict the properties of chemical entities with ease and reliability (269). This cost-effective tool enables the researchers to study and evaluate the drug likeliness properties which eventually resulted into saving of time and resources, and reduction in attrition rate during the drug discovery process (266),(270).

Table 5.10 depicts the drug likeliness properties of two novel MTDLs **(18)** and **(24)**. Physicochemical and drug likeness properties were evaluated on the basis of rules laid by Lipinski (271) and Veber (272). So far, they have remained the primary guide for evaluationand correlation of physical properties for successful drug development (273).

Both compounds **(18)** and **(24)** exhibited excellent adherence to rules without any violation, indicating that the synthesized compounds possessed oral drug like properties(274).

Table 5.10: Physicochemical properties of compound (18) and (24) by SWISS ADME

Parameters	Compound (18)	Compound (24)	Losartan	Terazosin
(A) Lipinski's Parameters				
Mol. Wt. (≤500)	390.44	407.51	422.91	387.43
Hbd (≤5)	1	1	2	1
Hba (≤10)	5	6	5	6
iLogP	3.4	3.92	2.59	2.9
Average LogP	2.27	2.59	3.86	1.14
Lipinski violations	0	0	0	0
(B) Veber's Parameters				
Nrb (≤10)	6	6	8	5
TPSA (≤140 $Å^2$)	100.53	76.74	92.51	103.04
MR	118.14	126.89	108.54	125.78
Veber violations	0	0	0	0
(C) Solubility				
ESOL Solubility (mg/ml)	0.0229	0.0360	0.00280	0.415
ESOL class	Moderately soluble	Moderately soluble	Moderately soluble	Soluble
Ali Solubility (mg/ml)	0.00832	0.0464	0.000479	0.368
Ali solubility class	Moderately soluble	Soluble	Moderately soluble	Soluble

Mol. wt.=molecular weight, Hbd=hydrogen bond donor, Hba=hydrogen bond acceptor, log P=an octanol-water partition co-efficient, TPSA=Total polar surface area, Nrb=No. of rotatable bonds, MR=Molecular refractivity, ESOL=Estimated aqueous solubility, Ali Solubility=Aqueous solubility. Value in the brackets shows upper and lower limit of particular parameter.

Molecular weight (MW) signifies the absorption and permeability of molecules through cell membrane. As a rule of thumb, molecular weight ≤500 Da is favoured for oral absorption. As mentioned in table 5.10, both MTDL **(18)** and **(24)** have molecular weight of 390.44 Da and 407.51 Da, respectively, thus satisfying the rule of Lipinski.

The partition coefficient holds critical importance in physiochemical and pharmacokinetic properties of molecules. It served as the classical descriptor of lipophilicity. The implicit

logP (ilogP) is the n-octanol/water partition coefficients of a particular molecule in two immiscible solvents and served as benchmark for logP estimation (275). SWISS ADME provides descriptive logP estimation including diverse markers and descriptors using different methods to provide accurate and precise estimation of value. Compound **(18)** and **(24)** showed consensus logP value (average obtained from 5 proposed methods) of 2.27 and 2.59, respectively which are well within the range of desired value for oral absorption (logP≤5).

The number of hydrogen bond donors and acceptors is a fundamental molecular descriptor to predict the oral bioavailability of small drug candidates (272) (276). It is generally assumed that hydrogen bond donors and acceptors impact on passive diffusion across cell membranes, a fundamental event during drug absorption and distribution (277). Any heteroatom with at least one bound hydrogen atom is referred to as a hydrogen bond acceptor. The H-bond acceptors determined for the intended compounds are reflected in table 5.10. Compound **(18)** and **(24)** showed Hba values of 5 and 6, respectively. Hba values for both standard compounds also fall within the range. While Hbd for compound **(18)** and **(24)** was predicted to be 1 which is significantly less than the Ro5 projected maximum limit(≤5).

Predictions of physicochemical properties according to Veber's parameters are listed in table 5.10 which relies upon Nrb and TPSA of molecules. Analysis of data provided by SWISS ADME revealed that compound **(18)** and **(24)** obeys both the Veber's parameters. The topological polar surface area (TPSA) is recognized as key determinant of drug absorption in the intestine (TPSA < 140 $Å^2$) and blood-brain barrier penetration (TPSA< 60 $Å^2$) (272). TPSA of compound **(18)** and **(24)** were predicted to be 100.53 $Å^2$ and 76.74 $Å^2$, respectively which satisfactorily obey the requirement for non-CNS drug with good oral absorption. Another useful indicator of drug likeness is number Nrb which gives assessment of molecular flexibility necessary to provide oral bioavailability of the drugs. Results showed compound **(18)** and **(24)** possess 6 rotatable bonds in their structure which falls within prescribed limit.

Establishment of meaningful correlations between the physicochemical properties and ADMET properties of novel entities are pivotal for drug discovery (278). Based on our analysis, both newly synthesized compounds exhibited favorable physicochemical properties in accordance to Lipinski's RO5 and Vebers's rule for oral bioavailable drugs and are comparable with the physicochemical properties of marketed drugs.

5.5.1 Radar chart and Brain Or IntestinaL EstimateD permeation method (Boiled-Egg) diagram of compound (18) and (24)

Radar provides graphical representation of physiological properties of molecules under investigation with reference to maximum limits of possible drug molecules (279), as shown in light pink colour in figure 5.9 and 5.10. It can be observed that the compound **(24)** followed the pattern of radar chart, and all the parameters lie within the range. Compound **(18)** also satisfactorily adhered to the limits.

As depicted in figure 5.9 and 5.10, the BOILED-Egg model helps in the computation of polarity and lipophilicity of derivatives as it gives datasets with accuracy and clear graphical outputs (280). In the BOILED-Egg model, white region depicts the high probability of passive absorption of the GI tract, whereas the yellow region (yolk) represents the high probability of the BBB penetration(281). In addition, the blue color indicates the active efflux of molecule by P-glycoprotein, represented as (PGP+), whereas the red color indicator shows the non-substrate of Pgp, represented as (PGP−) (279). Compound **(18)** is depicted as red dot and compound **(24)** as blue dot in figure 5.9 and 5.10, respectively. Both the compounds lie within intestinal absorption area. Moreover, compound **(24)** has Pgp efflux properties.

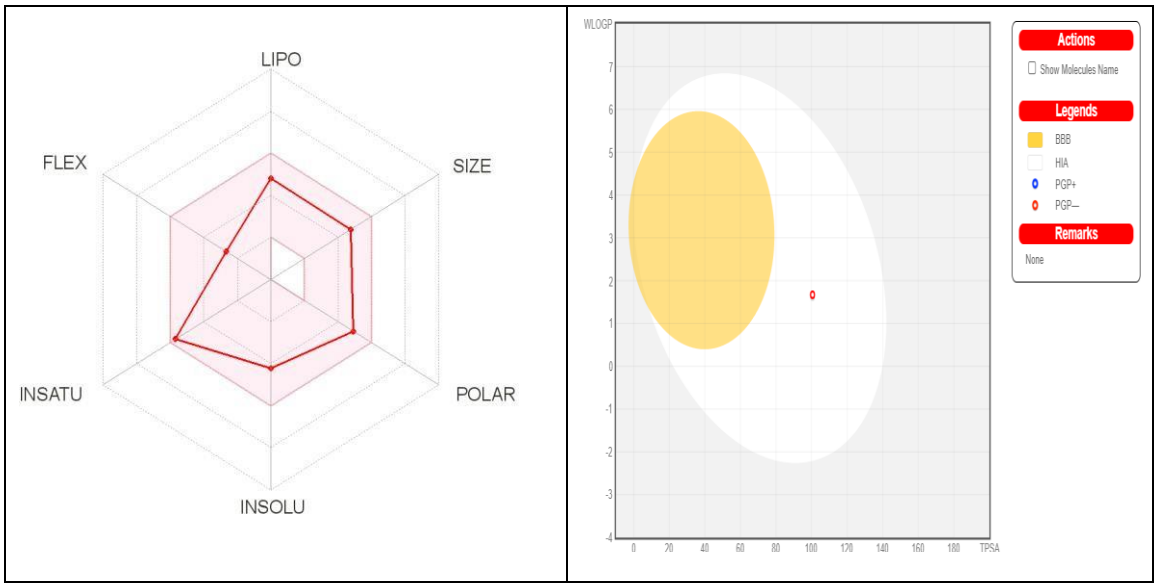

Figure 5.9: Radar chart and Boiled Egg diagram of compound **(18)**

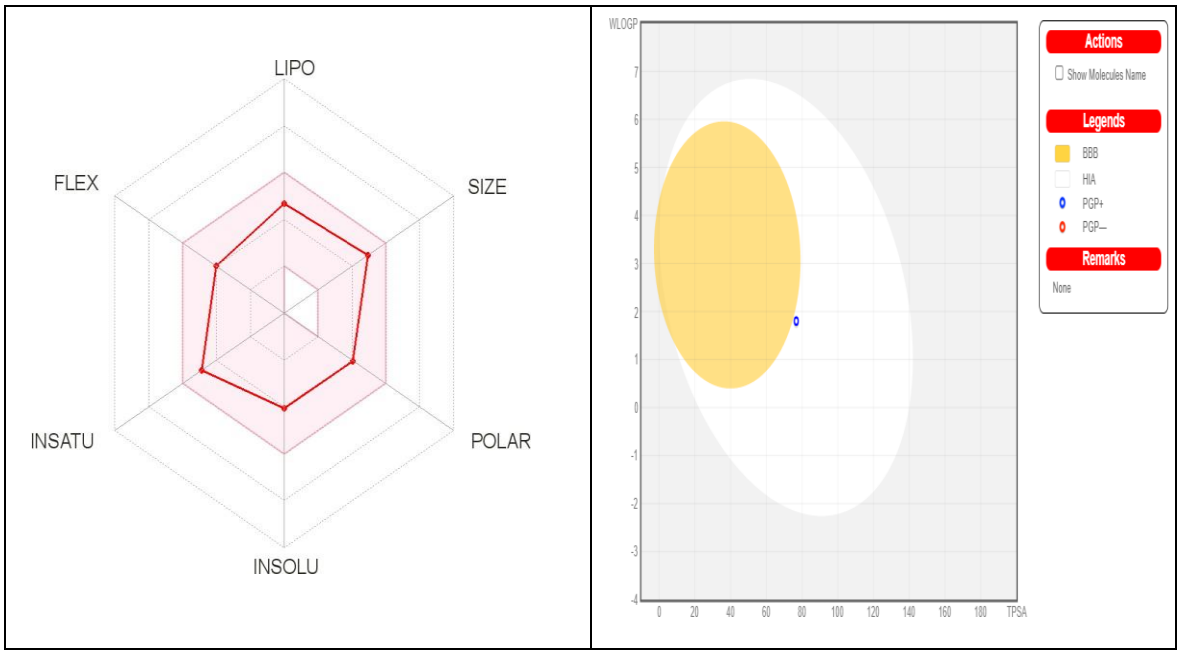

Figure 5.10: Radar chart and Boiled Egg diagram of compound **(24)**

5.6 ADME analysis and toxicity prediction of compound (18) and (24)

Table 5.11: ADME analysis and toxicity prediction of compound (18) and (24)

Parameter		Compound (18)	Compound (24)	Losartan	Terazosin
Absorption	GI absorption (%)	92.11	93.41	78.63	83.80
	Caco2 permeability	0.705	0.906	-0.082	0.839
	p-glycoprotein substrate	No	Yes	Yes	Yes
Distribution	VD_{ss} (human) (log L/kg)	-0.063	1.70	0.093	-0.42
	BBB permeability	No (-0.752)	No (-1.03)	No	No
	Fraction unbound	0.036	0.197	0.057	0.244
Metabolism	CYP 2D6 sub	No	No	Yes	No
	CYP 3A4 sub	Yes	Yes	Yes	Yes
	CYP 2C19 inh	No	No	Yes	No
	CYP2C9 inh	Yes	Yes	Yes	No
	CYP 3A4 inh	Yes	Yes	Yes	No
	CYP 2D6 inh	Yes	Yes	Yes	Yes
	CYP 1A2 inh	No	No	No	Yes

Parameter		Compound (18)	Compound (24)	Losartan	Terazosin
Excretion	Total clearance (log ml/min/kg)	0.275	0.958	0.795	0.284
	Renal OCT_2 substrate	No	No	No	No
Toxicity	AMES	No	No	No	No
	Carcinogenicity	No	No	No	No
	Skin sensitization	No	No	No	No
	LD_{50} (mg/kg B.W)	2.49	3.11	2.53	2.76
	LOAEL (oral rat chronic toxicity)	1.469	0.864	2.31	2.04

ADMET profile prediction is mentioned in table 5.11. Both the newly synthesized compounds were scrutinized by taking different important ADMET parameters into consideration. Compound **(18)** and **(24)** revealed encouraging overall ADMET profile. Absorption is the pivotal step for drugs to show their action. GI absorption of both the compounds **(18)** and **(24)** indicated high GI absorption (>90%) with excellent Caco2 permeability suggesting satisfactory permeation and absorption through intestine. Moreover, these results are in accordance with Boiled-Egg diagram connecting human intestinal absorption with topological factors.

Description of distribution process was predicted by pkCSM tool using the glycoprotein P (P-gp) substrate, blood–brain barrier (BBB) permeability and fraction unbound. Distribution of new chemical entities between the brain and peripheral system is an important factor for their pharmacological action and side effect. Both the compounds **(18)** and **(24)**are targeted for non-CNS condition, negative potential for BBB penetration is required attribute. Both compounds are predicted to be BBB impermeable satisfying the research need.Most drugs in plasma exist in equilibrium between an unbound state and a state in which they are bound to serum proteins.

Heme containing cytochromes are major group of enzymes involved in biotransformation of chemical molecules. It has been estimated that >75% of the marketed drugs are metabolized by CYPs. They are very important to study in the regards of fate of molecule in body and drug-drug interactions. Five major isoforms (CYP2C19, CYP3A4, CYP2D6, CYP1A2, CYP2C9) were taken into consideration for prediction and data indicates that

compound **(18)** and **(24)** are predicted to inhibit CYP2C9, CYP3A4, CYP2D6 while no effect was observed on other two isoforms. Newly synthesized compounds did not show any metabolic alert as this studied CYP isoforms are involved in more than 75% CYP related biotransformation of drug molecules (282).

The excretion profile showed clearance value of compound **(24)** within the normal range, while the clearance was reduced in case of compound **(18)**. However, both the compounds exhibit satisfactory clearance rate predicted by pKCSM tool. Renal OCT2 substrate analysis gives useful information about renal uptake, clearance, contraindications and systemic exposure of drugs (283). Results indicate (table 5.11) compounds under investigation are not OCT2 substrate and thus they will not be taken back by the kidneys and subsequently excreted in urine.

The toxicity panel revealed that the compound **(18)** and **(24)** did not reveal any alarming indication analysed by AMES, carcinogenicity and skin sensitization. Similar results were observed with standard drugs. LD_{50} values for newly synthesized compounds were close to the standard drugs suggesting the safety of synthesized compounds. In addition, 6,7-dimethoxyquinazoline served as a privileged scaffold for drug development reflecting its extensive use in exploration of approved and developing drugs

5.7 Acute toxicity study of compound (18) and (24) according to OECD guidelines

Acute toxicity assessment of compound **(18)** and **(24)** was carried out to further evaluate their safety in animals before *in-vivo* investigations. OECD provides extensive guidelines to ensure the use of safe and nonhazardous chemicals in animals and further translation to human. Quinazoline scaffold has been utilized by medicinal chemists as a privileged scaffold in the drug discovery process. Its utility can also be realized with the fact that there are a number of already approved drugs used in clinical practice bearing the quinazoline scaffold (284), (285). Many different investigations have reported the nontoxic nature of quinazoline derivatives up to the doses of 2000 mg/kg (286), (287). However, to ensure the safety of the test compounds **(18)** and **(24)**, their toxicological assessment was carried out by OECD guidelines 423. As mentioned earlier, 6,7-dimethoxyquinazoline analogues are utilized for clinical purposes, OECD guidelines provide waiver to skip the main test and allow the test compound by limit test. Accordingly, compound **(18)** and **(24)** were administered at the dose of 2000 mg/kg via oral route in 5 female animals. Guidelines have suggested the use of female animals as they are more prone to toxic phenotype than their counterpart. After single oral

administration of compounds **(18)** and **(24)**, there was no signof morbidity and/or mortality up to dose of 2000 mg/kg within 24 hrs. and during study period of 14 days.

None of the animals showed the alteration in the muscle activity, reflex activity and secretary activity during the observation period of 14 days after administration of compound **(18)** and **(24)**. Change in body weight is clear indicative of changes in general health of animals (288), (289). As per the guidelines by OECD, decline in body weight by 20% should be considered critical (290). The body weights of the animals were recorded on days 0, 7 and 14. All animals showed normal growth behavior with normal food and waterintake.

When awake, periodic observation of animals displayed normal grooming behavior and no alteration of skin or fur, abnormal locomotion or breathing, allergic response in the eye was observed. No untoward observations were made in this regard until end of the study protocol. No macroscopic or microscopic lesions were observed in vital organs, neither any architecture disruption nor oedema was observed in study animals.

Thus, it was concluded that compound **(18)** and **(24)** possess LD_{50} >2000 mg/kg and belong to the category 4 of safety criteria according to the OECD guidelines 423. These results indicate that newly synthesized compounds can be safe and could be developed in the future for cardiovascular disease.

5.8 Evaluation of compound (18) and (24) in UNX+DOCA salt induced hypertension

Recent studies in human and animals provides insight regarding the connection of hypertension and related cardiovascular diseases originating from dysregulation and hyperactivity of sympathetic nervous system and RAAS(291) (292). As reported in the previous study, the deoxycorticosterone acetate (DOCA)-salt model is ideal for defining the role of these two major pathways that plays critical role in the pathogenesis of essential hypertension(293), (294). DOCA-salt administration with unilateral nephrectomy has been the mainstay of model to study the protective effect of drugs in mineralocorticoid induced cardiorenal hypertension (295), (296). The administration of DOCA, in combination with salt loading, induces plethora of hypertensive phenotype such as increased renal sodium reabsorption and resultant hypervolemia (297). These conditions caused sympatho-excitation and increment in blood pressure due to enhanced smooth muscle tone and peripheral vascular resistance. The uncontrolled hypertension ultimately causes endothelial

dysfunction, cardiovascular remodeling, left ventricle hypertrophy(298), fibrosis(299), and heart failure as its consequences. Additionally, kidney damage with glomerulosclerosis and tubular fibrosis are also the cardinal feature of DOCA salt induced hypertension. Evidences also suggested pathomechanism of DOCA-salt evoked volume-dependent hypertension with end organ damage, increased oxidative stress and inflammation (300),(301). Accordingly, this model emphasizes the role of the sympathetic nervous system, activation of RAAS, reactive oxygen species (ROS) and inflammation in the development of renal and cardiovascular remodeling(302). This study highlighted the effect of persistent salt loading induced hypertension and role of developed multitargeted ligands i.e. compound **(18)** and **(24**) in the amelioration of developed anomalies (303).

5.8.1 Effect of compound (18) and (24) on physiological parameters in UNX+DOCA salt induced hypertension

Table 5.12: Effect of compound (18) and (24) on physiological parameters in UNX+DOCA salt induced hypertension

Groups	Weight (g)		Water intake (ml/rat)	Food intake (g/rat)
	0^{th} day	42^{nd} day		
NC	235.33±6.64	262.00±3.48	24±0.93	11.66±0.88
SC	236.33±5.24	254.00±1.63	24.66±0.80	10.83±1.01
UNX+DOCA (DC)	244.33±2.60	286.33±8.41	$71.83\pm2.21^{\#\#\#}$	11.66±1.45
DC + Compound **(18)** (5 mg/kg)	225.00±0.81	252.00±2.44	$39.66\pm1.62^{***}$	13.00±1.15
DC + Compound **(18)** (10 mg/kg)	229.05±5.52	266.66±3.33	$29\pm1.78^{***,\&\&,\wedge\wedge}$	13.33±1.20
DC + Compound **(24)** (5 mg/kg)	237.00±4.04	249.00±3.69	$42.33\pm2.66^{***}$	12.66±0.88
DC + Compound **(24)** (10 mg/kg)	234.00±1.00	245.33±6.22	$39.66\pm1.66^{***}$	13.00±1.52
DC+Los+Tera	243.5±6.94	252.5±6.12	$33.16\pm2.16^{***}$	11.33±1.20

Effect of compound **(18)** and **(24)** on physiological parameters. Values are expressed as mean±SEM (n=6). Data was analysed by one way ANOVA followed Bonferroni's multiple comparison post hoc test. #= compared to NC and SC, *=compared to DC, ^= compared to compound (24-10mg/kg), &=compared to Los+ Tera, $^{\&\&}$, **=p<0.01, ###,***=p<0.001

All the groups underwent unilateral nephrectomy followed by DOCA salt and 1% NaCl administration except normal and sham control animals for six weeks. Surgical intervention did not cause detrimental effects on weight and food intake of animals. There was

no significant difference observed amongst the groups. There was significant increase in waterintake of UNX+DOCA salt treated rats compared to NC and SC rats (SC vs. DC; 24.66±0.80 ml vs. 71.83±2.21 ml, $p<0.0001$). As depicted in table 5.12, there was no difference in weight of animals amongst groups observed suggesting surgical intervention did not interfere with normal growth process. Some of the studies have reported weight loss in DOCA salt treated rats as study progresses. Contrary to that, we have found non-significant weight gain, thus it was speculated that it may be due to dramatic increase in water intake in hypertensive rats. Administration of DOCA salt and 1% salt loading resulted into increased water intake as the study progressed (304) as shown in table 5.12. Reports have shown that consumption of sodium causes sensation of osmotic Na^+ receptors and increase in plasma osmolality (305). Changes in plasma osmolality serve as a initiator for induction of thirst and water intake and set the loop in motion (306). Studies have reported that increased salt consumption combined with fluid retention produce activation of RAAS and SNS nerve activity(307), and other vasoconstrictive agents such as vasopressin and endothelin release(308),(309). This global response of vasoconstriction resulted into initiation and maintenance of hypertension. Treatment with compound **(18)** and **(24)** produced significant improvement in water intake and natriuresis consumption at both the doses. Compound **(18)** at 5 mg/kg and 10 mg/kg reduced water intake significantly ($p<0.001$). Results revealed dose dependent action offered by compound **(18)** and significant difference was observed between two doses (5mg/kg vs. 10mg/kg, $p<0.001$). Compound **(24)** was also able to restore the balance between water intake and natriuresis. Here, results have shown superiority of compound **(18)** for maintaining the balancedepicting the significant difference ($p<0.001$ vs. compound **(24)**-10mg/kg) between compound **(18)** and **(24)**. Our results demonstrated that dual antagonism offered by compound **(18)** and **(24)** caused revival of intricate balance of osmolality and natriuresisthat are majorly governed by RAAS control.

5.8.2 Effect of compound (18) and (24) on hypertrophic response in UNX+DOCA salt induced hypertension

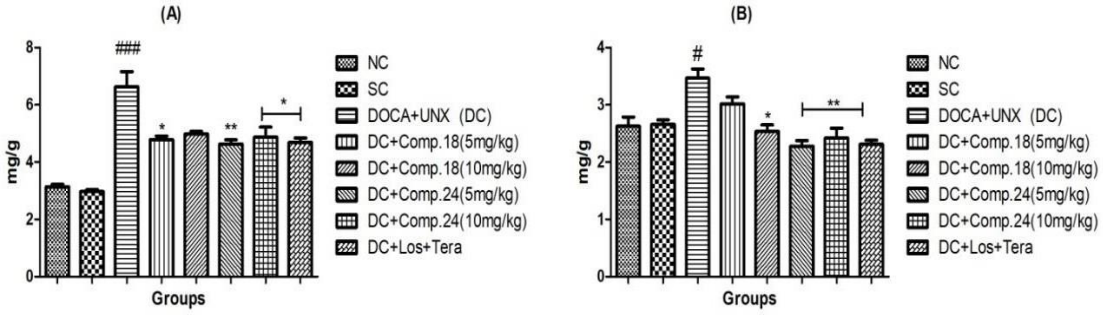

Figure 5.11: Effect of compound **(18)** and **(24)** on hypertrophic response in UNX+DOCA salt induced hypertension **(A)** kidney oedema index (KOI) **(B)** heart oedema index (HOI). Values are expressed as mean±SEM (n=6). Data was analysed by one way ANOVA followed by Bonferroni's multiple comparison post hoc test. #= compared to sham control. *= compared to UNX+DOCA. #,*=p<0.05, ##, **=p<0.01, ###,***=p<0.001

Uninephrectomized rats underwent DOCA and salt administration which showed marked elevation in kidney weight in previous investigations (295), (310). Our results are in accordance with previous findings as evident in figure 5.11 (A). Hypertensive rats showed almost 3-fold increase (p<0.001 vs. NC) in KW/BW ratio compared to normotensive rats. This observation can be attributed to increased workload implicated on the solitary kidney leading to stimulation of hypertrophic stimuli such as AngII, endothelin and catecholamines. Tissue specific activation of RAAS also promotes aldosterone release which further augments the process of fluid accumulation ultimately resulting into hypertrophic response (311).

Treatment with compound **(18)** and **(24)** abrogated this damage resulted into significantly reduced Kidney Oedema Index (KOI). Here, more beneficial result was observed only for compound **(18)** at 5 mg/kg than 10 mg/kg dose. However, no significant difference was observed between two dose levels [Compound **(18)** 5 mg/kg vs. 10 mg/kg, p>0.05]. Previous investigations also reported prevention in KOI by losartan and other ARB drugs (312). Standard drugs also exhibited similar degree of beneficial effect comparable with investigational compounds.

Sustained hypertension also produces significant increase in cardiac mass revealed by significantly increased Heart Oedema Index (HOI) in hypertensive rats as depicted in figure

5.11 (B). Chronic activation of Ang II and epinephrine is reported to increase left ventricular mass and diameter suggesting cardiac remodeling, increase end diastolic pressure and elevations in hypertrophic factor in heart(313),(314). Administration of compound **(18)** at 5 mg/kg did not show improvement ($p>0.05$) in HOI but dose of 10 mg/kg prevented hypertrophic response significantly [Compound **(18)** 10 mg/kg vs. DC, $p<0.05$] compared to hypertensive rats. While compound **(24)** at both doses exhibited their preventive potential in dose dependent manner ($p<0.001$ vs DC) compared to DC rats. Results obtained from current study highlighted the efficacy of targeting two systems together to mitigate the hypertrophic response as a consequence of uncontrolled hypertension.

5.8.3 Effect of compound (18) and (24) on hemodynamic alterations in UNX+DOCA salt induced hypertension

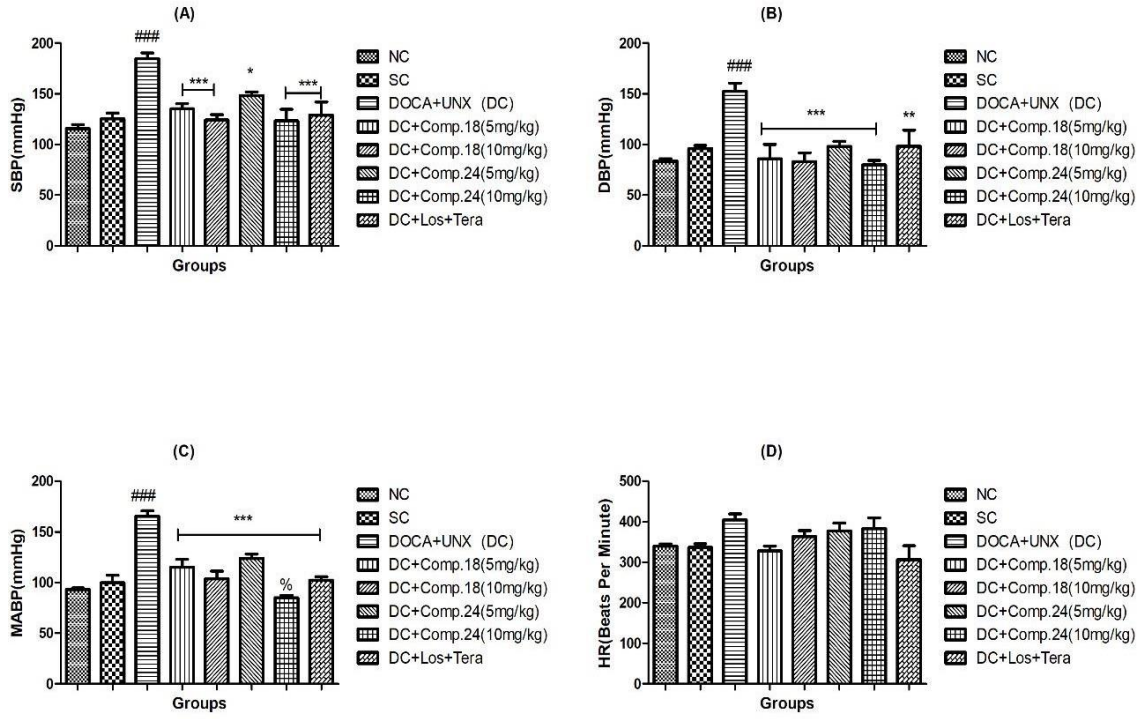

Figure 5.12: Effect of compound (18) and (24) on hemodynamic alterations in UNX+DOCA salt induced hypertension. (A) SBP (B) DBP (C) MABP (D) Heart rate. Values are expressed as mean±SEM (n=6). Data was analyzed by one way ANOVA followed by Bonferroni's multiple comparison post hoc test. #= compared to normal and sham control. *= compared to UNX+DOCA, $^{\%}$= compared to compound (**24**-5mg/kg) *,$^{\%}$=p<0.05, ##, **=p<0.01, ###,***=p<0.001 ns= non-significant. SBP= Systolic blood pressure, DBP=Diastolic blood pressure, MABP= Mean arterial blood pressure

UNX+DOCA treatment caused marked increase in SBP and DBP as depicted in figure 5.12 (A) by significant increase (NC vs. DC, 115.75±3.94 vs. 186.78±5.64, $p<0.0001$) as compared to normal and sham control animals. Treatment with compound **(18)** at both the doses produced excellent reduction in SBP [5 mg/kg (135.03±5.25), $p<0.0001$ vs. DC] and [10 mg/kg (122.32±5.22) $p<0.0001$ vs. DC]. While administration of compound **(24)** [5 mg/kg (148.42±3.06), $p<0.05$ vs. DC] and [10 mg/kg (123.34±11.42) $p<0.0001$ vs. DC] also produced potent antihypertensive effect by significant fall in BP. Combination of standard drugs showed comparable reduction in SBP (129.05±12.85, $p<0.0001$ vs. DC) to compound **(18)** and **(24)**. Treatment with compound **(18)** and **(24)** showed non-significant difference when compared to each other and dose dependent response was observed for developed compounds. DBP was [Figure 5.12 (B)] elevated drastically in hypertensive control compared to NC (NC vs. DC, 83.50±2.24 vs. 149.97±4.68, $p<0.0001$). Administration of compound **(18)** [5 mg/kg (85.73±14.32), $p<0.0001$ vs. DC] and [10 mg/kg (83.11±8.72), $p<0.0001$ vs. DC] produced significant reduction in DBP compared to DC group. Treatment with compound **(24)** [5 mg/kg (98.11±5.03), $p<0.0001$ vs. DC] and [10 mg/kg (79.87±4.40), $p<0.0001$ vs. DC] at both doses produced significant reduction in DBP compared to DOCA salt treated rats. Losartan and terazosin were able to nullify the effect of UNX+ DOCA salt evident by significant reduction in BP as evident in figure 5.12 (B).

Mean arterial blood pressure is considered as one of the definitive parameters for the evaluation of antihypertensive drug. Compound **(18)** [5 mg/kg (115.09±9.11), $p<0.0001$ vs. DC] and [10 mg/kg (103.62±10.58) $p<0.0001$ vs. DC] was able to ameliorate UNX+DOCA induced chronic rise in blood pressure. Treatment with compound **(24)** [5 mg/kg (123.49±5.62), $p<0.0001$ vs. DC] and [10 mg/kg (85.06±1.84), $p<0.0001$ vs. DC] also abolished the rise in MABP evoked by DOCA and NaCl salt loading. Here, compound **(24)** exhibited dose dependent reduction in blood pressure which was significantly lower [$p<0.05$ vs. compound **(24)**-5mg/kg] in 10 mg/kg treatment group. Animals treated with compound **(24)** has significantly reduced MABP than NC and SC animals. Combination of standard drugs also produced desired effect by reducing BP compared to DC (102.26±3.52, $p<0.0001$ vs. DC). It is evident from detailed hemodynamic assessment that treatment with both the NCEs produced excellent anti-hypertensive effect. Treatment with lower dose (5 mg/kg) produced comparable or slightly better action than combination of standard drugs, thus, it can be attributed to dual antagonistic potential.

Heart rate variability is associated with the UNX+DOCA salt model of hypertension. However, in our study we did not find any significant difference amongst different groups. Treatment with compound **(18)** and **(24)** did not cause any bradycardic or tachycardic response with their chronic treatment. On the contrary, treatment with combination of standard drugs showed reduced heart rate, this can be attributed to terazosin treatment, as terazosin treatment alone causes severe bradycardic response in animals.

DOCA administration along with salt intake is known to induce cardiorenal hypertension related to its sodium water retention effects(315). DOCA serves as a precursor to aldosterone, which is converted to aldosterone *in-vivo* through the action of the enzymes 11β-hydroxylase and subsequently aldosterone synthase. This *de-novo* formation of aldosterone from exogenously administered DOCA leads to sodium retention in the distal tubules of the kidney. Initially, increase in blood pressure is mediated mainly through plasma volume expansion and later accompanied by different pathomechanism of blood pressure such as sympatho-excitation and increased vasopressin levels (316), elevated central and peripheral RAAS system. Alteration of the central baroreflex involvement of NOX pathways and endothelin-I induced vasoconstriction are also signatory to DOCA-salt mediated hypertension.

Compound **(18)** and **(24)** exhibited marked effects at both doses of 5 mg/kg and 10 mg/kg revealed potent inhibition of two major governing systems and their cross talk involved in the pathogenesis of hypertension. Results showed non-significant difference between standard treatments and compounds under investigation. A very important observation needs to be considered that, for the lucid data interpretation we have only included the combination of standard drugs for the direct comparison of efficacy of compounds. Combination of standard drugs produces additive action compared to single therapy which emphasizes the role of cross talk between RAAS and SNS.

5.8.4 Effect of (18) and (24) on articular reactivity in UNX+DOCA salt induced hypertension

Table 5.13: Articular reactivity of compound (18) and (24) in UNX+DOCA salt induced hypertension

Groups	ΔP (mmHg)		
	Phenylephrine	**Angiotensin II**	**Acetylcholine**
NC	30.5±2.17	66.56±1.38	-56.32±9.58
SC	33.71±1.51	67.88±1.33	-51.76±3.01
UNX+DOCA (DC)	54.42±3.72$^{\#}$	106.84±4.97$^{\#\#}$	-45.47±8.41$^{\#}$
DC+ Compound **(18)** (5 mg/kg)	42.83±12.11	57.15±14.22**	-71.38±7.89**
DC+ Compound **(18)** (10 mg/kg)	31.42±5.16*	35.83±5.33***	-80.87±0.95**
DC+ Compound **(24)** (5 mg/kg)	26.98±0.83**	65.59±6.33**	-51.96±2.96
DC+ Compound **(24)** (10 mg/kg)	23.24±4.12**	49.85±5.99***	-63.73±6.32**
DC+Los+Tera	41.14±2.73	45.80±7.59***	-53.20±3.49

ΔP= indicates the difference in blood pressure between before and after phenylephrine or Ang II i.v. bolus. Bonferroni's multiple comparison post hoc test. #= compared to NC & SC control. *= compared to UNX+DOCA. *=p<0.05, ##, **=p<0.01, ###,***=p<0.001 ns= non-significant

Studies have reported an increase in sympathetic nerve activity, upregulation RAAS system and AT_1 receptor. To test these findings in this study; vasoactive agents such phenylephrine, Ang II and acetylcholine were injected as i.v. bolus (317). Hypertensive rats showed enhanced pressure response due to upregulation of SNS and RAAS system. While on the other hand, vasodilatory effect of ach is attenuated in disease control rats. This can be due to damaged endothelium resulted into reduced nitric oxide release and eNOS action (293). These results displayed in table 5.13 are in line with observation and proposed hypothesis. Articular reactivity to different agonists were assessed by i.v. bolus administration of vasoactive agents via jugular vein. UNX+DOCA salt treated showed heightened responses to selective α_1 agonist phenylephrine (5µg/kg). Disease control produced more pronounced increment ($p<0.001$) in ΔP compared to NC and SC rats as evident in table 5.13. Pre- treatment with compound **(18)** only at 10mg/kg showed significant inhibition of pressor response while both the doses of compound **(24)** produced significant inhibition when challenged against phenylephrine [(Compound **(24)**-5mg/kg, $p>0.05$), (Compound **(24)**-10 mg/kg, $p<0.05$)]. Combination of standard drug

produced lesser response compared to DC rats however it was not significant ($p>0.05$). Current study showed enhanced response to phenylephrine revealed up-regulation of adrenergic receptor, specifically α_1 receptors. Reid et.al. showed increased sympathetic nerve activity is also involved in DOCA-salt hypertension during the early phase (1–5 days after starting treatment) and developed phase(2–6 weeks after starting the treatment(318). Similarly, Ang II evoked potent rise in BP ($\Delta P= 66.56\pm1.38$ vs. 106.84 ± 4.97, NC vs. DC, $p<0.0001$) in hypertensive rats due to activation RAAS system. Treatment with NCEs and standard drugs abolished pressor response significantly. Current study highlights the impact of dual receptor inhibition on improvement of response to vasoactive agents.

Many studies have been reported regarding disturbed endothelial dysfunction in hypertension in *ex-vivo* conditions. We have studied effects of Ach on pressor response for indication of integrity and function of endothelial nitric oxide in *in-vivo*. Ach administration caused potent fall in BP in normotensive animals while hypertensive rats showed abrogatedresponse to Ach(319) (56.32 ± 9.58 vs. 45.47 ± 8.41, NC vs. DC, $p<0.05$). Treatment with compound **(18)** (10 mg/kg, $p<0.05$) showed excellent response to exogenous Ach which leads to fall in blood pressure. Treatment with compound **(24)** and standard drugs were ableto produce modest effect to Ach.

5.8.5 Effect of compound (18) and (24) on metabolic parameters in UNX+DOCA salt induced hypertension

Hypertension and metabolic anomalies are often progressed hand in hand, and they have cause-effect relationship and vice versa. DOCA salt treatment is believed to exhibit metabolic dysregulation because of overwhelming response of RAAS and SNS (320). As both these systems play vital role in the insulin signaling and mediated effects (321),(322). In addition, elevated level of mineralocorticoid levels is reported to hamper insulin signaling(323) and mineralocorticoid antagonist improve insulin sensitivity in animals(324),(325). Hypertensive rats showed non-significant change in glucose level after UNX+DOCA treatment compared to sham control animals. Treatment with NCE or standarddrugs did not produce any change in glucose homeostasis.

Table 5.14: Effect of compound (18) and (24) on metabolic parameters in UNX+DOCA salt induced hypertension

Group	Glucose	TG	TC	HDL
NC	141.57±3.35	55.16±1.28	44.32±2.09	55.21±2.14
SC	145.12±4.10	54.86±3.85	40.62±2.44	54.19±2.93
UNX+DOCA (DC)	147.97±6.05	76.40±6.13$^{\#}$	56.14±5.83	39.74±2.66$^{\#\#}$
DC+ Compound **(18)** (5 mg/kg)	132.87±8.63	58.70±1.64	50.41±3.08	60.01±1.61**
DC+ Compound **(18)** (10 mg/kg)	134.40±7.78	54.57±2.90*	46.16±2.31	56.71±1.61*
DC+ Compound **(24)** (5 mg/kg)	142.37±1.56	76.10±2.84	52.99±6.49	57.35±0.66*
DC+ Compound **(24)** (10 mg/kg)	137.40±2.89	64.20±4.10	46.86±3.29	57.30±3.68*
DC+Los+Tera	144.08±5.92	64.30±4.96	42.84±4.43	52.51±3.61

Data were analysed by Bonferroni's multiple comparison #= compared to NC & SC control. *= compared to UNX+DOCA. *=p<0.05, ##=p<0.01

DOCA salt treated rats showed elevated level of TG (p<0.05) compared to naïve animals while oral administration with compound **(18)** at 10 mg/kg dose was found to be effective in lowering of TG significantly. Treatment with other drugs was not able to alter this metabolic abnormality. HDL-C level was also dramatically decreased with DOCA treatment and significant correlation (DC vs. SC, p<0.001) was observed compared to NC or SC rats. All treatment regimens produced beneficial effects to raise this good cholesterol significantly. Total cholesterol was unaffected in all the groups as there was no significant change amongst the groups. The observed protective effects can be attributed to inhibition of dual system and subsequently prevent atherogenic response.

Evidence suggested that UNX+DOCA salt administration produce marked metabolic abnormalities (313), our results are in line with observation where we found mild metabolic abnormalities associated with UNX+DOCA salt treatment. Some of the studies have reported full-fledged metabolic alteration accompanying hypertension while we have observed only alteration in TG and HDL level. The reason for non-compliance could be the frequency and duration of the dose as many protocols intended to study chronic effect of DOCA induced hypertension and also the high salt loading diet study targeting central nervous pathway of RAAS activation (322).

5.8.6 Effect of compound (18) and (24) on Ach mediated endothelial relaxation and nitric oxide level in UNX+DOCA salt induced hypertension

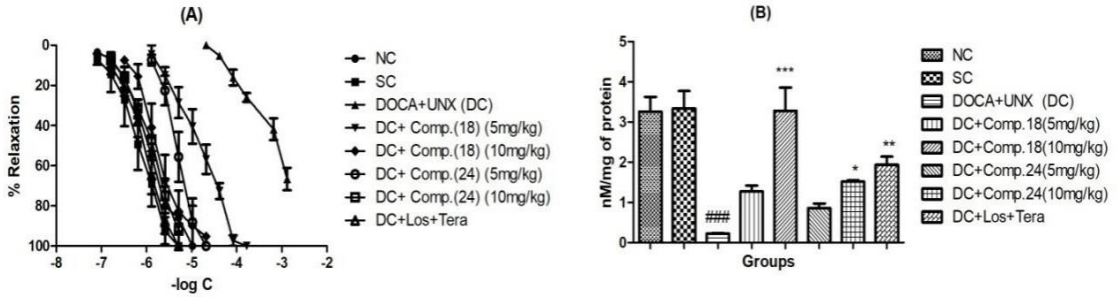

Figure 5.13: Effect of compound (18) and (24) on Ach mediated endothelial relaxation and nitric oxide level in UNX+DOCA salt induced hypertension. (A) Endothelial relaxation (B) Nitric oxide

Values are expressed as mean±SEM (n=6). Data was analysed by one way ANOVA followed by Bonferroni's multiple comparison post hoc test. #= compared to sham control. *= compared to UNX+DOCA. *=p<0.05, ##, **=p<0.01, ###,***=p<0.001

Ach mediated relaxation in large arteries provides index of endothelium damage inflicted by hypertensive stimuli. Normal control and sham control animals exhibited EC_{50} value of $1.076*10^{-6}$ µM while hypertension caused massive shift in EC_{50} value as DOCA salt treated rats showed 691.9 µM. Simultaneously, nitric oxide was measured to validate the observation made during tissue relaxation study. Hypertensive rats significantly reduced level of nitric oxide in plasma (3.25± 0.36 nM vs. 0.22±0.1 nM, p<0.0001) as compared to SC and NC rats. Treatment with compound **(18)** and **(24**) displayed leftward shift in relaxation curve with reduced EC_{50} value for Ach. Along with that, compound **(18)** and **(24)** significantly enhanced the depleted nitric oxide level compared to UNX+DOCA salt rats. Treatment with compound **(18)** at 10 mg/kg was able to restore nitric oxide level significantly compared to DC rats.

Persistent hypertension leads to erosion of endothelium in blood vessel lining resulted into decrease nitric oxide bioavailability (326). We have observed that hypertensive rats showed marred relaxation to acetylcholine due to enhance blood pressure resulted into denudationof NO mediated by unilateral nephrectomy and DOCA salt. Reports have been published regarding the decrease NO content in hypertension leading to compromised relaxation of blood vessel (327). One of the striking observations was made that aorta from hypertensiverats were more reactive to phenylephrine mediated contraction boosting the observation made in articular reactivity measurement and failed to produce 100% relaxation. Inhibition of this detrimental effect was reversed by novel multitargeted ligands under investigation as evident in figure 5.13

5.8.7 Effect of compound (18) and (24) on Protein Kinase C (PKC) and p-Akt protein expression in UNX+DOCA salt induced hypertension

To gain insight into molecular aspect of novel compounds, Protein kinase C (PKC) expression in aorta of study animals was measured. Hypertensive rats displayed significantly elevated level of PKC (NC vs. DC; $p<0.001$) as compared to NC animals. Treatment with dual antagonists significantly reduced the expression of PKC in rat aorta by inhibiting the cross talk between α_1 and AT_1 receptor. Treatment with compound **(18)** ($p<0.05$ vs. DC) and compound **(24)** (10 mg/kg vs. DC; $p<0.001$) was able to produce significantly reduced expression of PKC. PKC being the upstream signal in the G_q protein signal transduction control basal vascular smooth muscle (VSM) tone and myocardial contraction. Actions of PKC is also mediated by via calcium dependent and calcium independent signaling through MAPK pathway for contraction vascular smooth muscle. PKC, positioned upstream to the MAPK pathways is reported to modulate the increment of basal tone in hypertensive rats (328),

Henrion et al., reported the profound role of PKC in Ang II induced potentiation of norepinephrine-induced effects on vascular tone(329). Recent evidence also suggested contraction mediated by α_1 receptor in hypertensive ageing rat regulated by the PKC. Another reason to study the role of PKC is that both α_1 and AT_1 receptors signaling is mediated by G_q pathway. Considering the extensive cross talk between these two systems, PKC is believed to play the key regulator between them. One interesting fact is found to heterodimerize between the crosstalk of RAAS and SNS and interactions between α_1R and AT_1R exist at the second messenger level (330). The proposed molecular interactions in the second messenger pathway between the α_1R and AT_1R is a consequence of both receptors coupling to Gq-proteins. These may result in decrease calcium mobilization and MAPK activation leading to reduced VSM contraction. Our results demonstrate that novel compounds may act on PKC, a critical regulator of receptor crosstalk and responsible for achieved beneficial effects.

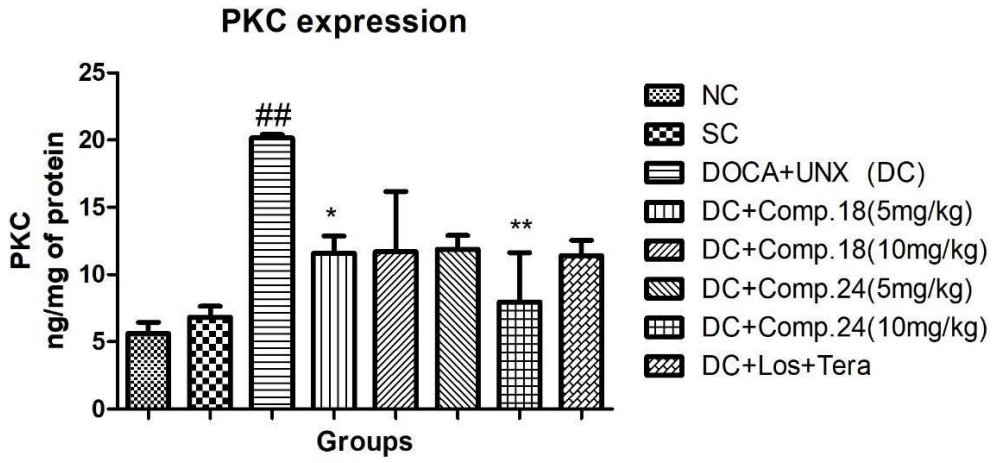

Figure 5.14: Effect of compound (18) and (24) on Protein Kinase C expression in aorta of DOCA salt hypertensive rats. Values are expressed as mean±SEM (n=6). Data was analyzed by one way ANOVA followed by Bonferroni's multiple comparison post hoc test. #= compared to sham control. *= compared to UNX+DOCA. *=p<0.05, ##, **=p<0.01

On the other hand, increased activity of PKC leads to MAPK activation which subsequently activate numerus second messengers such as PI_3K, ERK1/2. Especially, PI_3K was found be expressed in DOCA salt hypertensive rats however its downstream component, p-Akt level was decreased (331). Current study showed decreased p-Akt level in rat aorta of hypertensive rat. Reduced p-Akt level is highly related to decreased eNOS enzyme and reduced NO production. Novel compound **(24)** showed an increase in p-Akt level in aorta after six weeks of treatment. Our results are in accordance with previous report where chronic blockade of RAAS and SNS increased p-Akt expression (332).

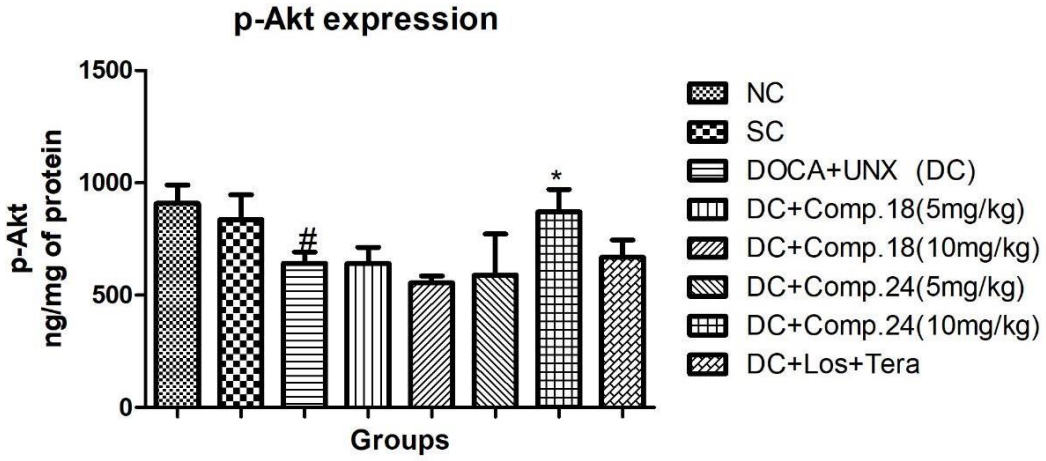

Figure 5.15: Effect of compound (18) and (24) on p-Akt expression in aorta of DOCA salt hypertensive rats. Values are expressed as mean±SEM (n=6). Data was analyzed by one way ANOVA followed by

Bonferroni's multiple comparison post hoc test. #= compared to sham control. *= compared to UNX+DOCA. *,# = $p<0.05$

5.8.8 Effect of compound (18) and (24) on cytokine imbalance in UNX+DOCA salt induced hypertension

Table 5.15: Effect of compound (18) and (24) on cytokine levels in UNX+DOCA salt induced hypertension

Group	IL-6 (pg/ml)	TNF-α (pg/ml)	PRA (ng/ml)
NC	796.09±170.05	275.9±13.01	6.01±0.24
SC	936.06±219.58	269.40±13.81	5.78±0.34
UNX+DOCA (DC)	2766.05±447.98$^{\#\#}$	918.73±14.89$^{\#\#\#}$	2.51±0.79$^{\#\#}$
DC+ Compound **(18)** (5 mg/kg)	1106.41±263.46*	678.23±38.88**	5.17±0.23**
DC+ Compound **(18)** (10 mg/kg)	862.66±125.47**	466.9±55.76$^{***,@@}$	4.66±0.14*
DC+ Compound **(24)** (5 mg/kg)	1249.33±250.00	854.4±8.08	3.12±0.42*
DC+ Compound **(24)** (10 mg/kg)	572.66±17.40$^{**,\%}$	619.15±14.58$^{***,\%}$	4.37±0.39**
DC+Los+Tera	786.00±288.63**	376.40±10.69$^{***,\wedge\wedge}$	5.18±0.15**

Values are expressed as mean±SEM (n=6). Data was analyzed by one way ANOVA followed by Bonferroni's multiple comparison post hoc test. #= compared to sham control. *= compared to UNX+DOCA., @= Compared to compound **(18)** – 5 mg/kg, %= Compared to compound **(24)** – 5 mg/kg, ^=compared to compound **(24)** – 10 mg/kg, *,%=$p<0.05$, ##, **,@@,^^=$p<0.01$, ###,***=$p<0.001$ ns= non-significant

We have studied the role cytokine imbalance as a causative factor in hypertension progression. Studies reported that hypertension is associated with many circulating inflammatory factors (333). Increased inflammatory factors are also related to the increased risk of hypertension in normotensive individuals. Inflammation in the brain has received increased attention as a cause of sympatho-excitation (334). Hence, an inflammatory-sympathetic mechanism is a key element in the pathogenesis of hypertension. On the other hand, overactive RAAS system, produce ROS and activate NADPH oxidase, this oxidative stimulus caused activation and release of cytokine which further increase the blood pressure and induce inflammatory changes in heart and kidney.

Elevated cytokine level is responsible for initiation and sustenance of blood pressure in DOCA salt induced hypertension. TNF-α promotes sodium retention, vasoconstriction, hypertrophy and oxidative injury during the development of hypertension in DOCA-salt

Hypertension (335). Hypertensive animals showed significant elevation in IL-6($p< 0.001$ vs. DC) and TNF-α ($p<0.0001$ vs. DC) level compared to normal control animals. Treatment with compound **(18)** and **(24)** at both the doses produce beneficial effect by reducing cytokine imbalance significantly. Combination of standard drug found to be more effective in reducing detrimental level of cytokine level in plasma as compared to hypertensive rats.Increase level of IL-6 and TNF-α caused decrease in NO bioavailability and further contributed to maintenance of blood pressure. (336)

Many lines of evidence suggest that DOCA salt induced hypertension is renin independent as it is marked by decreased plasma rennin activity (337). It is speculated that there is elevated renal perfusate pressure in solitary kidney in uninephrectomized rats which cause diminished renin release and subsequent activation of sympathetic nerve and spillover of norepinephrine. DMLs target both receptors together resulting into amelioration of the cytokine imbalance and helps to normalize the blood pressure.

5.8.9 Effect of compound (18) and (24) on urinary indices in UNX+DOCA salt induced hypertension

Table 5.16: Effect of compound (18) and (24) on urinary parameters in UNX+DOCA salt induced hypertension

Group	Urine output(ml)	Sodium (µmol/l)	Potassium (µmol/l)	Uric acid (µmol/l)	Urea (ng/ml)	Creatinine (mg/dl/day)	Creatinine Clearance	Albumin (µg/day)
NC	11.74 ± 1.76	268.361 ± 9.962	45.000 ± 1.426	306.480 ± 19.153	12.508 ± 1.547	22.167 ± 0.795	2.800 ± 0.208	12.153 ± 0.334
SC	9.66 ± 2.028	263.279 ± 5.658	44.360 ± 7.246	301.662 ± 17.096	10.274 ± 1.398	22.083 ± 0.961	2.683 ± 0.044	14.084 ± 0.220
UNX+DOCA (DC)	44 ± 4.726$^{###}$	184.262 ± 11.858$^{###}$	66.608 ± 1.986^{ns}	535.876 ± 16.836$^{###}$	49.564 ± 4.552$^{###}$	7.083 ± 0.417$^{###}$	1.133 ± 0.145$^{###}$	28.912 ± 4.481$^{#}$
DC+ Compound (18) (5 mg/kg)	30.16 ± 2.333***	268.852 ± 7.166**	57.073 ± 6.497^{ns}	399.127 ± 10.683^{ns}	40.280 ± 4.099^{ns}	11.500 ± 1.127^{ns}	1.313 ± 0.144^{ns}	18.962 ± 0.759^{ns}
DC+ Compound (18) (10 mg/kg)	18.16 ± 3.844**	264.590 ± 8.273***	39.512 ± 7.617^{ns}	444.340 ± 17.954**	15.888 ± 1.348***	13.250 ± 0.661$^{**,@}$	2.250 ± 0.189*	18.348 ± 1.535^{ns}
DC+ Compound (24) (5 mg/kg)	13.5 ± 2.906$^{***,@@}$	228.033 ± 13.983***	50.762 ± 2.688^{ns}	392.827 ± 24.037***	21.900 ± 1.372***	11.333 ± 0.982^{ns}	1.850 ± 0.202^{ns}	15.892 ± 2.830*

Group	Urine output(ml)	Sodium (µmol/l)	Potassium (µmol/l)	Uric acid (µmol/l)	Urea (ng/ml)	Creatinine (mg/dl/day)	Creatinine Clearance	Albumin (µg/day)
DC+ Compound (24) (10 mg/kg)	13.5 ± 3.844$^{***,@@,\$\$}$	222.459 ± 4.926$^{**,\$\$,\&\&}$	31.829 ± 13.994*	369.480 ± 20.403$^{***,\&}$	13.956 ± 1.652***	17.417 ± 1.228$^{***,\%\%}$	2.393 ± 0.301**	12.966 ± 1.854**
DC+Los+Tera	17.83 ± 3.930*	258.853 ± 6.695^{ns}	37.454 ± 3.155^{ns}	465.463 ± 11.772^{ns}	16.854 ± 3.789^{ns}	15.817 ± 1.099**	1.943 ± 0.038^{ns}	20.378 ± 0.303^{ns}

Values are expressed as mean±SEM (n=6). Data was analyzed by one way ANOVA followed by Bonferroni's multiple comparison post hoc test. #= compared to sham control. *= compared to UNX+DOCA., @= compared to compound **(18)** – 5 mg/kg, $=compared to compound **(18)** – 10 mg/kg, %= compared to compound **(24)** – 5 mg/kg, &=compared to Los+Tera *,$^{@,\%,\&}$ = p<0.05, ##, **,$^{\%\%}$ =p<0.01, ###,***=p<0.001 , ns= non-significant

Urinary parameters are important when studying mineralocorticoid induced hypertension since the major affected organ is the kidney. Hypertension mediated overload leads to functional damage to the kidney which may be suggested by changes in excretion of electrolytes, creatinine, protein and glucose(338),(339) Accordingly, it was decided to evaluate a battery of parameters which provide an index of renal function.

UNX+DOCA (DC) treatment showed a significant ($P<0.001$) increase in urine output compared to both normal control (NC) and sham control (SC) groups It is known that mineralocorticoids like DOCA favors sodium/water retention and in turn supports excretion of potassium. In contrast to this finding, we found that urinary output was increased about 4-fold in DOCA-salt treated animals. One possible reason for this outcome is that as this group was supplemented with 1% NaCl and 0.2% KCl in drinking water which increases the osmolarity of the drinking solution thus leading to increased volume intake and ultimately output(340),(341). Compound **(18)** (5 mg/kg & 10 mg/kg) group showed significant ($P<0.001$) decrease in urine output when compared to UNX+DOCA (DC) treated rats. Compound **(24)** (5 mg/kg & 10 mg/kg) treatment showed significant ($p<0.001$) decrease in urine output when compared to UNX+DOCA (DC) animals. Los + tera showed significant ($p<0.001$) decrease in urine output when compared to UNX+DOCA (DC) animals.

UNX+DOCA (DC) treatment showed a significant ($p<0.001$) decrease in urinary sodium levels when compared to sham control (SC) and normal control (NC) animals. Treatment with Compound **(18)** at 5 mg/kg & 10 mg/kg showed a significant ($p<0.001$) increase in sodium when compared to UNX+DOCA salt-treated group. Compound **(24)** (5 mg/kg & 10 mg/kg) treatment showed significantly ($p<0.01$ & $p<0.001$ respectively) increased sodium levels when compared to UNX+DOCA (DC) animals. Treatment with losartan + terazosin showed significant ($p<0.001$) increase in the sodium levels when compared with UNX+DOCA (DC) group. This was suggestive of increased sodium retention in the positive control group which might contribute to increased vascular volume factoring the rise in blood pressure. This data are in agreement with the findings reported by investigators. (316),(342).

Kidneys are known to effectively excrete creatinine in the urine and block the spillage of glucose and proteins in the urine. However, when renal structure is marred due to mineralocorticoid insult which can consequently cause reduce creatinine excretion A decline in glomerular filtration rate was also evident from the creatinine clearance values

which were reduced in the DOCA-salt group as compared to the control group(343). UNX+DOCA (DC) treated rats showed significant ($p<0.001$) decrease in creatinine levels and creatinine clearance compared to the normal control (NC) and sham control (SC) animals. Compound **(18)** at 10mg/kg showed significant ($p<0.01$) increase in creatinine levels when compared to UNX+DOCA (DC) treated rats. Compound **(18)** at 5 mg/kg reflected non-significant increase in creatinine levels when compared to disease control (DC) rats. Compound **(24)** (10 mg/kg) treatment showed significant ($p<0.001$) increase in creatinine levels when compared to UNX+DOCA (DC) animals. Compound **(24)** (5 mg/kg) treatment showed non-significant increase in creatinine level when compared to disease control (DC) animals. The treatment with Los+tera showed a significant ($p<0.001$) increase in creatinine levels when compared to UNX+ DOCA treated rats.

Mineralocorticoids induced insult on kidney resulted into significant presence of albuminuria (DC vs. SC; $p<0.001$) in urine of DOCA salt treated rats. One of the possible explanations for these abnormalities could be due to uncontrolled hypertensive response on the solitary kidney which leads to cellular and vascular damage. This can lead to architectural damage in the kidney and as a consequence leakage of macro and micro molecules could occur in filtrate. Treatment with compound **(18)** and **(24)** produced significant prevention response by reducing blood pressure as well as could be local inhibition of RAAS. Compound (24-10mg/kg) was found be the most effective in reducing the negativechanges inflicted by DOCA salt Current observations are coincided well withhistopathological observations.

The above battery of parameters provides necessary evidence of the damage produced by mineralocorticoid induced hypertension due overwhelming RAAS inhibition. Compound **(18)** and **(24)** certainly present protective roles in abrogating this pathological response andimproving renal function. These results also encourage us the investigation of novel compounds in chronic kidney disease (CKD) propagated by dual inhibition of RAAS and SNS in future.

5.8.10 Effect on compound (18) and (24) on oxidative stress parameters in UNX+DOCA salt induced hypertension

5.8.10.1 Effect on compound (18) and (24) on oxidative stress parameters in heart of UNX+DOCA salt induced hypertension

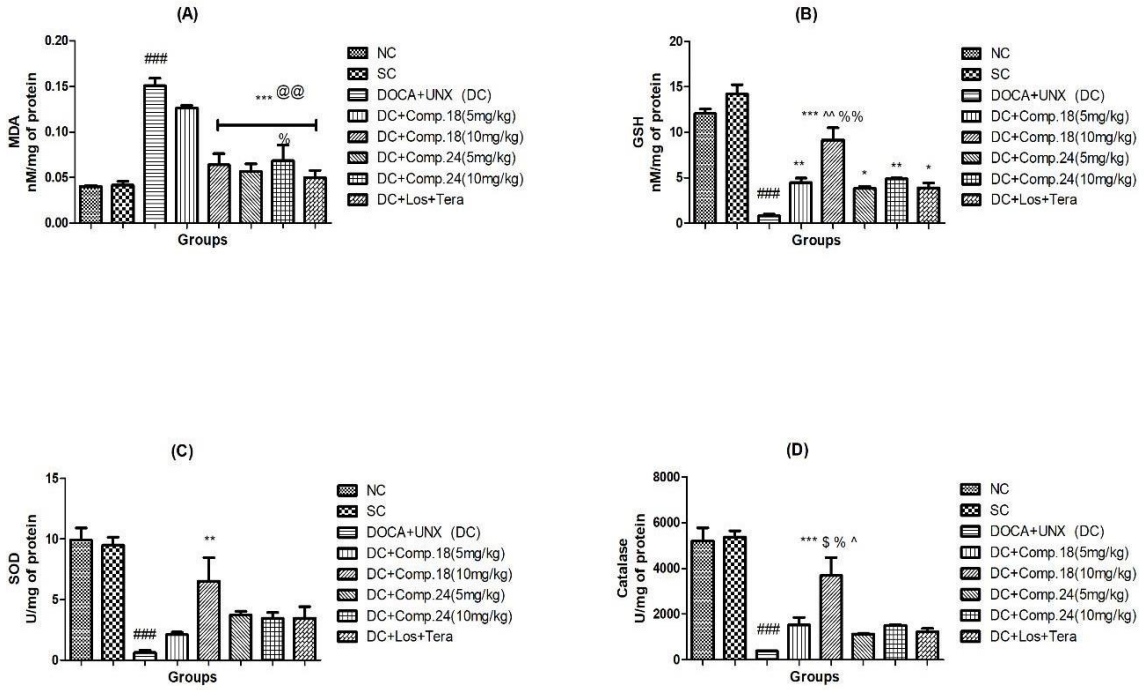

Figure 5.16: Effect of compound (18) and (24) on oxidative stress parameters in heart of UNX+DOCA salt induced hypertension. (A) MDA (B) GSH (C) SOD (D) Catalase. Values are expressed as mean±SEM (n=6). Data was analyzed by one way ANOVA followed by Bonferroni's multiple comparison post hoc test. #= compared to sham control. *= compared to UNX+DOCA., @= compared to compound (**18**-5mg/kg), $=compared to compound (**18**-10mg/kg) %= compared to compound (**24**-5mg/kg), &=compared to Los+Tera, *,$^{@,\%,\&}$ = p<0.05, ##, **,$^{\%\%}$ =p<0.01, ###,***=p<0.001 , ns= non-significant

UNX+DOCA salt induced significant lipid peroxidation evident by dramatic increase in MDA content in heart homogenate (p<0.001). Treatment with compound **(18)** (5 mg/kg) was found to be ineffective to reverse this effect however other treatments produced favorable effect by reducing MDA content significantly (p<0.001) figure 5.16 (A). Antioxidant protection was markedly affected as evident in figure 5.16 (B) by significant (p<0.001) low level of GSH in hypertensive rats compare to normal control. Treatment with compound **(18)** and **(24)** and standard drugs caused significant (p<0.01) elevation in GSH content.

As depicted in figure 5.16 (C) and (D), UNX+DOCA treatment showed detrimental effects on antioxidant defense by significantly reduced SOD and catalase level in heart

homogenates (p<0.001). Treatment with compound **(24)** (10mg/kg) restored this balance by significantly increase (p<0.001) preventive enzyme in tissue samples.

5.8.10.2 Effect on compound (18) and (24) on oxidative stress parameters in kidney of UNX+DOCA salt induced hypertension

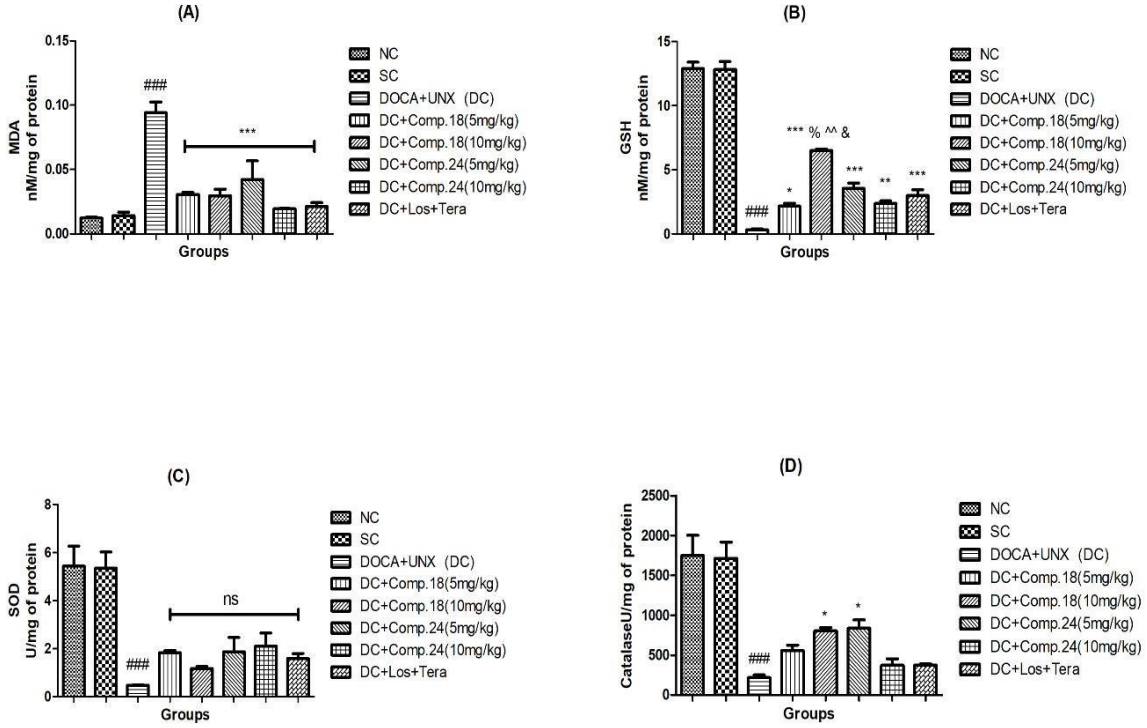

Figure 5.17: Effect of compound (18) and (24) on oxidative stress parameters in kidney of UNX+DOCA salt induced hypertension. (**A) MDA (B) GSH (C) SOD (D) Catalase.** Values are expressed as mean±SEM (n=6). Data was analysed by one way ANOVA followed by Bonferroni's multiple comparison post hoc test. #= compared to sham control. *= compared to UNX+DOCA. *,#=p<0.05, **=p<0.01, ###,***=p<0.001 ns= non-significant

Analysis of kidney homogenates suggests elevated levels of MDA and GSH, and reduced level of protective antioxidant such as SOD and catalase in hypertensive rats. Increased production of ROS, demonstrated in micro puncture studies in the kidney macula densa of spontaneously hypertensive rats (SHR) is attributed to a decrease in the bioavailability of nitric oxide (344). This may directly induce vasoconstriction and increase tubulo-glomerular feedback, resulting in enhanced renal vascular resistance and hypertension (345). Lipid peroxidation is greatly increased in DOCA salt treated rats showed involvement of ROS generation in pathogenesis of hypertension (346).

Administration of standard drugs and NCEs reduced MDA content significantly after 45 days.

Antioxidant defense is severely affected by UNX+DOCA salt treatment evident by significant reduction in GSH, SOD, catalase. Compound **(18)** and **(24)** markedly reduce oxidative by increasing GSH and catalase content. However, treatment was found to be non-significant as far as elevation in SOD is concerned.

The mechanisms involved in angiotensin II-induced vascular O_2•− production is well characterized. ROS production by angiotensin II can be separated into an acute phase involving protein kinaseC (PKC), c-Src, growth factor receptors transactivation and translocation of cytosolic p47phox to the membrane(347) (348) and a sustained phase involving up-regulation of NADPH oxidase subunits(349). Potent blockade of SNS and RAAS by compounds under investigation prevented generation of ROS mediated by Ang II and epinephrine directly or by inhibiting the stimulation of endothelin release.

5.8.11 Effect of compound (18) and (24) on histopathological changes in UNX+DOCA salt induced hypertension

The vascular tissues like heart, aorta and kidney are prime organs susceptible to damage inflicted by mineralocorticoid induced cardiorenal remodeling (350). Hypertension is associated with vascular dysfunction, with changes are seen at the histological and cellular level in vessels from hypertensive animals and human patients. Uncontrolled hypertension accelerates the damage to these target tissue and results in eventual organ failure and cardiovascular death and disability.

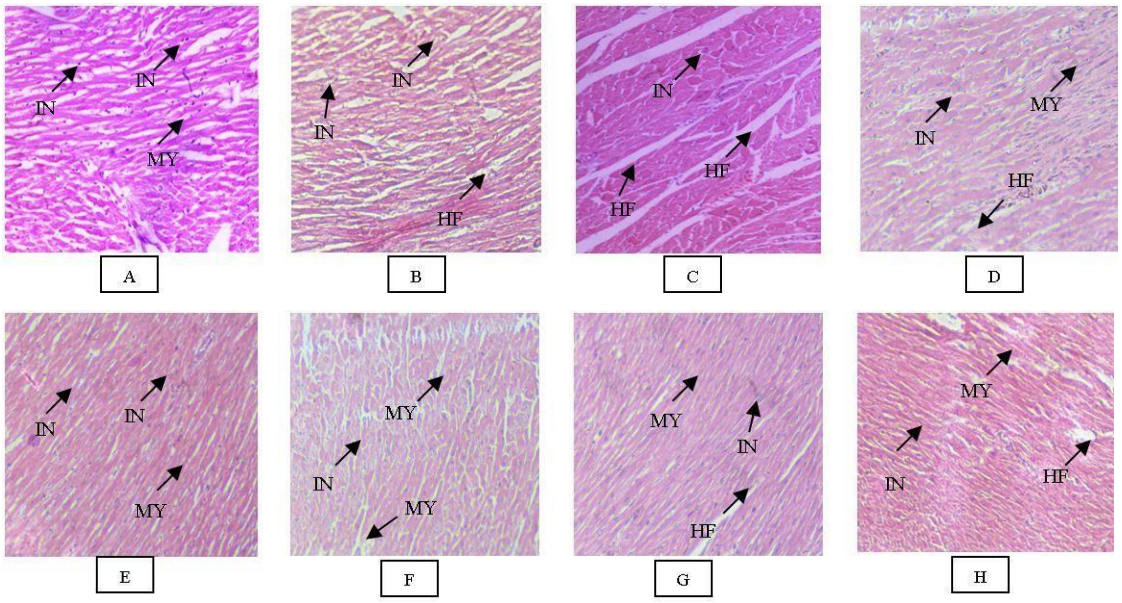

Figure 5.18: Effect of compound **(18)** and **(24)** on histopathological changes (heart) in UNX+DOCA salt induced hypertension in H&E staining. **(A)** NC **(B)** SC **(C)** UNX+DOCA **(D)** Compound (**18**-5mg/kg) **(E)** Compound (**18**-10mg/kg) **(F)** Compound (**24**-5mg/kg) **(G)** Compound (**24**-10mg/kg) **(H)** Los+tera. Sections were analysed under 20X magnification. MY= Myocytes, IN=Intact nucleus HF=Hypertrophic response.

The normal control group and Sham animals showed normal cardiomyocyte cell (MY) morphology indicated by regular cardiac myocytes arrangement including intact nucleus (IN) (Figure 5.18A). UNX+DOCA salt treatment inflicted damage to cardiac myocytes reflected by increased hypertrophic response (HF) (Figure 5.18B) which is indicated by the enlargement of the cardiac muscle size as an adaptation of the increased work of the heart to pump blood due to hypertension. In addition, tissue architecture was also disturbed in comparison to normal myocyte arrangement as observed in control animals. Figure 5.18 also suggests increased matrix deposition and disarranged myocytes with significant eosinophils accumulation. Treatment with novel dual receptor antagonists halt this damage by inhibiting hypertrophic response produced by RAAS and SNS. Both novel chemical entities **(18)** and **(24)** (Figure 5.18 E, G) at 10 mg/kg showed marked improvement, revealed by normal myocytes size and decrease of matrix component. This qualitative response is in accordance with observed elevated heart oedema index in DOCA salt uninephrectomized hypertensive rats.

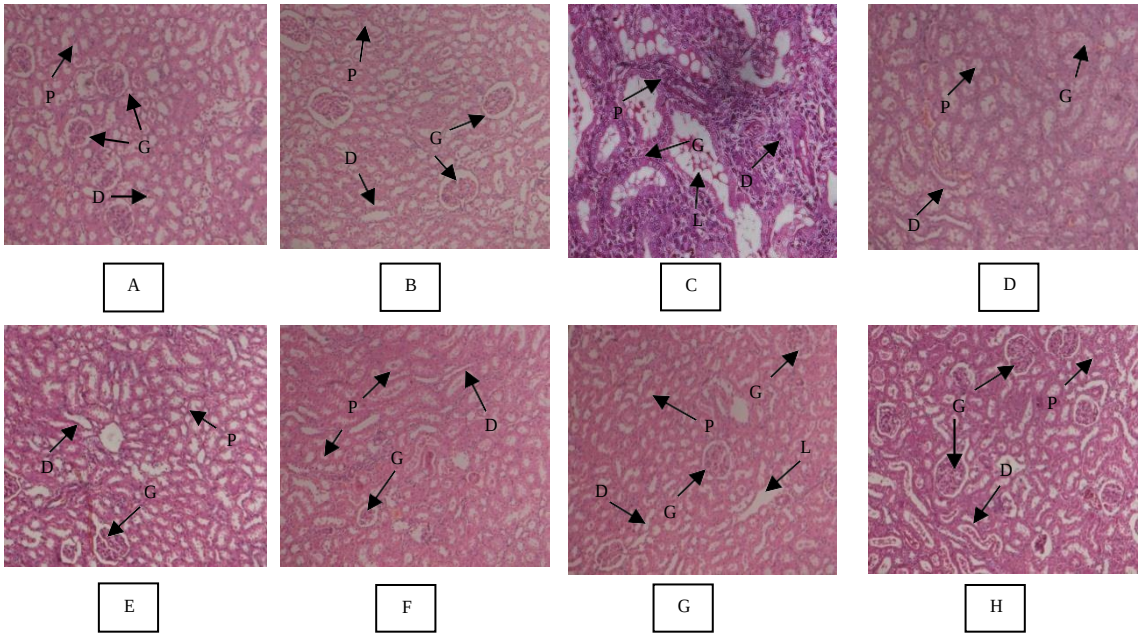

Figure 5.19: Effect of compound **(18)** and **(24)** on histopathological changes in kidney by UNX+DOCA salt induced hypertension in **H&E** staining. **(A)** NC **(B)** SC **(C)** UNX+DOCA **(D)** Compound (**18**-5mg/kg) **(E)** Compound (**18**-10mg/kg) **(F)** Compound (**24**-5mg/kg) **(G)** Compound (**24**-10mg/kg) **(H)** Los+tera. Sections were analysed under 20X magnification. G=Glomerulus, P=Proximal convoluted tubules (PCT), D= Distal convoluted tubules (DCT)

Unilateral nephrectomy and DOCA salt caused number of changes in the solitary kidney including tubular swelling, infiltration of inflammatory cells and matrix deposition in parenchyma compared to the normal architecture of glomeruli and tubules in the normal and sham control group (351). DOCA salt treatment also produced dilation of tubules, pretentious leakage, tubular nephritis with glomerulus damage as shown in Figure 5.19 (C). Our observations are in line with previous findings suggesting six weeks of DOCA salt treatment in UNX rats exhibited glomerulosclerosis, arterial wall thickening, and cloudy swelling of tubules, interstitial inflammation, and fibrosis compared to control rats. Treatment with compounds **(18)** and **(24)** prevented these pathological changes compared to hypertensive rats (Figure 5.19 D-H). Compound **(18)** treatment shows the reversal of tissue damage, however, at both the doses, mild presence of tubular nephritis is observed. Compound **(24)** showed better protection against DOCA salt treatment and both treatment group exhibited significant protection characterised by reduced tubular swelling, clear tubular DCT and PCT were observed. Treatment with compound **(24)** 10 mg/kg produced pronounced protection against DOCA salt induced kidney injury secondary to hypertension (Figure 5.19 F-G). ARB and ACE inhibitors are reported to prevent renal inflammatory

response in different models of hypertension such as 1K-1C, 2K-1C models. Combination of standard treatment also showed preventive response to glomeruli, but a thickening of the endothelial membrane was observed. Treatment with novel compounds showed decreasedrenal damage and intact glomeruli and no proteinous leakage as compared to the model control group in Figure 5.19 (C).

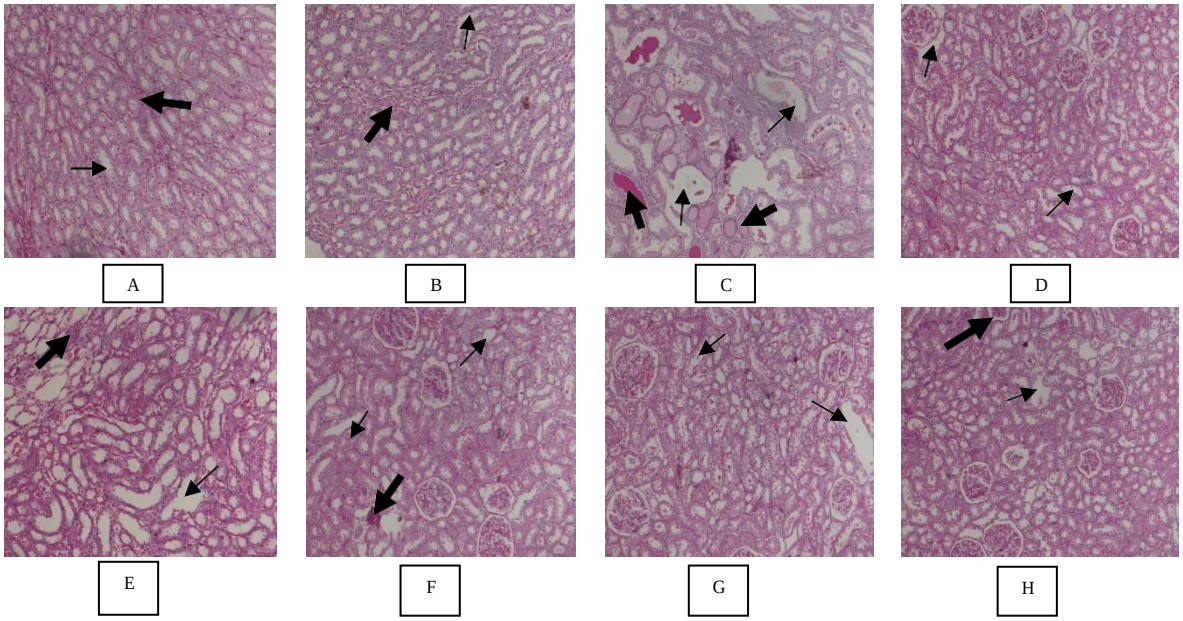

Figure 5.20: Effect of compound **(18)** and **(24)** on histopathological changes in kidney by UNX+DOCA salt induced hypertension by **PAS** staining. **(A)** NC **(B)** SC **(C)** UNX+DOCA **(D)** Compound (**18**-5mg/kg) **(E)** Compound (**18**-10mg/kg) **(F)** Compound (**24**-5mg/kg) **(G)** Compound (**24**-10mg/kg) **(H)** Los+tera. Sections were analysed under 20X magnification. Thick arrows showed presence of fluid accumulation in renal tubules while thin arrows indicate intratubular presence of polysaccharides.

The treatment with DOCA salt in uninephrectomized rats for six weeks resulted in significant kidney damage due to increased pressure exerted on the remaining kidney as shownin figure 5.20 (C). Periodic acid Schiff staining is a widely used staining procedure to detectthe presence of polysaccharides and glycolipids in the kidney. The treatment with DOCA salt +UNX caused accumulation of polysaccharides in distal convoluted tubules (indicated by thick arrows). It also showed marked presence of glycogen and mucin products stained as magenta color in renal medulla. Treatment with compound **(18)** and **(24)** significantly reduced the infiltration of complex carbohydrates into the kidney structure as evident by clear tubules and less presence of glycogen products as evident in figure 5.20 (D, E, F, G). Both compounds showed dose dependent protection against kidney damage. Compound

(24) at 10 mg/kg caused reversal of hypertensive damage inflicted by DOCA+UNX treatment.

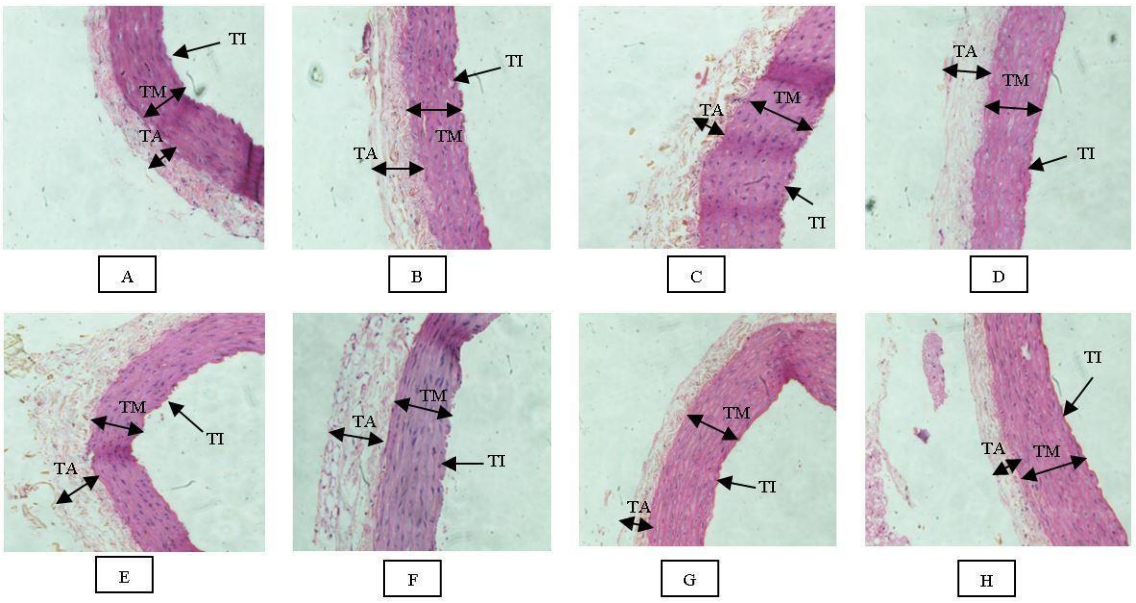

Figure 5.21: Effect of compound **(18)** and **(24)** on histopathological changes in aorta by UNX+DOCA salt induced hypertension in **H&E** staining **(A)** NC **(B)** SC **(C)** UNX+DOCA **(D)** Compound (**18**-5mg/kg) **(E)** Compound (**18**-10mg/kg) **(F)** Compound (**24**-5mg/kg) **(G)** Compound (**24**-10mg/kg) **(H)** Los+tera. Sections were analysed under 20X magnification.

Hypertension is associated with structural and functional alterations of blood vessels. Sustained hypertension induced by UNX+DOCA caused aortic remodeling characterized by increased medial thickness, smooth muscle cell layers, adventitial area and media/lumen ratio in hypertension. Role of collagen and elastin is believed to be adaptive factor in response to elevated blood pressure in conduit vessels, arterioles and veins (352). Basic histological differences in the composition of aorta from normal and hypertensive rats are highlighted by H&E staining. The figure 5.21 (A) revealed that the aorta of normal control rats showed no histological changes, while in model control rats, there were thickening of tunica media (TM) and alteration of tunica intima (TI), increased numbers of smooth muscle cells [figure 5.21(C)]. Treatment with compound **(18)** and **(24)** for six weeks in hypertensive rats ameliorated pathological changes in conduit vessels. The tunica media thickness (TM) and amount of necrotic smooth muscle cells were substantially reduced by the administration of NCEs at 10 mg/kg. The sham control group showed similar morphology as compared with the model control group [Figure 5.21(B)].

5.9 Evaluation of compound (18) and (24) in L-NAME induced hypertension

5.9.1 Effect of compound (18) and (24) on physiological parameters in L-NAME induced hypertension

Table 5.17: Effect of compound (18) and (24) on physiological parameters in L-NAME induced hypertension

Groups	Weight (gm)		Water intake (ml/rat)	Food intake (gm/rat)
	0^{th} day	28^{th} day		
NC	229.16±1.15	261.33±3.17	22.5±1.11	12.25±1.25
L-NAME(DC)	226±5.39	214.16±10.20	23.66±0.80	13.25±0.75
DC+ Compound **(18)** (5 mg/kg)	227.66±3.17	240.33±6.35	22.33±0.95	13.00±1.47
DC+ Compound **(18)** (10 mg/kg)	216.66±1.85	266.66±3.33	24.16±0.87	11.50±1.84
DC+ Compound **(24)** (5 mg/kg)	228.6±8.21	232.4±9.19	24.5±1.72	12.50±1.70
DC+ Compound **(24)** (10 mg/kg)	234.00±1.00	245.33±6.22	25.16±2.61	12.00±2.61
DC+Los+Tera	243.5±6.94	252.5±6.12	24.66±1.30	12.75±1.31

Values are expressed as mean±SEM (n=6). Data was analysed by one way ANOVA followed by Bonferroni's multiple comparison post hoc test.

There was no significant difference in weight observed at the initiation of the study amongst study groups. During 4 weeks period, study animals showed normal growth behavior and weight gain. L–NAME treated animals tend to show slight drop in weight however it was insignificant. Compound **(18)** (5 mg/kg & 10 mg/kg) showed comparatively increased body weights on 28^{th} day when compared with disease control (DC) group. Similarly, compound **(24)** (5 mg/kg & 10 mg/kg) also showed marked increase in body weights when compared to disease control (DC) group. Treatment with los + tera showed an increase in body weights of animals on 28^{th} day when compared with the disease control (DC) group.

On observing the water intake of study animals, it was seen that the L-NAME (DC) animals had a non-significant difference in water intake when compared to the normal control (NC) animals. The treatment groups exhibited similar water intake. The results have shown us that L–NAME administration either in DC rats or in treatment rats does not produce any effect on sodium ingestion or electrolyte imbalance resulted into volume independent form of hypertension.

5.9.2 Effect of compound (18) and (24) on hemodynamic parameters in L-NAME induced hypertension

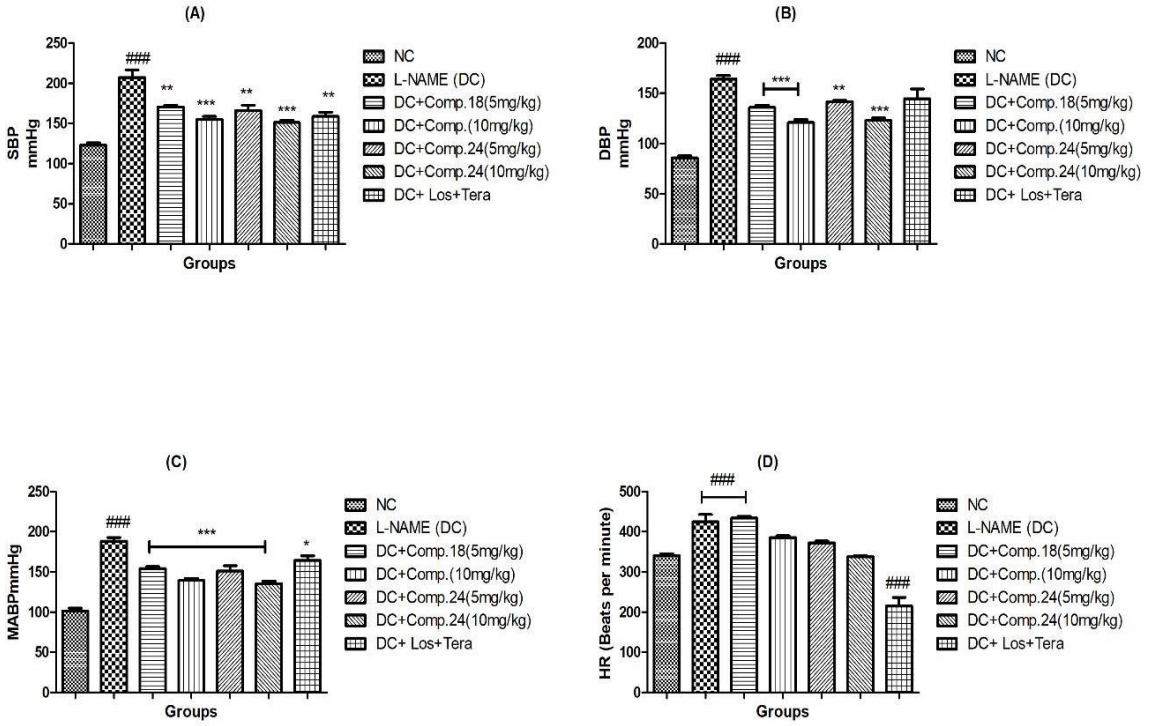

Figure 5.22: Effect of compound (18) and (24) on hemodynamic parameters in L-NAME induced hypertension. (A) SBP (B) DBP (C) MABP (D) Heart rate. Values are expressed as mean±SEM (n=6). Data was analysed by one way ANOVA followed by multiple comparison post hoc test. #= compared to sham control. *= compared to L-NAME. *=p<0.05, ##, **=p<0.01, ###,***=p<0.001 ns= non-significant. SBP= Systolic blood pressure, DBP=Diastolic blood pressure, MABP= Mean arterial blood pressure

Administration of L-NAME for 4 weeks resulted chronic rise in systolic blood pressure (NC vs. DC; 122.75±3.25 mmHg vs. 225.74±10.36mmHg; p<0.0001) compared to normal control animals. Treatment with compound **(18)** at 5 mg/kg (170.80±2.04 mmHg vs. 225.74±10.36 mmHg, p<0.001) and 10 mg/kg (154.91±3.95 mmHg vs. 225.74±10.36 mmHg, p<0.0001) resulted into significant fall in blood pressure by 24% and 31%, respectively. Compound **(18)** displayed dose dependent reduction in SBP, however, treatment with compound **(24)** also decreased SBP significantly in response to L-NAME after 4 weeks. Dose of 5 mg/kg (165.65±5.96 mmHg vs. 225.74±10.36 mmHg, p<0.001) and 10 mg/kg (151.24 mmHg± vs. 225.74±10.36mmHg, p<0.001) produced significant decrease in BP compared to DC rats. Both NCEs exhibited comparable potency regarding their blood pressure lowering effect. Combination of standard drugs also provide significant reduction (p<0.001) in blood pressure compared to DC animals.

Diastolic pressure was significantly reduced (85.63±2.08 mmHg vs. 164.18±1.23 mmHg; p<0.0001) in hypertensive rats as compared to normal rats. Both the compounds showed excellent action reducing raised diastolic pressure in dose dependent manner. Compound **(18)** at 5 mg/kg (135.96±1.73 mmHg vs.164.18±1.23 mmHg; p<0.0001) and 10 mg/kg also reduced elevated pressure significantly (120.83±3.89 mmHg vs. 164.18±1.23 mmHg; p<0.0001).

Administration of compound **(24)** also showed comparable protective action to compound **(18)** reflecting equal potency as depicted in figure 5.22. Both the doses of compound **(24)** produced significant reduction in DBP as compared to L-NAME treated rats. Treatment with combination of standard drugs failed to reduce DBP significantly (144.62±8.31 mmHg vs. 164.18±1.23 mmHg, p>0.05) compared to DC rats. These results demonstrate the superior action provided by DMLs compared to individual or combination therapy.

MABP is one of the unique and emphasized parameter for evaluation of antihypertensive action of drugs. Chronic inhibition of nitric oxide synthetase resulted into dramatic increase in MABP as evident in figure 5.22 (C). L-NAME administration cause significant elevation in MABP (101.85 ±2.95 mmHg vs. 188.51±4.55; p<.0001) compared to NC rats. Concomitant administration of compound **(18)** and **(24)** with L-NAME caused significant fall in MABP with compound **(24)** at 10 mg/kg (135.32±3.14 mmHg vs. 188.51±4.55 mmHg, p<0.0001) exhibited highest efficacy in reducing MABP. Combination of standard drugs produced significant drop in MABP (164.70±5.31 vs. 188.51±4.55 mmHg, p<0.05). However, both the compound displayed superior action compared to standard drugs as evenat the dose of 5 mg/kg, NCEs revealed excellent reduction in blood pressure.

The major function of endothelium is to provide platform for the release of myriad vasoconstrictive and vasodilatory chemicals resulted into maintenance of BP. Lokette et al. reported loss of endothelium dependent relaxation in arteries of hypertensive rats (353). Additionally, endothelial dysfunction is believed to be the key factor in pathogenesis of hypertension. Reduced NO level is observed even from the early stage of hypertension. Apart of dilatory effect, NO is critically involved in vascular resistance and growth. Several line of research utilized inhibition of nitric oxide synthase enzyme to produce chronic rise in blood pressure (354),(355). However, we found that widely utilized dose of L-NAME 40mg/kg and even higher doses via oral route did not produce hypertensive changes in study animals. Thus, obtained results encourage us to explore and optimize the dose of L-NAME via parental route. Administration of 15 mg/kg L-NAME via i.p. route resulted

into chronic and persistent rise in blood pressure. This model also emphasizes the role of increase in Ang II and SNS activity apart from nitric oxide deprivation. Reports have suggested that that cross talk of α_1 and AT_1 receptor in L-NAME induced hypertension via combination of losartan and prazosin provides significant improvement in hemodynamic alterations compared to inferior response produced by single drug treatment(356), (357). The above results with critical observation from literature enable us to put forward the therapeutic potential of novel compounds in chronic blockade of NO induced resistant form of hypertension (358).

5.9.3 Effect of compound (18) and (24) on articular reactivity in L-NAME induced hypertension

Table 5.18: Articular reactivity of compound (18) and (24) in L-NAME induced hypertension

Groups	ΔP (mmHg)		
	Phenylephrine	**Angiotensin II**	**Acetylcholine**
NC	30.5±2.17	66.56±1.38	-56.32±9.58
L-NAME (DC)	48.27±10.23	97.17±14.92$^{\#\#}$	-31.07±5.99$^{\#}$
DC+ Compound **(18)** (5 mg/kg)	34.79±2.61	100.17±10.29	-56.47±9.84
DC+ Compound **(18)** (10 mg/kg)	38.04±5.27	77.45±6.97	-65.74±3.20*
DC+ Compound **(24)** (5 mg/kg)	36.96±5.12	96.11±3.89	-52.33±5.06
DC+ Compound **(24)** (10 mg/kg)	40.65±3.03	68.64±2.55$^{\#}$	-71.05±10.15*
DC+Los+Tera	40.56±4.71	76.93±9.92	-57.27±8.62

ΔP= indicates the difference in blood pressure between before and after phenylephrine or Ang-II i.v. bolus. Bonferroni multiple comparison post hoc test. #= compared to NC. *= compared to DC. *=p<0.05, $^{\#\#}$, =p<0.01,

Articular activity was assessed by i.v bolus administration of vasoactive agents. Administration of 5 µg/kg phenylephrine produced increment in blood pressure however the rise observed was not as expected and hypertensive rats showed insignificant difference (p>0.05) compared to NC rats. Treatment with investigational compound **(18)** and **(24)** also did not produce significant difference compared to NC or DC rats. The plausible explanation for this observation is rapid metabolism of phenylephrine in *in-vivo* response. In contrast arterial strip showed enhanced contraction against α_1 agonist.

Ang II administration produce significant rise (NC vs. DC, p<0.001) in blood pressure in L-NAME treated rats. This observation is suggestive of upregulation of RAAS and AT_1 receptor. Animals treated with compound **(18)** and **(24)** abrogated the Ang II mediate dramatic rise in BP. Animals treated with only compound **(24)** at 10 mg/kg dose exhibited significant (Compound **(24)**-10mg/kg vs. DC; p<0.05) inhibition in pressor response.

Systemic chronic blockade of nitric oxide by L-NAME produced significant reduction in Ach mediated fall in blood pressure (359), (360). Treatment with both compounds at 10 mg/kg showed pronounced reversal of endothelial function revealed by significant improvement in Ach response. These are in accordance with nitric oxide level possibly due to increase p-Akt level which mediate eNOS induced NO synthesis.

5.9.4 Effect of compound (18) and (24) on hypertrophic response in L-NAME induced hypertension

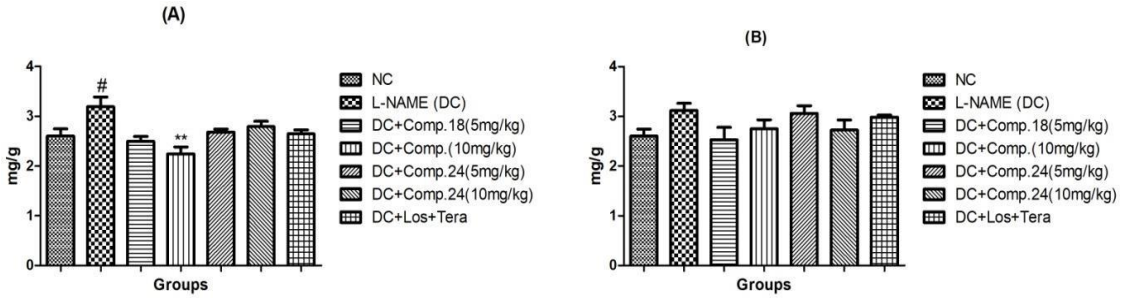

Figure 5.23: Effect of compound (18) and (24) on hypertrophic response in L-NAME induced hypertension (A) heart oedema index (B) kidney oedema index (KOI). Values are expressed as mean±SEM (n=6). Data was analysed by one way ANOVA followed by Bonferroni's post hoc test. #= compared to normal control. *= compared to L-NAME (DC). #,= p<0.05, ##, **=p<0.01

There was a significant increase in HW/BW in DC rats compared to NC rats after 4 weeks of L-NAME treatment (NC vs. DC; 2.60±0.14 vs 3.19±0.19; p<0.05) Treatment with Compound **(18)** (10 mg/kg) resulted into significant reduction in oedema index (DC vs. Compound (18-10mg/kg); 3.19±0.19 vs. 2.24±0.09; p<0.001). Treatment with compound **(18)** at both doses reduce HOI but only later dose showed significant difference compared to hypertensive rats.

Chronic rise in blood pressure directs myocardium towards the hypertrophic response initially. This is accompanied by increased myocardial size. However persistent elevated blood pressure and hypertrophic response tuned into maladaptive response which eventually leads to left ventricular hypertrophy and left ventricular ejection fraction.

Different hypertrophic stimuli are such as Ang II, endothelin and epinephrine. Our results also demonstrate the similar increase in cardiac mass which is significantly inhibited by receptor blockade produced by novel MTDL **(18)** and **(24)**, thus abolished hypertrophic response. On the other hand, we have observed that L-NAME administration caused slight increase in kidney oedema index however it was found to be non-significant compared to NC rats (2.60±0.14 vs. 3.19± 0.13, $p>0.05$). However, recent evidences of *in-vitro* and *in-vivo* studies suggested that decreased nitric oxide bioavailability act as a stimulus of renin release from collecting duct and activate RAAS system (361), (362). Other studies have reported the change in kidney mass after L-NAME administration (359). This discrepancy in the observations can be because of the dose and duration of L-NAME administration as L-NAME treatment was continued for eight weeks in reported studies(363), (364).

We have observed that, all treatment protocols with compound **(18)** and **(24)**, along with combination of standard drugs did not cause any change in KW/BW compared to NC or DC rats showed decrease KW/BW ratio however it was non-significant when evaluated statistically.

5.9.5 Effect of compound (18) and (24) on endothelial dysfunction and plasma nitric oxide level in L-NAME induced hypertension

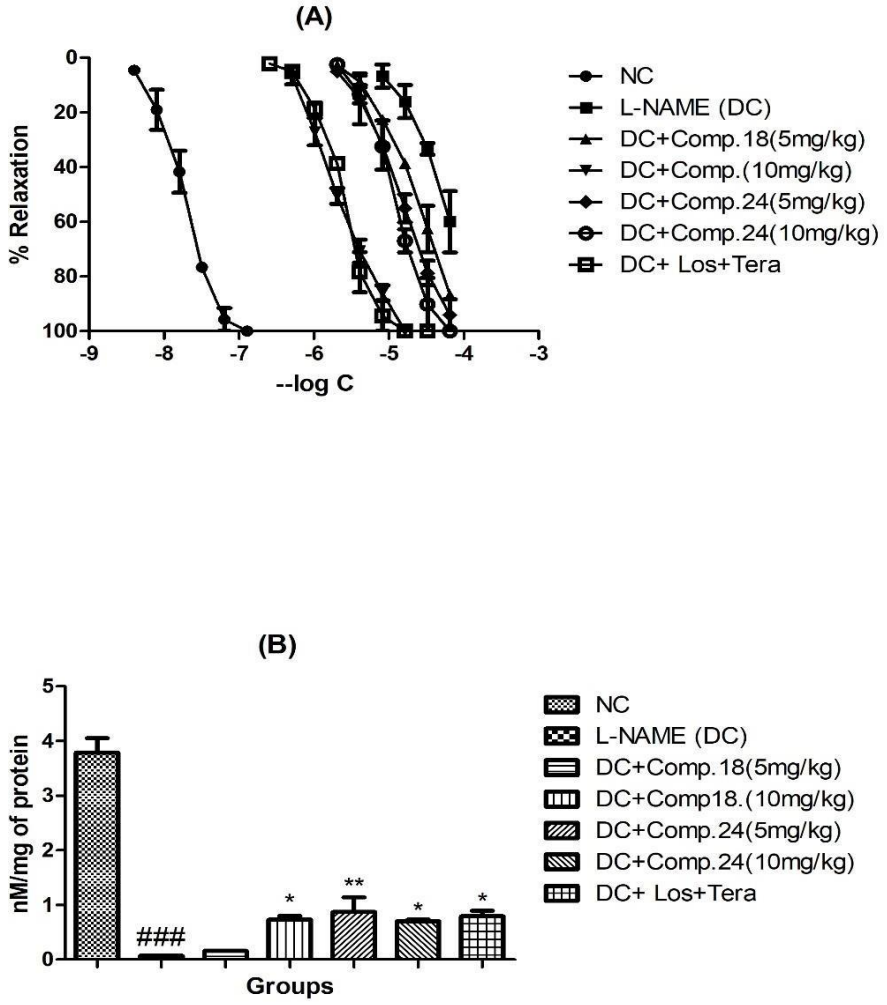

Figure 5.24: Effect of compound (18) and (24) on Endothelial dysfunction and Plasma nitric oxide level in L-NAME induced hypertension. Values are expressed as mean±SEM (n=6). Data was analysed by non-linear regression variable slope and one way ANOVA followed by Bonferroni's multiple comparison post hoc test. #= compared to normal control. *= compared to L-NAME-. *=p<0.05, **=p<0.01, ###,***=p<0.001 ns= non-significant.

L-NAME administration for 4 weeks resulted into significant fall in nitric oxide level (p<0.0001) as compared to normal control animals (365). Aorta from hypertensive rats exhibited poor relaxation against PE by Ach. There was distinct rightward shift observed in hypertensive rats with high EC_{50} for Ach (NC vs. DC, 0.0175µM vs. 59.74µM). These observations are in correlation with increased shear stress and poor NO bioavailability resulted into endothelial dysfunction. It is also noteworthy that contractile response of aorta from hypertensive rats showed more pronounced response for longer period of time. This

observation also led us to the discovery of upregulation of α_1 receptor is L-NAME treated rats.

Treatment with compound **(18)** and **(24)** at 5 mg/kg dose did not improve the endothelial relaxation induced by Ach suggestive of potent damage to endothelium, however at the dose of 10 mg/kg both the compounds revived the Ach mediated vasodilator response. Compound **(18)** ($p<0.05$ vs DC) improved the level of NO mildly but significantly compared to hypertensive rats. Here it is important to note that compound **(24)** ($p<0.001$ vs DC) exhibited superior response compared to endothelium when utilized in incremental manner which led us to speculation that compound might possess vasodilator activity. Combined data of blood pressure we can put forward that concomitant administration of compound **(18)** and **(24)** with L-NAME was able to ameliorate blood pressure changes and improved vascular hemostasis.

5.9.6 Effect of compound (18) and (24) on cytokines level in L-NAME induced hypertension

Table 5.19: Effect of compound (18) and (24) on cytokines level in L-NAME induced hypertension

Group	IL-6 (pg/ml)	TNF-α (pg/ml)	PRA (ng/ml)	NF-kβ (ng/ml)
NC	1251 ± 30.41	269.40±13.81	6.01±0.24	5.81±1.93
L-NAME (DC)	1622.66±101.33$^{\#\#}$	623.90±7.69$^{\#\#\#}$	8.09±0.26$^{\#\#}$	8.45±1.84
DC+ Compound **(18)** (5mg/kg)	1494.33±3.33^{ns}	359.23±4.34***	5.17±0.23$^{\$\$\$}$	5.53±2.30^{ns}
DC+ Compound **(18)** (10mg/kg)	996.00±17.32***	223.90±2.59***	5.78±0.34***	5.76±2.25
DC+ Compound **(24)** (5mg/kg)	1387.66±18.78	593.56±9.77	5.18±0.14***	5.76±2.25
DC+ Compound **(24)** (10mg/kg)	827.66±41.76***	359.40±7.65***	4.37±0.39***	3.56±0.19
DC+Los+Tera	1166.0±30.55***	208.06±10.99***	5.17±0.23***	4.50±1.19

Values are expressed as mean±SEM (n=6). Data was analysed by non-linear regression and one way ANOVA followed by Bonferroni's multiple comparison post hoc test. #= compared to sham control. *= compared to L-NAME. *=p<0.05, ##, **=p<0.01, ###,***=p<0.001 ns= non-significant

L-NAME treatment showed significant ($p<0.001$ vs NC) increase in IL-6 levels compared to normal control (NC) animals as per the previous reports (366). Treatment with compound **(18)** at 5 mg/kg group showed non-significant depletion in IL-6 levels when compared to L-NAME treated (DC) group. A significant change ($P<0.001$) was observed between the compound **(18)** (10 mg/kg) group and L-NAME treated group. Compound **(24)** (5 mg/kg) group showed non-significant decrease in IL-6 levels when compared to disease control (DC) animals. Compound **(24)** (10 mg/kg) showed a significant decrease in IL-6 levels when compared to L-NAME (DC) treated animals. Standard (Los + Tera) treatment showed significant ($P<0.001$) decrease in IL-6 levels compared to L-NAME treated group (DC).

Chronic inhibition of nitric oxide provoked significant ($p<0.001$) increase in TNF-α levels compared to normal control (NC) rats. Treatment with compound **(18)** (5 mg/kg & 10 mg/kg) groups showed significant ($p<0.001$) depletion in TNF-α levels when compared to L-NAME treated (DC) groups. Treatment with compound **(24)** (5 mg/kg & 10 mg/kg) groups showed significant (5 mg/kg & 10 mg/kg vs. DC, $p<0.001$, $p<0.001$ respectively) depletion in TNF-α levels when compared to L-NAME treated (DC) groups. Standard treatment significantly ($p<0.001$) decreased TNF-α levels compared to L-NAME treated rats.

L-NAME treatment showed a significant ($p<0.001$) increase in plasma renin levels compared to normal untreated rats. Compound **(18)** (5 mg/kg & 10mg/kg) group displayed significant ($p<0.001$) decrease in plasma renin levels when compared to L-NAME (DC) treated rats. Treatment with compound **(24)** (5 mg/kg & 10mg/kg) groups showed a significant ($P<0.001$) decrease in plasma renin levels when compared to L-NAME treated hypertensive rats. Standard treatment showed significantly ($p<0.001$) decreased plasma renin levels compared to L-NAME treated hypertensive rats.

L-NAME treatment showed a non-significant decrease in NF-kβ levels compared to normal untreated (NC) rats. Treatment with compound **(18)** (5 mg/kg & 10 mg/kg) groups showed a non-significant decrease in NF-kβ levels when compared to L-NAME treated (DC) hypertensive rats. Treatment with compound **(24)** (5 mg/kg & 10mg/kg) groups showed a non-significant decrease in NF-kβ levels when compared to L-NAME treated hypertensive rats. Standard (Los + Tera) treatment showed non-significant decrease in NF-kβ levels compared to L-NAME treated hypertensive rats.

5.9.7 Effect of compound (18) and (24) on urinary indices in L-NAME induced hypertension

Table 5.20: Effect of compound (18) and (24) on urinary indices in L-NAME induced hypertension

Group	Urine output (ml)	Sodium (µmol/l/day)	Potassium (µmol/l/day)	Uric acid (µmol/l/day)	Albumin (ng/ml/day)
NC	18.33±2.51	344.08±14.17	226.53±26.78	226.53±26.78	12.08±0.43
L-NAME(DC)	17.33 ± 3.21^{ns}	348.98 ± 5.84^{ns}	264.49 ± 50.95^{ns}	245.51 ± 31.33^{ns}	$24.81\pm2.41^{\#\#}$
DC+ Compound (18) (5mg/kg)	15.16 ± 2.25^{ns}	338.36 ± 10.50^{ns}	337.89 ± 45.55^{ns}	264.49 ± 50.95^{ns}	$15.49\pm1.65^{*}$
DC+ Compound (18) (10mg/kg)	16.00 ± 2.64^{ns}	333.32 ± 24.30^{ns}	278.41 ± 50.47^{ns}	337.89 ± 45.55^{ns}	$13.67\pm2.72^{**}$
DC+ Compound (24) (5mg/kg)	15.33 ± 3.21^{ns}	335.71 ± 13.18^{ns}	307.52 ± 11.59^{ns}	278.41 ± 50.47^{ns}	18.28 ± 0.84^{ns}
DC+ Compound (24) (10 mg/kg)	17.66 ± 3.05^{ns}	364.69 ± 26.54^{ns}	275.88 ± 29.92^{ns}	284.74 ± 24.40^{ns}	$12.82\pm4.00^{**}$
DC+Los+Tera	15.16 ± 2.46^{ns}	348.36 ± 6.45^{ns}	284.74 ± 24.40^{ns}	307.52 ± 11.59^{ns}	16.82 ± 0.84^{ns}

Values are expressed as mean±SEM (n=6). Data was analysed by non-linear regression and one way ANOVA followed by Bonferroni's multiple comparison post hoc test. #= compared to sham control. *= compared to L-NAME *=p<0.05, ##, **=p<0.01, ns= non-significant

L-NAME administration did not produce any significant change in urinary excretion volume, handling of electrolytes such sodium and potassium and creatinine (367). On the contrary, many studies have reported disturbed urinary profile upon chronic administration of L-NAME. L-NAME (DC) treated rats showed a non-significant decrease in urine output compared to normal control (NC) group. Compound **(18)** (5 mg/kg & 10 mg/kg) group showed non-significant decrease in urine output when compared to L-NAME (DC) treated rats. Compound **(24)** (10 mg/kg) treatment showed non-significant increase in urine output whereas compound **(24)** (5 mg/kg) showed non-significant decrease in urine output when compared to L-NAME (DC) animals. Los + Tera showed non-significant decrease in urine output when compared to L-NAME (DC) animals.

L-NAME (DC) treatment showed a non-significant increase in Urinary sodium levels when compared to Normal control (NC) animals. Treatment with compound **(18)** (10mg/kg& 5 mg/kg) showed a non-significant decrease in sodium when compared to L-NAME (DC) treated group. Compound **(24)** (10 mg/kg & 5 mg/kg) treatment showed non-significant increase and decrease in sodium levels when compared to L-NAME (DC) animals. Treatment with losartan + terazosin (DC+ Los + Tera) showed a similar pattern in sodium levels when compared with L-NAME (DC) group.

L-NAME (DC) treatment showed a non-significant decrease in potassium levels when compared to Normal control (NC) animals. Treatment with compound **(18)** (5mg/kg) showed a better non-significant increase in potassium when compared to compound **(18)** at 10 mg/kg. Treatment with compound **(24)** at 5 mg/kg & 10mg/kg showed non-significant increase in potassium levels when compared to L-NAME (DC) animals. There was a non-significant increase in the potassium levels when losartan + terazosin (DC + Los + Tera) was compared with L-NAME (DC) group.

L-NAME (DC) treatment showed a non-significant increase in urinary uric acid compared to Normal control (NC) group. Compound **(18)** (5 mg/kg & 10 mg/kg) group showed non-significant increase in urinary uric acid when compared to L-NAME (DC) treated rats. Compound **(24)** (5 mg/kg & 10 mg/kg) treatment had non-significant effect on increasing the uric acid levels when compared to L-NAME (DC) animals. On treatment with standard combination (Los + Tera), there was non-significant increase in urine uric acid levels seen when compared to L-NAME (DC) animals.

The L-NAME (DC) treatment group showed a significant increase in albumin levels compared to normal control (NC). Compound **(18)** (5 mg/kg & 10 mg/kg) group showed

significant decrease in albumin levels when compared to L-NAME (DC) treated rats. Compound **(24)** at 5 mg/kg treatment showed non-significant effect on decreasing the albumin levels when compared to L-NAME (DC) animals. While treatment of compound **(24)** at 10 mg/kg showed significant decrease in albumin levels when compared to disease control (DC) group. Los + tera showed non-significant decrease in albumin levels when compared to L-NAME (DC) animals.

Different groups have reported the change in urine profile with chronic L-NAME treatment. However, contrary to that we did not observe natriuresis, kaluria and other urine abnormalities in L-NAME treated rats.

5.9.8 Effect on compound (18) and (24) on oxidative stress parameters in heart of L-NAME induced hypertension

5.9.8.1 Effect on compound (18) and (24) on oxidative stress parameters in heart of L-NAME induced hypertension

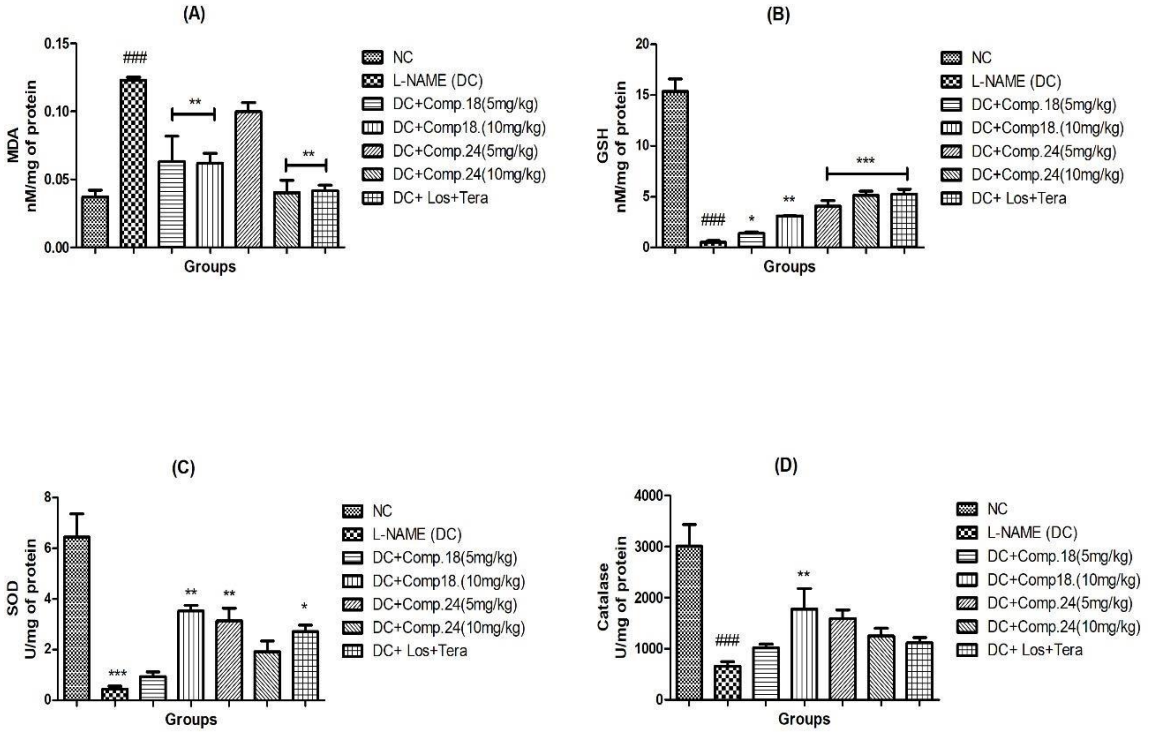

Figure 5.25: Effect of compound (18) and (24) on oxidative stress parameters in heart of L-NAME induced hypertension. (A) MDA (B) GSH (C) SOD (D) Catalase. Values are expressed as mean±SEM (n=6). Data was analysed by one way ANOVA followed by Bonferroni's multiple comparison post hoc test. #= compare to sham control. *= compared to L-NAME-. *=p<0.05, **=p<0.01, ###, ***=p<0.001 ns= non-significant.

Different studies have highlighted excessive amounts of ROS in essential hypertensive patients and various animal models of hypertension (368),(369). Chronic rise in blood pressure produced vascular $O_2^{\bullet-}$ generation which rapidly reacts with NO to produce peroxynitrite ($ONOO^-$) resulting in impaired NO bioavailability. In L-NAME hypertensive rats, positive correlation has been studied with increases in the level of plasma MDA and vascular $O_2^{\bullet-}$ with elevated SBP.

L- NAME treatment resulted into imbalance in redox system revealed by significant increase in MDA content ($p<0.0001$) and pronounces decrease in GSH, catalase and SOD content ($p<0.0001$). Treatment of compound **(18)** (5 mg/kg and 10 mg/kg) provided protective action against MDA reduction and GSH elevation against L-NAME hypertensive rats. SOD and catalase were also increased significantly after of compound **(18)** and **(24)** at 10 mg/kg for 28 days. Combination of standard drugs also provided comparable effect against MDA, GSH, SOD level, however, catalase level was not improved by los+tera against oxidative stress insult caused by L-NAME as depicted in figure 5.25.

5.9.8.2 Effect of compound (18) and (24) on oxidative stress parameters in kidney of L-NAME induced hypertension

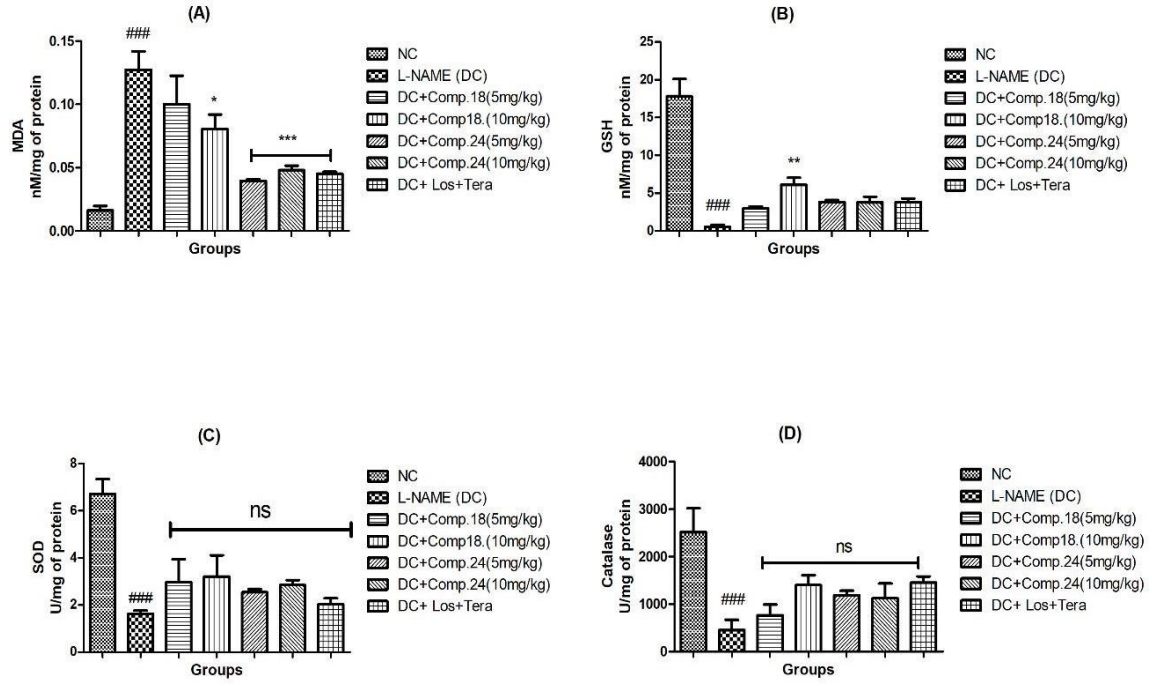

Figure 5.26: Effect of compound (18) and (24) on oxidative stress parameters in kidney of L-NAME induced hypertension. (A)MDA (B) GSH (C) SOD (D) Catalase. Values are expressed as mean±SEM

(n=6). Data was analysed by one way ANOVA followed by Bonferroni's multiple comparison hoc test. #= compared to sham control. *= compared to L-NAME-. *=p<0.05, **=p<0.01, ###,***=p<0.001 ns= non-significant.

L-NAME induced inhibition produce detrimental changes in kidney redox defense evident by significant increase in MDA and reduced GSH, catalase and SOD level. Treatment with compound **(18)** and **(24)** showed mild improvement in parameters as evident in figure 5.26. SOD and catalase levels remain unaltered after 4 weeks of antihypertensive agent in kidney homogenates.

5.9.9 Effect of compound (18) and (24) on histopathological changes in L-NAME induced hypertension

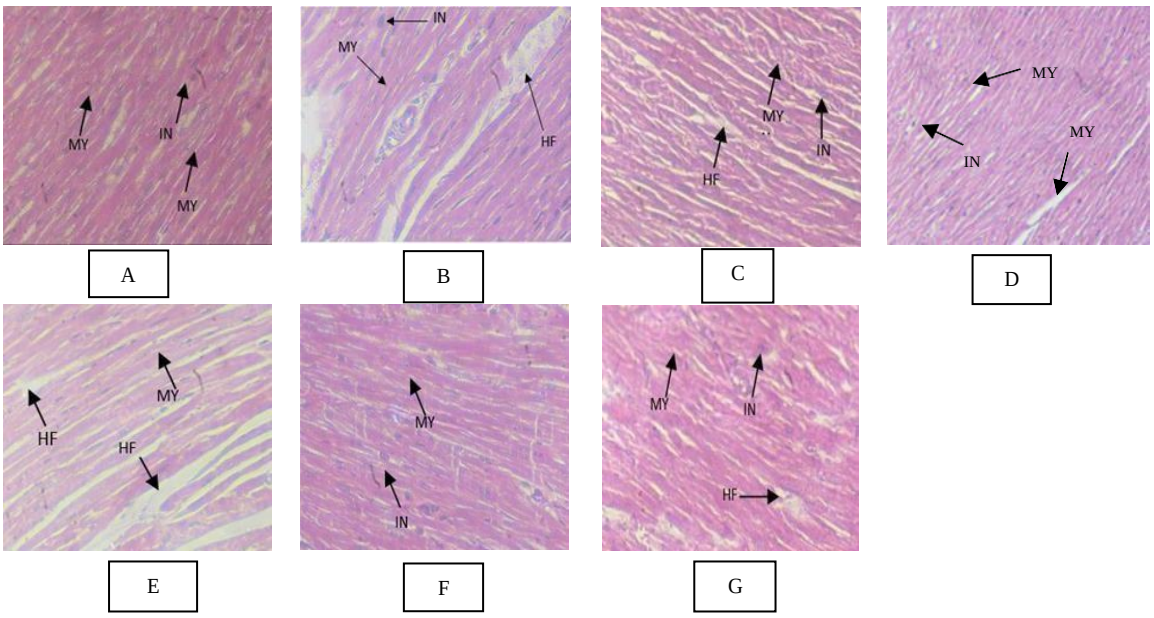

Figure 5.27: Effect of compound **(18)** and **(24)** on histopathological changes in heart by L-NAME induced hypertension in **H&E** staining. **(A)** NC **(B)** L-NAME **(C)** Compound (**18**-5 mg/kg) **(D)** Compound (**18**-10 mg/kg) **(E)** Compound (**24**-5 mg/kg) **(F)** Compound (**24**-10 mg/kg) **(G)** Los+tera. Sections were analysed under 20X magnification.

Treatment with L-NAME caused structural alteration in heart as observed in figure 5.27 (B). The figure suggests that L-NAME treatment produced significant hypertrophy of myocytes, increased matrix deposition and disarranged cardiac myocytes. On the contrary, figure 5.27 (A) showed histopathology of normal heart marked by absence of hypertrophic response and regulated myocytes arrangement. Treatment with compound **(18)** at 5 mg/kg showed mild improvement while at 10 mg/kg showed reversal of hypertrophic response as

evident by figure 5.27 (C, D). Treatment with compound **(24)** at 5 mg/kg did not show marked improvement against L-NAME induced tissue damage while 10 mg/kg showed restoration of normal myocardial architecture and decreased hypertrophic response. Treatment with standard drugs showed decreased hypertrophic response but presence of tissue architectural damage was still observed.

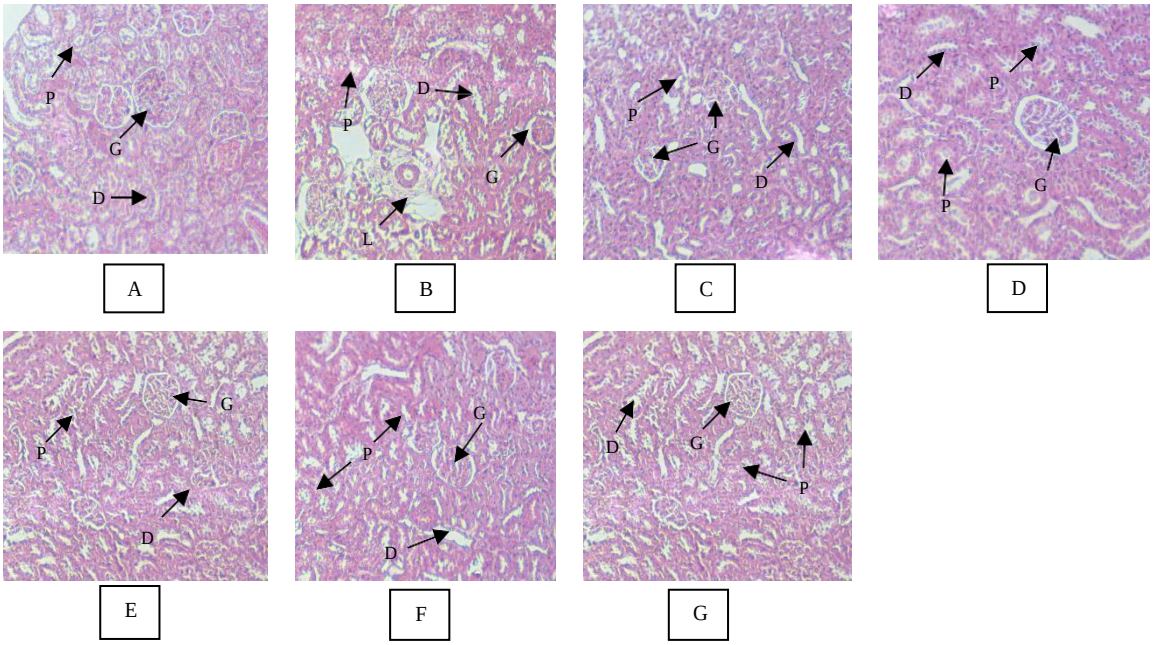

Figure 5.28: Effect of compound **(18)** and **(24)** on histopathological changes in kidney by L-NAME induced hypertension in **H&E** staining. **(A)** NC **(B)** L-NAME **(C)** Compound (**18**-5 mg/kg) **(D)** Compound (**18**-10 mg/kg) **(E)** Compound (**24**-5 mg/kg) **(F)** Compound (**24**-10 mg/kg) **(G)** Los+tera. Sections were analysed under 20X magnification.

Kidney of L-NAME treated rats exhibited marked tissue damage evident by disruption of glomeruli and renal medulla while kidney from normal rats displayed normal glomeruli and presence of distal and proximal convoluted tubules (figure 5.28A). Number of glomeruli were also diminished in L-NAME treated group (figure 5.28B). Treatment with compound **(18)** resulted into marked improvement in histological feature of kidney as displayed in figure 5.28 C, D. Treatment with 5 mg/kg showed low degree of inflammation and matrix deposition by tissue architecture damage while treatment with 10 mg/kg dose revealed significant improvement in histological feature marked by well characterised glomeruli and renal tubules (Figure 5.28E). Treatment with compound **(24)** at 5 mg/kg and 10 mg/kg was also able to ameliorate tissue damage caused by L-NAME treatment. Standard treatment also revealed marked improvement in tissue architecture after L-NAME treatment.

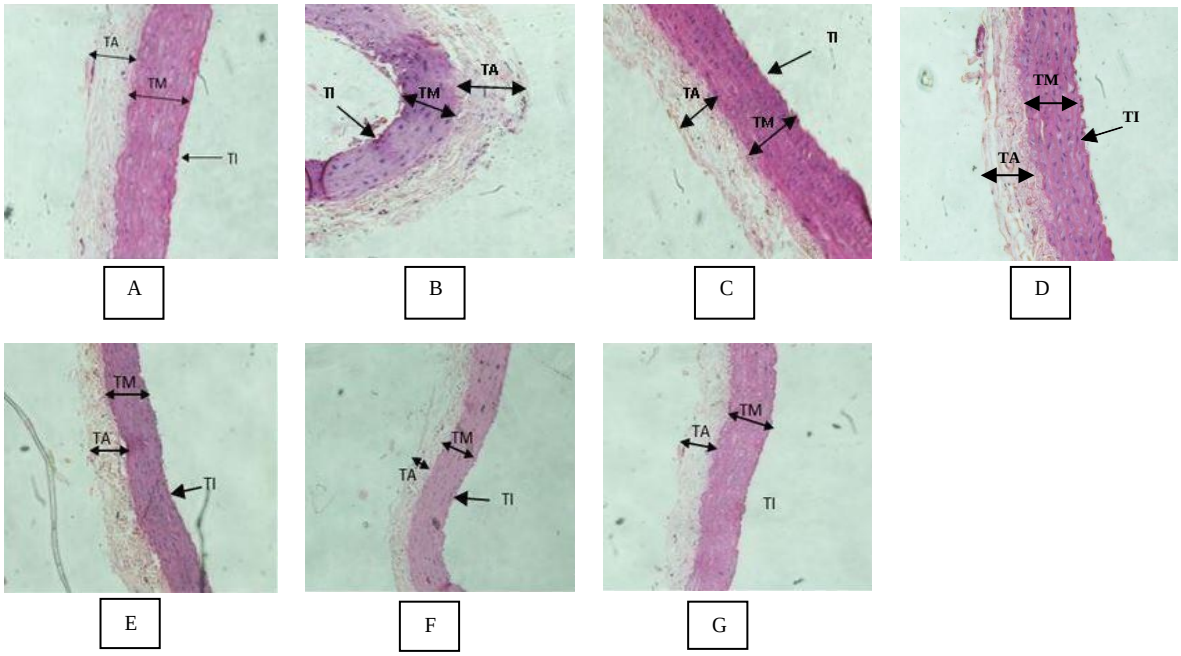

Figure 5.29: Effect of compound **(18)** and **(24)** on histopathological changes in aorta by L-NAME induced hypertension in **H&E** staining. **(A)** NC **(B)** L-NAME **(C)** Compound (**18**-5 mg/kg) **(D)** Compound (**18**-10 mg/kg) **(E)** Compound (**24**-5 mg/kg) **(F)** Compound (**24**-10 mg/kg) **(G)** Los+tera. Sections were analysed under 20X magnification.

Aorta from normal rats showed well defined layers of tunica media and tunica adventitia with thin prominent tunica intima as evident by figure 5.29 (A). Treatment with L-NAME produced disruption of tunica adventitia with presence of inflammatory cells in tunica media region (Figure 5.29B). Treatment with 5 mg/kg and 10 mg/kg of compound **(18)** produced improvement in histological features of aorta whereas aorta from 10 mg/kg dose treated rats showed similar histology to normal control rats. Compound **(24)** also provides significant damage caused by diminished nitric oxide level compared to L-NAME treated rats (figure 5.29 E, F). Combination of standard drugs also revealed significant improvement against L-NAME induced aortic remodeling.

5.10 Evaluation of compound (18) and (24) in cardiometabolic disorders in rats

5.10.1 *In-silico* study of compound (18) and (24) with targets of CMets

In-silico study studies such as docking and molecular dynamics study provides comprehensive insights regarding the putative binding and interactions of ligands for particular protein target. The most promising compounds compound **(18)** and **(24)** were docked with Dipeptidylpeptidase-IV (DPP4) enzyme (PDB code: 6B1E) and Peroxisome Proliferator Activated Receptor (PPARγ) (PDB code: 7AWC), two very important targets of CMets. Utilization of these two targets have been well documented for diabetes and other metabolic conditions.

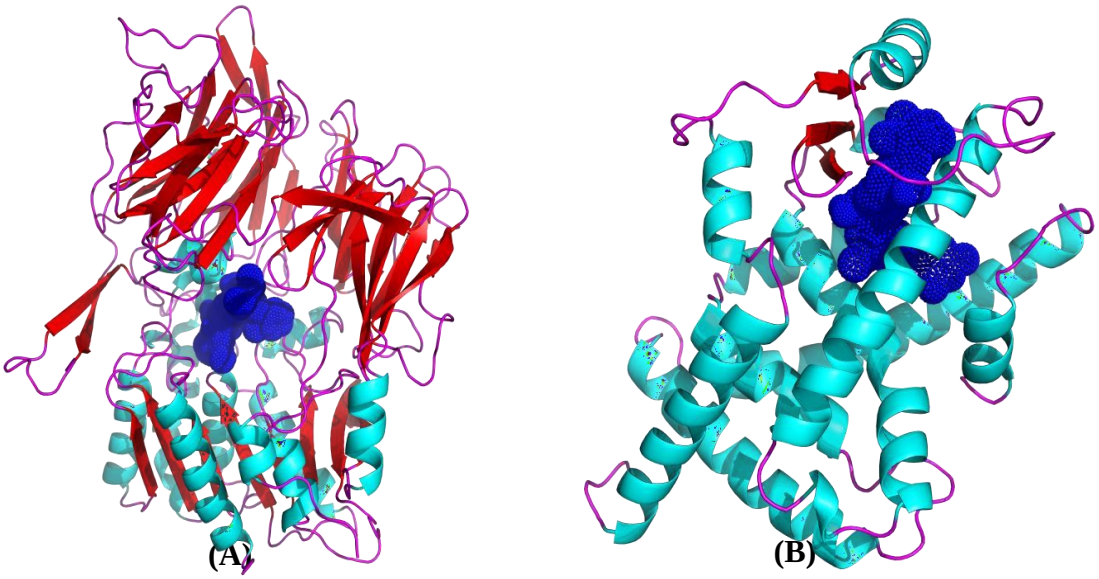

(A) **(B)**

Figure 5.30: Binding site of molecules on (A) DPP4- overlapping of compound **(18)** and **(24)** with structure of DPP4 with vildagliptin and (B) PPARγ- overlapping of compound **(18)** and **(24)** with structure of PPARγ with Rosiglitazone. Ligands are shown in deep blue color.

5.10.1.1 *In-silico* study of compound (18) and (24) with DPP4 enzyme

Molecular docking was performed to get the deeper insight of the binding site of the molecules along with interactions. Both the ligands showed excellent binding score. In case of the DPP4 protein, compound **(18)** and **(24)** exhibited the glide score of -6.966 and -7.554, respectively, whereas co-crystallized reference with vildagliptin exhibited the score of -7.724. Binding site of the test molecules and standard drug with DPP4 protein is shown

in the figure 5.30 (A). Blue dotted areas showed the binding of compound **(18), (24)** and vildagliptin in same ligand binding domain (LBD) in the pocket.

2D interactions of the molecule with the receptor were given in figure 5.31. Here, H-bond is only shown as AUTODCOK VINA only showed H-bond interactions in 2D images. As depicted in figure 5.31 (A), 4-NH_2 group on quinazoline scaffold in compound **(18)** formed the H bond with Ser209 with bond length of 2.93 Å while another H bond interactions is observed by –CN group with Tyr 547 with 3.17Å bond length. Interestingly these both residues form the hydrogen bond with the co-crystallized ligand (standard drug-Vildagliptin) as well. Here, it was also observed that quaternary nitrogen of piperazine interacts with Glu205 by salt bridge (not shown in image).

Compound **(24)** exhibited excellent interactions with the LBD of DPP4 enzyme. Oxygen of methoxy group at 6th position in quinazoline ring formed the H-bond with Tyr 631 residue with the distance of 2.93 Å. While nitrogen of 4-NH_2 group in quinazoline ring formed H bond with Gly206 with 3.27 Å bond length [Figure 5.31 (B)]. Apart from these strong favourable interactions, other noteworthy interactions were also observed. Quinazoline scaffold showed pi-pi stacking Phe357 residue and 2-methylbenzene with Tyr666 (not shown in image).

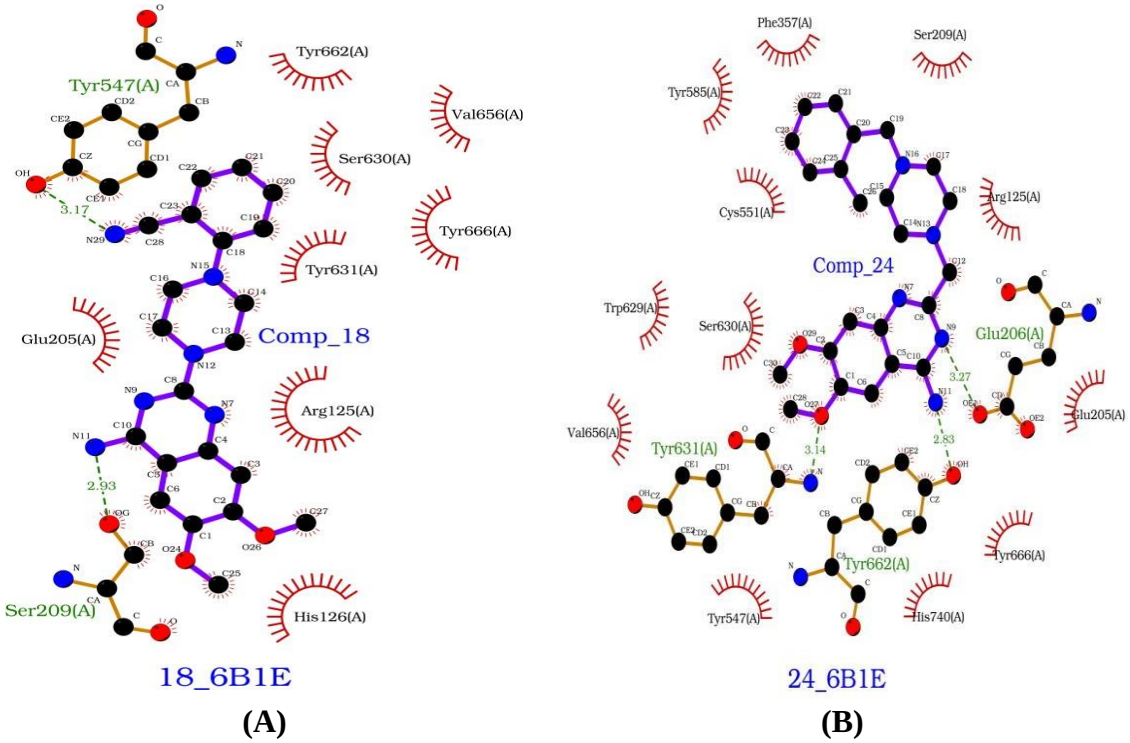

Figure 5.31: Interactions of (A) compound **(18)** and (B) compound **(24)** with the DPP4. Hydrogen bonds are shown in green with donor-acceptor distance.

5.10.1.2 *In-silico* study of compound (18) and (24) with PPARγ receptor

Figure 5.32 depicts the binding site of ligands within the pocket of PPARγ (PDB code: 7AWC). Blue dotted area showed the superimposed region of two newly synthesized compounds with rosiglitazone in LBD of PPARγ. In the case of PPARγ very similar interaction pattern is observed through docking. 7AWC had a co-crystallized ligand, rosiglitazone which was used as the reference molecule. The binding site of molecules on the PPARγ is shown in figure 5.30 (B). Rosiglitazone shows many non-bonded interactions withmultiple amino acids of PPARγ, similar pattern can be seen in compound **(24)**. Compound **(18)** strongly interacted with Leu340 via H- bond with 2.73 Å distance and with Ser342 residue with 2.98 Å [Figure 5.32 (A)].

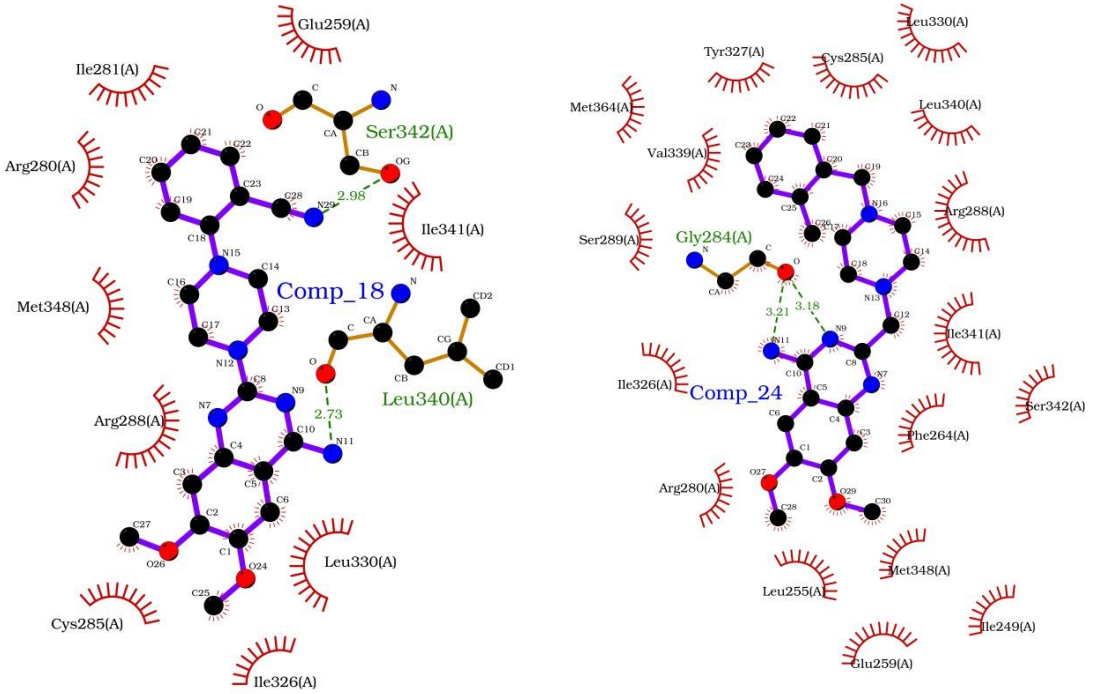

Figure 5.32: Interactions of (A) compound **(18)** and (B) compound **(24)** with the PPARγ. Hydrogen bonds are shown in green colour with donor-acceptor distance.

In case of compound **(24)**, nitrogen at 9th position in quinazoline ring formed H-bond with Gly284 with 3.18 Å, while nitrogen of 4-amino group interacted with Gy284 by H-bond 3.21 Å interacts with Gly284 by forming two hydrogen bonds. 2D interactions diagram of compound **(24)** were given in figure 5.32 (B). Amino acid residue like Cys285, Arg288, Ile326, Leu330, and Ile341 were interacting with both ligands (image not shown).

5.11 Evaluation of compound (18) and (24) in 20 % fructose induced cardiometabolic disorders in rats

There has been an epidemic increase in CMets as a result of hypercaloric diet (HD) intake and sedentary habits. Both obesity and overweight are conditions associated with metabolic dysfunction, decreased insulin sensitivity and diabetes. On the other hand, insulin resistance (IR) is known to be a key factor for the development of vascular damage such as endothelial dysfunction and impaired vascular relaxation (370).

The metabolic syndrome (MS), characterized by the clustering of hypertension, insulin resistance, and dyslipidemia are common risk factors for cardiovascular disease and type-2 diabetes. To achieve optimal prevention of cardiovascular outcomes in hypertensive patients, a multi-factorial approach is required, combining lifestyle modification, blood pressure lowering, and control of hyperglycemia and dyslipidemia.

Both renin angiotensin system (RAS) and adrenergic system play a critical role in the control of physiological and pathological cardiorenal functions (371). Indeed, Ang II induced vasoconstriction and remodeling through AT_1R has been involved in the pathogenesis of diabetic vascular dysfunction. In addition recent research highlighted the role of cross talk of α_1/AT_1 receptor in obesity and diabetes (372),(373).

Additionally, damage produced by metabolic disturbances can change adrenergic or Ang II receptors functionality, increasing the crosstalk between α_1 and AT_1 receptors (374). Indeed, an increased α_1/AT_1 crosstalk has been proposed as an early damage indicator of metabolic disturbances (374)

Long-term high fructose consumption is known to induce hyperglycemia, hypertriacylglycerolemia, insulin resistance and hypertension in the rats (375), (376). The potential mechanism proposed by which hyperinsulinemia causes hypertension and other metabolic disturbances are believed to be Na^+ retention, sympathetic nerve activation and activation of RAAS system accompanied by endothelial dysfunction and inflammation(377),(378).

5.11.1 Effect of compound (18) and (24) on physiological parameters in 20% fructose induced CMets

Table 5.21: Effect of compound (18) and (24) on physiological parameters in 20% fructose induced CMets

Groups	Weight (gm)		Water intake (ml/rat)	Food intake (gm/rat)
	0^{th} day	60^{th} day		
Normal Control (NC)	185.33±3.71	227 ±4.7	26±0.9	11.66±0.88
20% Fructose (DC)	181.3±1.76	243.33±4.40	18.5±1.65	10.83±1.01
DC+ Compound **(18)** (10mg/kg)	176.±7.21	227.37±3.71	24±1.41	13.00±1.15
DC+ Compound **(18)** (20mg/kg)	177.5 ±3.67	227 ±4.72	19.6±0.98	13.33±1.20
DC+ Compound **(24)** (10mg/kg)	200±10.81	234±7.02	21.66±2.37	12.66±0.88
DC+ Compound **(24)** (20mg/kg)	202.00±7.57	226.56±9.61	17±0.94	13.00±1.52
DC+Los+Tera	188.33±8.17	246 ±4.16	23.33±1.08	11.33±1.20

Values are expressed as mean±SEM (n=6). Data was analyzed by one way ANOVA followed by Bonferroni's multiple comparison post hoc test. Weight of animals at 0^{th} day and 60^{th} day were evaluated by paired t-test.

Male Wistar rats weighing around 180-200 g were taken for study and the mean difference of weight did not differ more than 10%. All the animals were switched to 20% fructose solution instead of RO drinking water at initiation of the study except for control animals. Animals were weighed every 15 days for 8 weeks. Current showed study showed that animals under study did not show any significant difference amongst groups and showed normal increase in body weights which is contrary to other studies which have shown significant increase in body weight as compared to normal rats(379),(380). These discrepancies in the results can be due to the different age of animals as well as the duration of the study (381). Fluid intake was measured during study and fructose fed rats showed increase in fluid intake in first half of the study and later it was less than the RO water consuming rats. These changes can be attributed to the sweet taste of fructose leading increase intake initially and reduced palatability with time. Study groups showed no significant difference in food intake during experimental protocol. Despite the decrease in fluid intake, fructose has energy value of 4 kcal/g caused net increase in calorie consumption in animals lead to myriad metabolic changes (382).

5.11.2 Effect of compound (18) and (24) on metabolic parameters in 20% fructose induced CMets

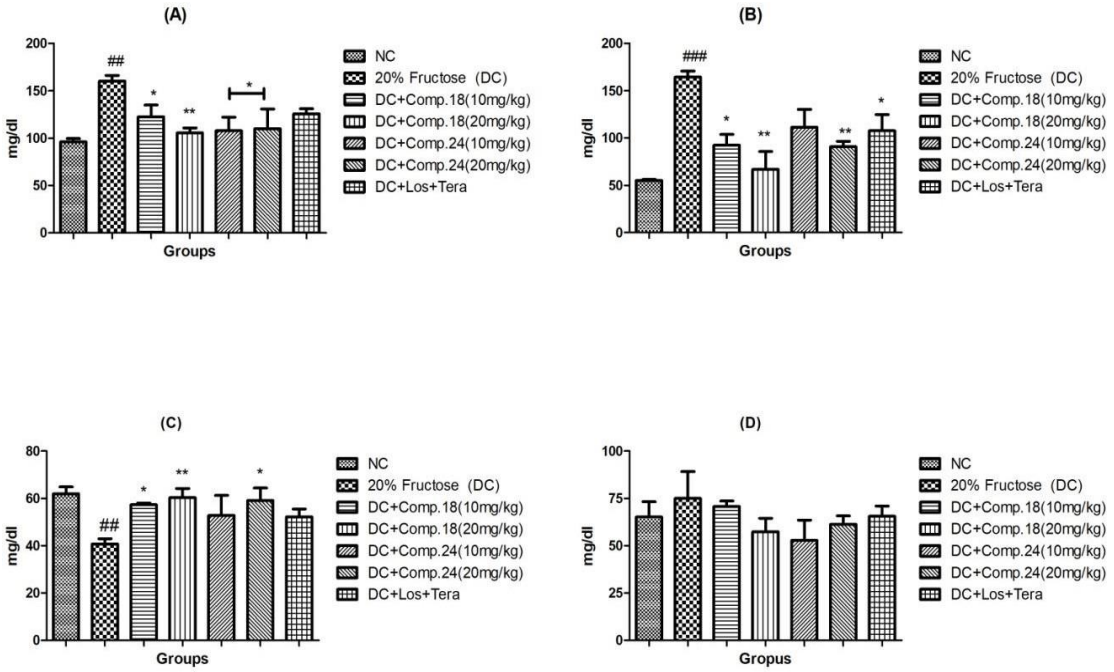

Figure 5.33: Effect of compound (18) and (24) on metabolic parameters in 20% fructose induced CMets. (A) Glucose (B) Triglycerides (C) High density lipoprotein (HDL) (D) Total Cholesterol. Values are expressed as mean±SEM (n=6). Data was analysed by one way ANOVA followed by Bonferroni's post hoc test. #= compared to normal control. *= compared to 20% fructose. #,*=p<0.05, ##, **=p<0.01, ns= non-significant.

Long-term high fructose consumption is known to induce hyperglycemia, hypertriacylglycerolemia, insulin resistance and hypertension in the rat. Fructose by its virtue of diabetogenic effect produced significant elevation in fasting plasma glucose level (NC vs. DC; 96.49±3.29 vs. 160. 44±5.90 mg/dl; p<0.01) after 60 days compared to water drinking rats. Compound **(18)** at both doses showed significant reduction (10mg/kg; 122.71±12.41 vs. 160. 44±5.90 mg/dl; p<0.05) and (20mg/kg; 105.73± 5.19 vs.160. 44±5.90 mg/dl; p<0.01) in glucose level compared to fructose fed rats.

These effects can be associated with strong interactions of novel compounds with ligand binding domain of PPARγ and DPP 4 proteins. Previous also showed the beneficial role of SNS and RAAS blockade in Fructose and high fat diet induced CMets(383),(384). These encouraging effects are independent of its receptor antagonism effect as it provides superior reduction in glucose level compared to standard drugs. Compound **(24)** at both doses of 10 mg/kg and 20mg/kg also produced beneficial effect comparable to compound **(18)**.

Fructose feeding is accompanied by dyslipidemia, particularly dramatic increase in triglycerides in plasma. These effects can be attributed to the fact that chronic fructose consumption reduced lipoprotein lipase activity and suppressed the insulin signaling. 20% fructose consumption for 8 weeks caused significant elevation in TG level (NC vs. DC; 55.16±1.28 vs. 164.36±6.36 mg/dl, p<0.001) as compared to naïve animals. Treatment with compound **(18)** and **(24)** at 20 mg/kg showed beneficial effect by preventing the effect on fructose significantly [Compound **(18)** vs. DC; 66.93±18.88 vs. 164.36±6.36 mg/dl, p<0.01] and [Compound **(24)** vs. DC; 90.93±4.56 vs. 164.36±6.36 mg/dl, p<0.01). Treatment with standard drugs also improved metabolic profile significant decrease in TG level (107.75± 17.12 vs. 164.36±6.36 mg/dl, p<0.05 as compared to fructose fed rats.

There was no significant change observed in cholesterol level in fructose fed rats as compared to normal control rats. While increase in cholesterol level is subjected to discrepancies in the result reported as many study found significant alterations in cholesterol and derived atherogenic lipids. These can be speculated as researchers have used high fat to high fructose diet and also combination of high fat diet with fructose feeding. No significant change was observed amongst groups as well. High density lipoprotein (HDL), a protective lipid acts by increasing the transport of peripheral LDL to liver and thus reducing its plasma level. Fructose consumption produced a marked decrease in HDL level after 8 weeks of ingestion. ARB blockers have been reported to increase HDL level and decrease atherogenic index (385). Compound **(18)** and **(24)** exhibited protective effect by significantly increasing HDL level at 20mg/kg as compared to disease control rats.

5.11.3 Effect of compound (18) and (24) on glycemic parameters in 20% fructose induced CMets

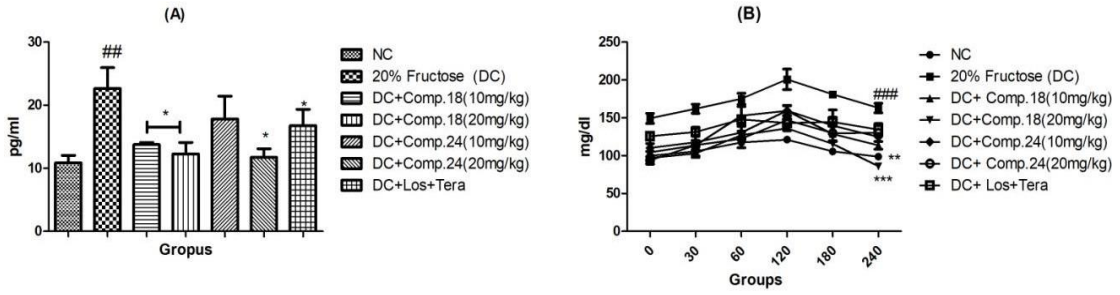

Figure 5.34: Effect of compound (18) and (24) on glycemic parameters in 20% fructose induced CMets. (A) Insulin (B) Oral Glucose Tolerance Test (OGTT) Values are expressed as mean±SEM (n=6). Data

was analysed by one way ANOVA followed by Bonferroni's post hoc test. #= compared to normal control. *= compared to 20% fructose. #, *=p<0.05, ##, **=p<0.01, ***=p<0.001.

After 8 weeks of 20% fructose ingestion in drinking water resulted in significant elevation insulin level compared to normal rats. Insulin resistance is the hallmark feature of cardiometabolic disorder and its one of the metabolic anomalies induced by fructose administration in rodents as well as in human(386) (375).Activation of SNS by fructose feeding leads to prominent role for excess ([Caþ2]i) in the mediation of insulin resistance syndrome is suggested(387). It is conceivable that activation of certain classical isoforms of PKC contributes independently to disruption of insulin signaling in adipocytes, as PKC activators have been shown to interfere with this signaling in cultured adipocytes, whereas a specific inhibitor of classical PKCs up-regulates insulin-stimulated glucose transport(388),(389). Oral glucose tolerance test was performed at 2g/kg, exhibited significant difference (NC vs. DC; 92.82±5.59 vs. 162.93±6.33 mg/dl; p<0.001) in glucose level even after 240 minutes. These results accompanied with elevated insulin level revealed insulin resistance in fructose fed rats.

Previous researches have showed activation of SNS and RAAS system followed by fructose consumption leads to malfunction of insulin signaling, β-cell dysfunction due to angiotensin-mediated increases in oxidative stress (390), inflammation, and free fatty acids concentrations, as well as glucotoxicity, lipotoxicity, and advanced glycation end products potentially contribute to insulin resistance related to RAS activation(391). Treatment with compound **(18)** resulted into significant difference in glucose during OGTT protocol associated with significantly (10mg/kg; 113.57±5.09 vs. 162.93±6.33 mg/dl; p<0.001) and (20mg/kg; 85.12±2.85 vs. 162.93±6.33 mg/dl; p<0.001) decrease level of insulin in rat plasma. These results shed lights on the beneficial effects of dual RAAS and SNS blockadeproduced by the compounds under investigation. This beneficial effect can also be postulated to its DPP4 and PPARγ modulatory activity which is independent of its receptorantagonism. Compound **(24)** also showed significant difference in glucose level comparedto fructose fed rats during treatment. Combination of standard drug also showed modest improvement in insulin resistance as depicted in figure 5.34.

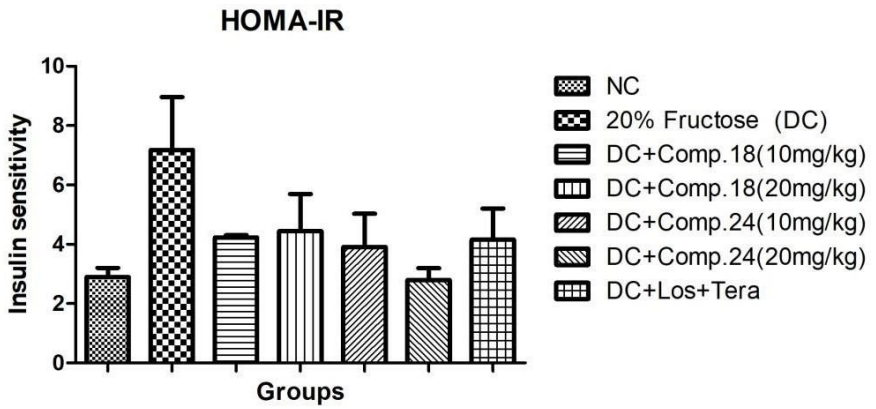

Figure 5.35: Effect of compound (18) and (24) on insulin sensitivity index by HOMA-IR. Values are expressed as mean±SEM (n=6). Data was analysed by one way ANOVA followed by Bonferroni's post hoc test.

The overall result is that HOMA-IR and QUICKI as surrogate measures provide a reasonable and reliable approximation of formal measures of insulin resistance when applied to rats and mice as they do in humans(392).The Homeostasis Model Assessment of IR (HOMA-IR) has proved to be a robust tool for the surrogate assessment of IR obtained by combining fasting plasma glucose and insulin level (393). Normal control animals showed a mean value of 2.89±0.9 HOMA-IR index. These are in line with reported value of acceptable limits for HOMA-IR value (394). Treatment with 20% fructose caused a marked increase in index (7.18±1.78). However, they were found to be insignificant when compared statistically. Treatment with compound **(18)** and **(24)** for six weeks offered better glycemic control by improving insulin resistance in OGTT and reduced level of glucose in serum. HOMA-IR value was found to be 4.23±0.06 for compound **(18)** and 2.79±0.39 for compound **(24)** at 20mg/kg dose. Combination of standard drug provides comparable control in comparison to compound **(18)** but compound **(24)** offered superior improvement in surrogate marker of IR.

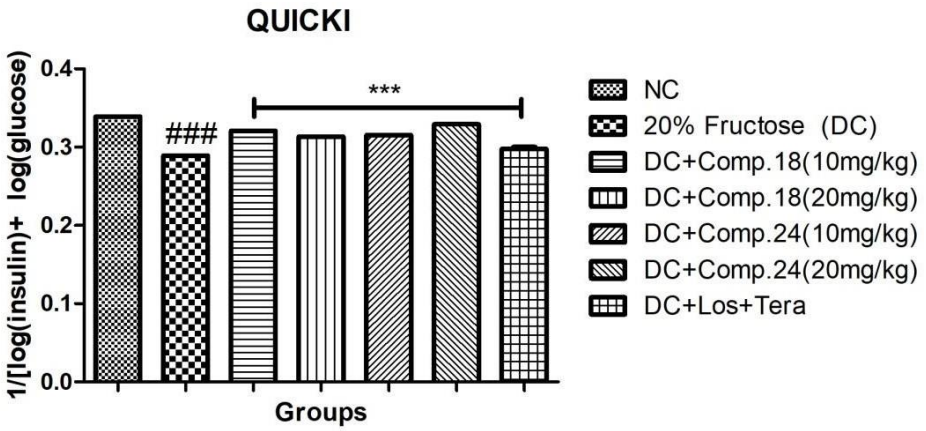

Figure 5.36: Effect of compound (18) and (24) on insulin sensitivity index by QUICKI. Values are expressed as mean±SEM (n=6). Data was analysed by one way ANOVA followed by Bonferroni's post hoc test. #= compared to normal control. *= compared to 20% fructose. ###, ***=p<0.001.

QUICKI score is also the reliable surrogate marker for confirmation of insulin resistance. Fructose fed rats showed significant reduction in QUICKI score suggesting impaired insulin and glucose turnover. Our results are consistent with previous findings where fructose feeding whether by diet or in drinking water disturbed insulin signaling (395),(396). Treatment with both the new compounds **(18)** and **(24)** produced marked improvement revealing its protective role insulin resistance induced by chronic fructose feeding. Combination of standard drugs also showed comparable results with NCEs under investigation. These results combined with OGTT results indicate the involvement of enhanced SNS and RAAS stimulation responsible for induction of metabolic disturbances

5.11.4 Effect of compound (18) and (24) on hemodynamic parameters in 20% fructose induced CMets

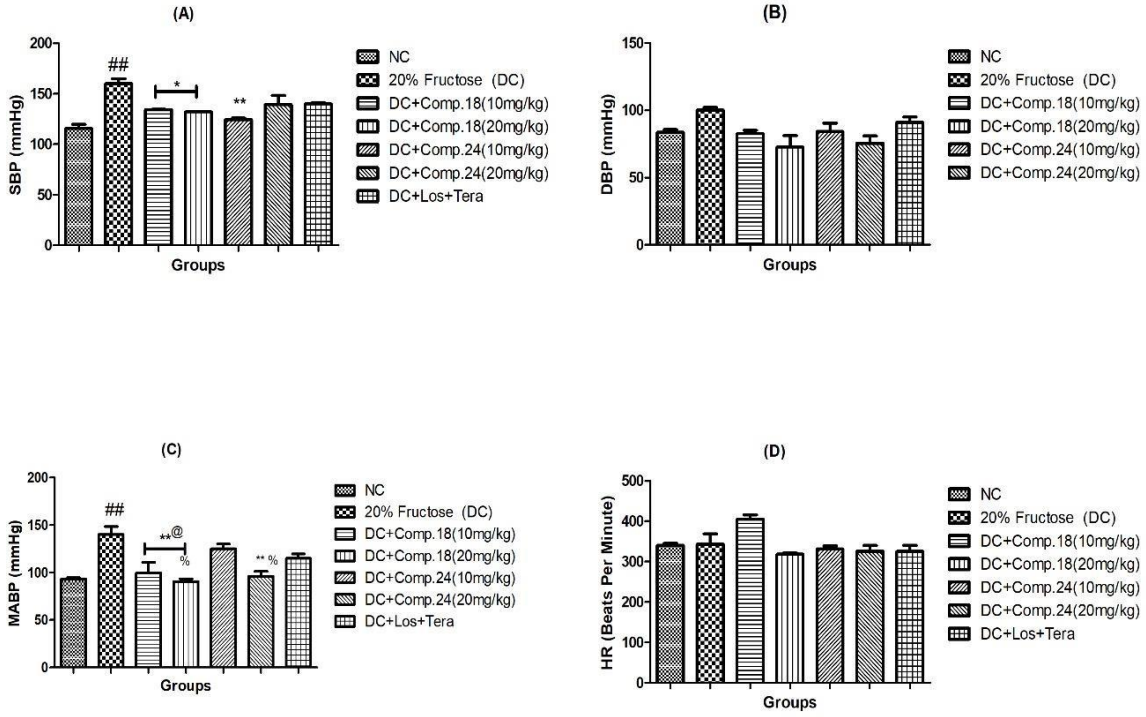

Figure 5.37: Effect of compound (18) and (24) on hemodynamic parameters in 20% fructose induced CMets. (A) SBP (B) DBP (C) MABP (D) Heart rate. Values are expressed as mean±SEM (n=6). Data was analysed by one way ANOVA followed by Bonferroni's post hoc test. #= compared to normal control. *= compared to 20% fructose. *=p<0.05, ##, **=p<0.01, ns= non-significant. SBP= Systolic blood pressure, DBP=Diastolic blood pressure, MABP= Mean arterial blood pressure

Fructose feeding has been recognized as the perpetrator to increase the blood pressure via increase reabsorption of salt from proximal convoluted tubule resulted into increase in activation of RAAS (384), On the other hand, increase uptake of salt increase the synthesis of fructose in body thus initiate the vicious positive feedback of salt and sugar interaction(397). Administration of fructose via drinking water or high fructose diet is associated with increase in blood pressure due to insulin resistance and activation of sympathetic nervous system associated increase spillover of catecholamine (398).

Fructose fed rats showed significant elevation in SBP (160.34± 3.32 vs. 115.75±3.75 mmHg; p<0.001) after 8 weeks of administration compared to normal control animals. Compound **(18)** at 10 mg/kg (134.17±0.56 vs.160.34± 3.32 mmHg, p<0.05) and 20 mg/kg (132.10±10.17 vs. 160.34± 3.32 mmHg, p<0.05) exhibited significant reduction in blood

pressure. Compound **(24)** showed significant reduction at 10 mg/kg (124.18±1.56 vs.160.34± 3.32 mmHg, p<0.001) compared to fructose fed rats. While combination of losartan and terazosin did not show significant reduction compared to fructose fed rats.

Diastolic pressure showed non-significant difference between fructose control and normal control animals. Treatment with compound **(18)** and **(24)** revealed decrease in blood pressure however it was not significant compared to fructose administered rat or normal control animals.

Mean arterial blood pressure (NC vs. FC; 93.30±1.30 vs. 140.03±7.34 mmHg; p<0.001) showed significant elevation after 60 days 20% fructose feeding in drinking water. Treatment with compound **(18)** was able to reduce MABP significantly compared to fructose fed rats. At 10 mg/kg (99.45±11.24 vs. 140.03±7.34 mmHg; p<0.001) and 20 mg/kg (90.43±2.97 vs. 140.03±7.34 mmHg; p<0.001). Higher dose of compound **(18)** showed reduction in MABP compared to 10 mg/kg however it was not significant.

Few studies have reported increase in heart rate after fructose feeding however current study reported no change in heart rate during study period amongst different groups (399).

5.11.5 Effect of compound (18) and (24) on articular reactivity in 20% fructose induced CMets

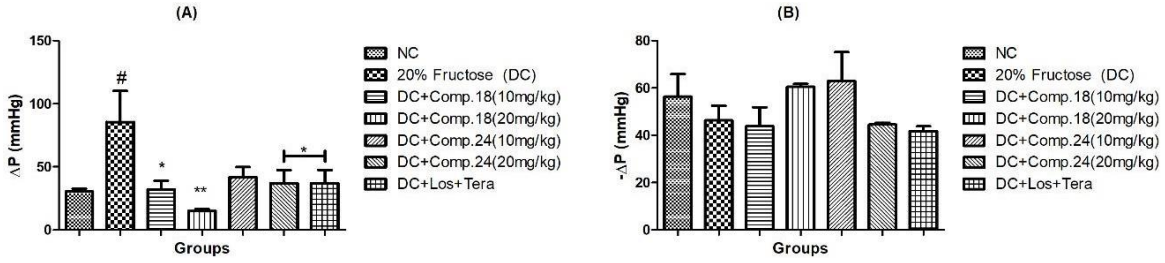

Figure 5.38: Effect of compound (18) and (24) on articular reactivity in 20% fructose induced CMets. (A)Phenylephrine (B) Acetylcholine. Values are expressed as mean±SEM (n=3). Data was analysed by one way ANOVA followed by Bonferroni's post hoc test. #= compared to normal control. *= compared to 20% fructose. #*=p<0.05, ##, **=p<0.01, ns= non-significant

Articular reactivity provides the idea about the receptor up-regulation and its association with physiological response (400). Previous study have reported the activation and up-regulation of SNS system and especially alpha$_1$D receptor subtype in fructose fed rats and in humans(401),(402). After 60 days of fructose administration, rats showed significantly enhanced (NC s. FC; 30.5±2.17 vs. 85.61±20.12, p<0.01) response to exogenous

phenylephrine administration compared to water drinking rats. Dual inhibition of RAAS and SNS by compound **(18)** at 5mg/kg; 32.23±5.43 vs. 85.61±20.12mmHg $p<0.01$, 10mg/kg; 15.11±1.15 vs. 85.61±20.12mmHg $p<0.01$) and compound **(24)** produced significant reduction in heightened vasomotor activity with concomitant fructose administration as perthe previous observations (403). Compound **(18)** at higher dose of 20 mg/kg suppressed the reactive response to phenylephrine more potently than the normal rats. These results displayed dose dependent inhibition of receptors with chronic administration of NCEs. Combination of standard drugs also reduced the change in blood pressure significantly compared to fructose fed rats.

Acetylcholine is potent vasodilator acting by up regulation of eNOS enzyme and subsequent nitric oxide production. 20% fructose administration weakened the vasorelaxant effect of Ach compared to normal animals however this effect was not significant. Treatment with compound **(18)** and **(24)** restores the vasodilation mediated by Ach revealing improved endothelial dysfunction. These results can be correlated with strong hypotensive effect of NCE and reversal of insulin resistance induced by concomitant administration of fructose.

5.11.6 Effect of compound (18) and (24) on adipocytokines in 20% fructose induced CMets

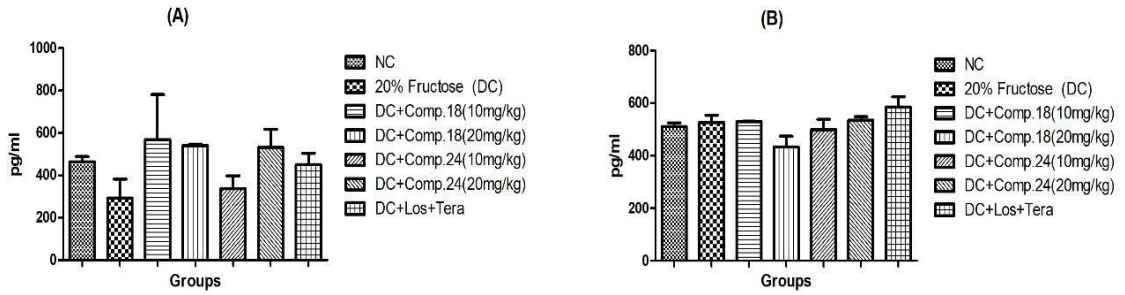

Figure 5.39: Effect of compound (18) and (24) on adipocytokines in 20% fructose induced CMets.
(A) Adiponectin (B) Leptin Values are expressed as mean±SEM (n=6). Data was analysed by one way ANOVA followed by Bonferroni's post hoc test.

Adipocytokines function plays vital role in management of metabolic function of body and many adipocytokines were implicated in the initiation and progression of metabolic and cardiovascular disease (404). Adiponectin, a protective cytokine was measured in the rats switched to 20% fructose for 8 weeks. Animals showed reduction in adiponectin level

However, it was not significant compared to normal rats. Treatment with compound **(18)** atboth doses increase in adiponectin level these can be due to their multifunctional effect on PPARγ receptors and DPP4 enzyme which are key regulators of adipogenesis. Treatment with compound **(24)** did not produce pronounce effect on adiponectin level as compared to compound **(18).** Combination of standard drugs did not show significant elevation as compared other treatment groups highlighting the superiority of novel compounds with additional favorable effects on key targets of metabolic disorders (405), (406).

5.11.7 Effect of compound (18) and (24) on liver and heart in 20% fructose induced CMets

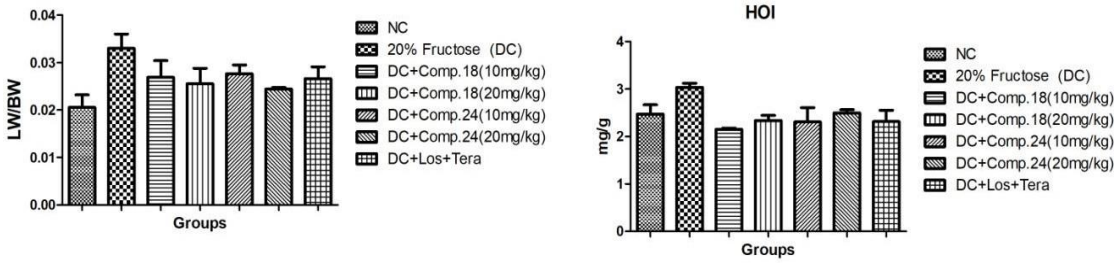

Figure 5.40: Effect of compound (18) and (24) on liver and heart in 20% fructose induced CMets.
(A) Liver weight /Body weight (LW/BW) (B) Heart oedema index (HOI). Values are expressed as mean±SEM (n=4). Data was analysed by one way ANOVA followed by Bonferroni's post hoc test.

Eight weeks of fructose feeding resulted in an increase in fat and glycogen production reflected by an increase in liver weight to body weight ratio. These results are in the agreement with previousstudy exhibiting *de-novo* lipogenesis induced by chronic fructose administration (407). Treatment with compound **(18)** and **(24)** were able to reduce the load inflicted by fructosefeeding however it was not found statistically significant. Heart oedema index was also modestly increased in fructose fed rats showed impaired left ventricular function induced by combined activation of vasoactive systems and mal function of insulin signaling. Compound **(18)** and **(24)** by their virtue of action inhibited activation of SNS and RAAS and reduced the burden on cardiovascular system.

5.11.8 Effect of compound (18) and (24) on histopathological changes in 20% fructose induced CMets

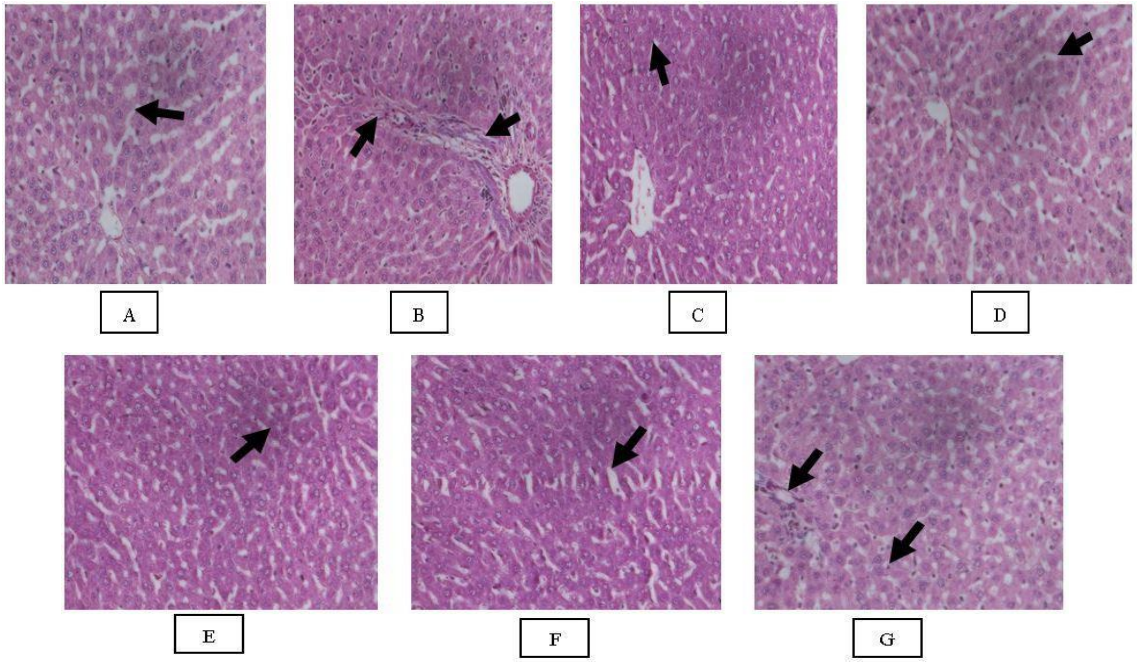

Figure 5.41: Effect of compound **(18)** and **(24)** on histopathological changes in liver by 20% fructose induced CMets. **(A)** NC **(B)** 20% Fructose **(C)** Compound (**18**-10mg/kg) **(D)** Compound (**18**-20mg/kg) **(E)** Compound (**24**-10mg/kg) **(F)** Compound (**24**-20mg/kg) **(G)** Los+tera (10 mg/kg each). Sections were analysed under 20X magnification.

Liver microscopy from normal rats presented round normal central, sinusoids, with absence of steatosis. There was no inflammatory infiltration of cells detected in normal rats. Fructose consumption is believed to produce significant alteration displayed by enlarged hepatolobular cells. However, in contrast many studies have reported absence of the mentioned symptoms. Current protocol of fructose consumption leads to mild alterations in liver architecture presented by accumulation of inflammatory cells from blood vessels running from central vein to portal vein. Treatment with compound **(24)** at 20 mg/kg displayed slight enlargement of lobules, however, no major abnormalities was detected. Treatment with novel compounds **(18)** and **(24)** showed normal liver tissue histology with smooth oblong sinusoids and absence of inflammatory cells infiltration.

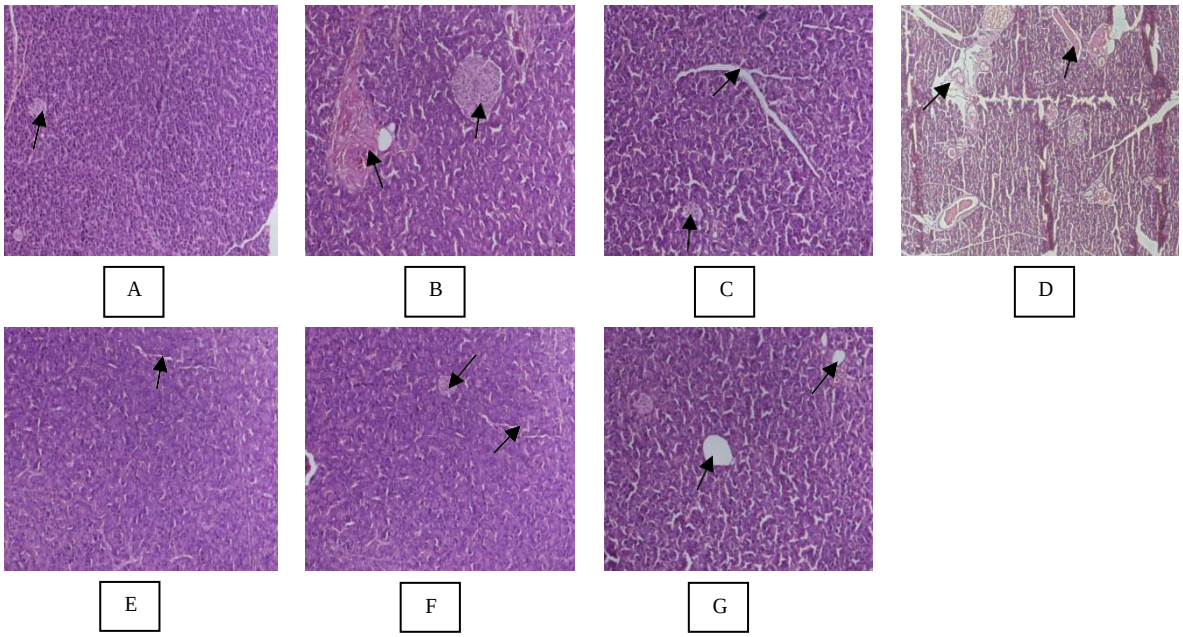

Figure 5.42: Effect of compound **(18)** and **(24)** on histopathological changes in pancreas by 20% fructose induced CMets. **(A)** NC **(B)** 20% Fructose **(C)** Compound (**18**-10mg/kg) **(D)** Compound (**18**-20mg/kg) **(E)** Compound (**24**-10mg/kg) **(F)** Compound (**24**-20mg/kg) **(G)** Los+tera (10 mg/kg each). Sections were analysed under 20X magnification.

Pancreas of normal rats revealed normal histopathological attributes marked by normal islet cells and normal dilation of exocrine and endocrine glands. 20% fructose administration for six weeks resulted in mild pancreatic damage exhibited by expansion of islet cells and infiltration of inflammatory cells (figure 5.42). Similar studies with high fructose administration displayed mild to intense pancreatic damage. Treatment with compound **(18)** showed improvement in pancreatic structure and normalization of islet size. Dose of 20 mg/kg improved the tissue architecture in comparison to 10 mg/kg. Similarly, administration of compound **(24)** also caused reversal of damage inflicted by fructose consumption.

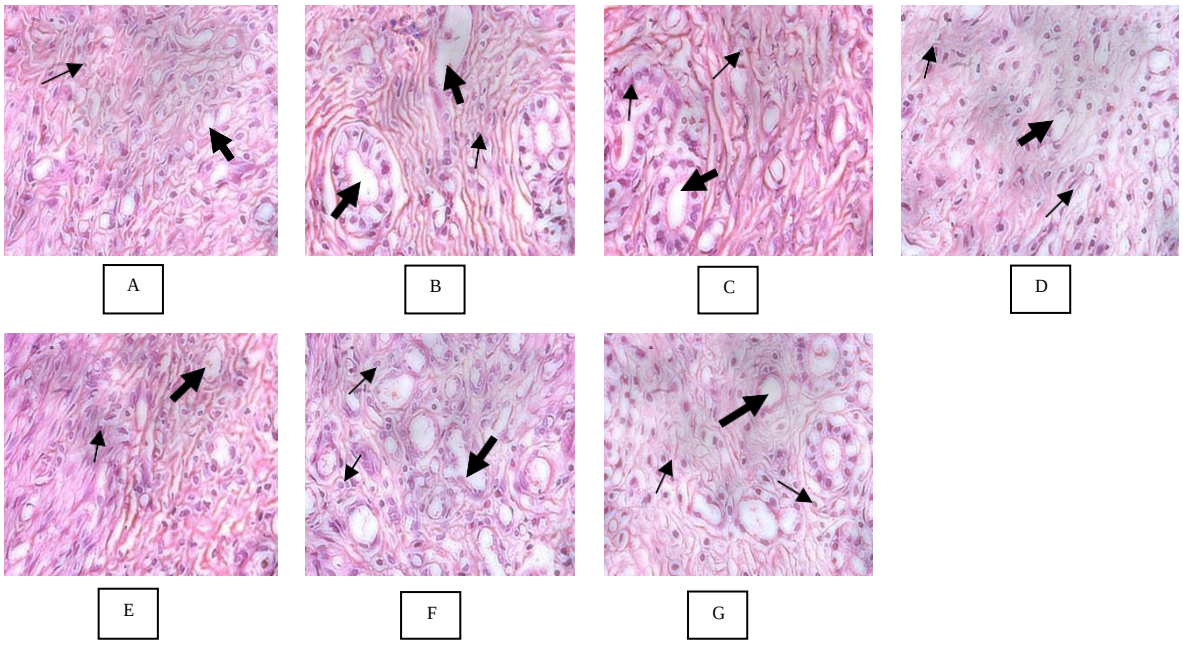

Figure 5.43: Effect of compound **(18)** and **(24)** on histopathological changes in adipose tissue by 20% fructose induced CMets. **(A)** NC **(B)** 20% Fructose **(C)** Compound (**18**-10mg/kg) **(D)** Compound (**18**-20mg/kg) **(E)** Compound (**24**-10mg/kg) **(F)** Compound (**24**-20mg/kg) **(G)** Los+tera (10 mg/kg each). Sections were analysed under 20X magnification.

Histological interpretation of white adipose tissue (WAT) suggested significant enlargement in adipocytes diameter while adipocytes visualized from normal rats showed regular arrangement. Sections obtained from the fructose fed rats showed noteworthy inflammation represented by leukocytes infiltration. These results indicate the imbalance in adipocytokine level observed by leptin and adiponectin level. Treatment with compound **(18)** resulted into the improvement of metabolic response in WAT characterized by regular adipocytes size and reduced inflammation. The protection was higher in 20 mg/kg group of compound **(18)**. While compound **(24)** treatment at 10 mg/kg was marked by presence of inflammatory cells, treatment with 20 mg/kg dose produced beneficial effect, however, noticeable hypertrophy of adipocytes was observed compared to normal control group.

5.12 Pharmacological screening and evaluation of compound (14) and (50) for FXa inhibition

5.12.1 *In-vitro* FXa inhibition *and ex-vivo* assay for evaluation of antithrombotic activity

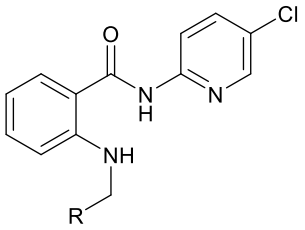

Series I

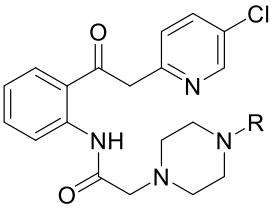

Series II

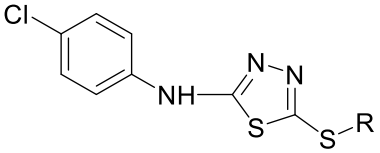

Series III

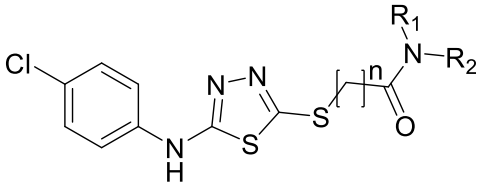

Series IV

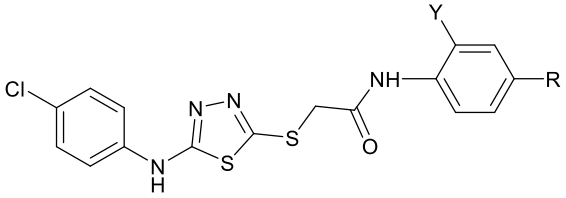

Series V

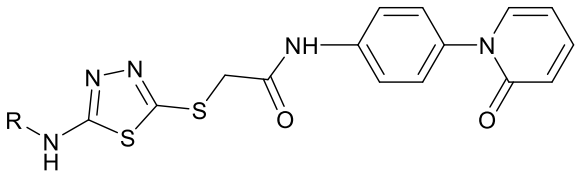

Series VI

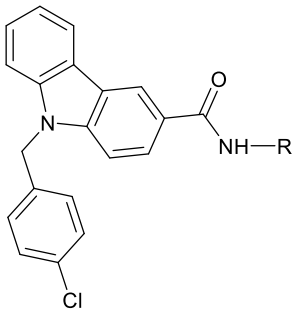

Series VII

Series I: FXa inhibition, PT and aPTT time measurement of 2-Aminobenzamide derivatives (Benzyl substitutions)

In-vitro enzyme inhibition assay for FXa was performed for the novel compounds at a concentration range from 0.001 µM to 100 µM by using a human Factor Xa enzyme and chromogenic substrate (S-2765). The hydrolysis of the substrate by the enzyme resulted in the change of absorbance at 405 nm which indicates the enzyme inhibition and IC_{50} values were calculated accordingly. IC_{50}, PT and aPTT time of 2-aminobenzamide derivatives are mentioned in table 5.22 and 5.23.

Table 5.22: IC_{50} values, PT and aPTT time of compounds (1-17)

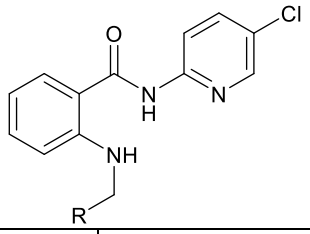

Compound	Where -*R* is	IC_{50} ± SEM (µM)	PT (sec)	aPTT (sec)
1	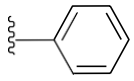	>100	22	19
2	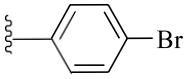	23.7 ± 3.4	22	15
3	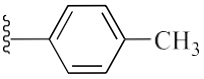	18.4 ± 2.6	21	30
4	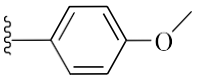	11.5 ± 1.3	22	34
5	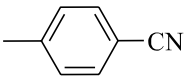	85.56±2.76	20	18
6	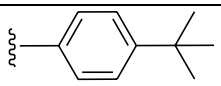	41.0 ± 3.2	21	30
7	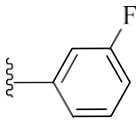	48.3 ± 2.9	24	30
8	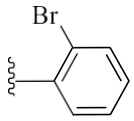	23.2 ± 8.4	23	37.5
9	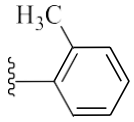	>100	20	19
10	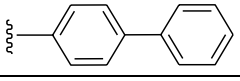	35.3 ± 2.3	22	35

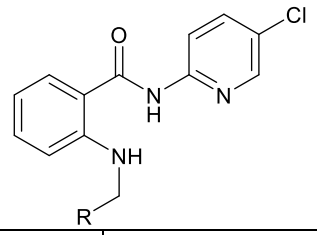

Compound	Where -*R* is	IC_{50} ± SEM (µM)	PT (sec)	aPTT (sec)
11	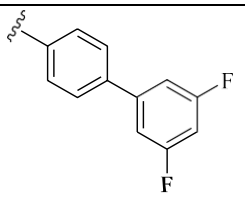	**5.4 ± 1.0**	24	**40**
12	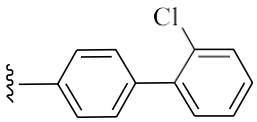	**1.3 ± 0.8**	24	**40**
13	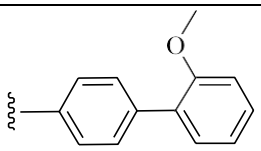	12.5 ± 2.2	22	35
14	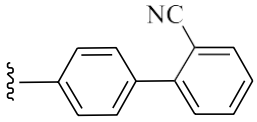	**0.7 ± 0.2**	25	**45**
15	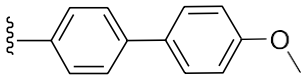	>100	21	28
16	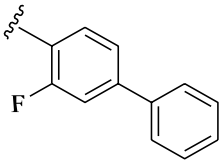	30.0 ± 6.4	23	30
17	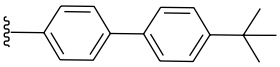	52.5 ± 5.7	9	35

Compounds exhibiting significant inhibition of the enzyme FXa in the preliminary screening were evaluated further by *ex-vivo* measurements of prothrombin time and aPTT time. These studies are important in the development of anti-thrombotic agents as it is the reflection of efficacy of new agent on coagulation cascade and clot formation. Substitution at the 4th position of compound **(1)** resulted into compounds **(2-6)** with improvement of FXa inhibition however it was far higher than the standard drug. Substitution at 2nd and 3rd position also resulted into sub molar potency of compounds.

Increase in aromaticity by means of substituted benzyl replacement resulted into favorable results and IC_{50} of compounds were greatly improved **(11-15).** Compound **(14)** was found

to be the most potent compound of synthesized compounds. *Ex-vivo* study by PT and aPTT time showed considerable improvement in parameters as compound **(14)** exhibited highest prolonging activity.

Series II: FXa inhibition, PT and aPTT time measurement of 2-Aminobenzamide derivatives (Piperazinyl substitutions)

Table 5.23: IC_{50} values, PT and aPTT time of compounds (18-23)

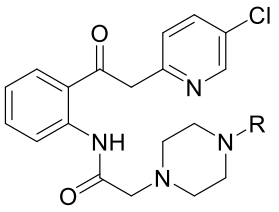

Compound	Where -*R* is	IC_{50} ± SEM (µM)	PT (sec)	aPTT (sec)
18	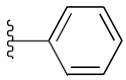	95.2± 5.21	21	44
19	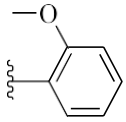	>100	20	39
20	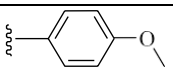	>100	19	41
21	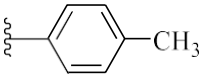	96.23 ± 6.78	24	35
22	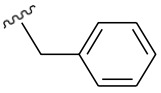	57.5 ± 8.6	25	52
23	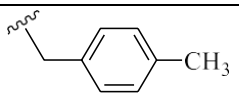	>100	22	44

Substitution of benzyl ring in series I with substituted piperazinyl resulted in compounds **(18-23)**. However, it is observed that insertion of heterocyclic ring produced detrimental effect on potency of compounds as evident in table 5.23. The compound exhibited very high IC_{50} values and showed poor activity against FXa. However, the newly synthesized compoundretained their PT and aPTT prolongation properties.

Series III: FXa inhibition, PT and aPTT time measurement of 1,3,4 thiadiazole derivatives (Benzyl Substitutions)

Table 5.24: IC_{50} values, PT and aPTT time of compounds (24-30)

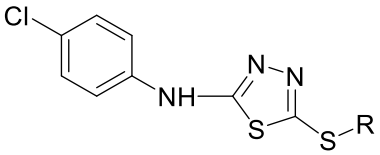

Compound	Where -*R* is	IC_{50} ± SEM (µM)	PT (sec)	aPTT (sec)
24	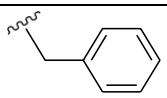	> 100	21.29	42.12
25	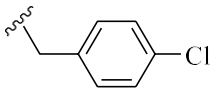	> 100	17.955	47.97
26	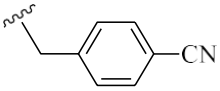	> 100	23.436	42.12
27	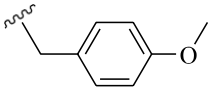	> 100	20.223	42.51
28	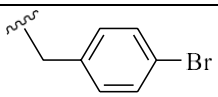	> 100	20.79	58.11
29	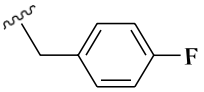	> 100	22.869	59.67
30	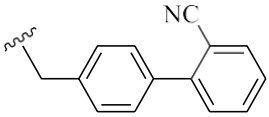	9.55 ± 1.3	30.996	56.16

Series IV: FXa inhibition, PT and aPTT time measurement of 1,3,4 thiadiazole derivatives (Aminoalkyl Substitutions)

Table 5.25: IC_{50} values, PT and aPTT time of compounds (31-39)

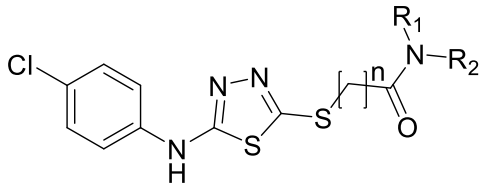

Compound	N	Where -NR_1R_2 is	IC_{50} ± SEM (µM)	PT (sec)	aPTT (sec)
31	1	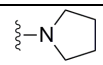	> 100	22.11	48.75
32	1	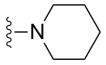	> 100	22.491	50.7
33	1	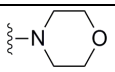	> 100	29.673	44.85
34	2	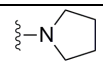	> 100	28.917	85.02
35	2	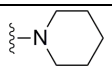	> 100	32.508	70.2
36	2	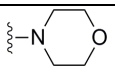	> 100	38.934	69.03
37	3	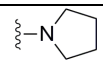	> 100	38.367	173.55
38	3	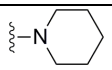	> 100	27.027	85.02
39	3	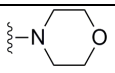	> 100	38.556	68.64

The antithrombotic potential of the 1,3,4-thiadiazole derivatives was checked by screening all the synthesized compounds against FXa inhibition and their IC_{50} values were determined according to the procedure mentioned earlier. Table 5.24 and 5.25 shows the inefficiency of benzyl substituted compounds (**24-30**) and aminoalkyl derivatives (**31-39**) for FXa inhibition as evident by their IC_{50} values > 100 µM. Amongst the benzyl substituted compounds, compound (**30**) has substituted biphenyl group as the P4 motif which showed higher FXa inhibitory activity (IC_{50} = 9.55 µM).

Series V: FXa inhibition, PT and aPTT time measurement of 1,3,4 thiadiazole derivatives (Heterocyclic Substitutions)

Table 5.26: IC_{50} values, PT and aPTT time of compounds (40-52)

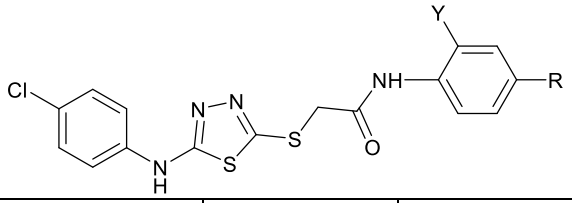

Compound	Y	Where -*R* is	IC_{50} ± SEM (µM)	PT (sec)	aPTT (sec)
40	H		> 100	22.30	47.97
41	H		> 100	17.38	52.65
42	H		> 100	27.02	52.26
43	H		16.5 ± 2.7	28.16	62.79
44	H	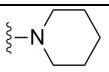	18.8 ± 1.8	27.02	59.28
45	H	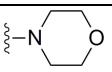	6.5 ± 1.1	37.04	80.34
46	H	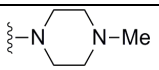	4.98 ± 1.0	24.57	64.74
47	H	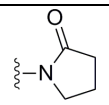	**2.05 ± 0.8**	51.97	92.04
48	H	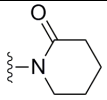	**0.79 ± 0.13**	55.94	117
49	H	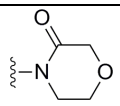	**0.35 ± 0.12**	125.30	246.87
50	H	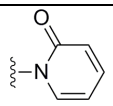	**0.22 ± 0.08**	110.94	173.55
51	H	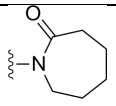	**2.56 ± 1.3**	38.36	85.02
52	F	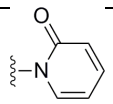	**0.47 ± 0.13**	125.30	120.12

Compounds (**40-42**) having 4-chloroaniline (**40**), 4-fluoroaniline (**41**) and 4-methoxyaniline (**42**) showed poor FXa inhibitory activity (IC_{50}>100 µM). Different heterocyclic substitutions like pyrrolidine, piperidine, morpholine and N-methylpiperazine were introduced at *para* position of aniline to obtain compounds (**43-46**). The resultant compounds displayed moderate to good FXa inhibitory activity as evident by their IC_{50}

values of 16.5 µM, 18.8 µM, 6.5 µM and 4.9 µM, respectively (table 5.26). The pyrrolidine ring in compound (**43**, IC_{50} = 16.5 µM) was replaced by pyrrolidinone ring resulting in compound (**47**, IC_{50} = 2.05 µM) exhibiting excellent improvement in FXa inhibitory activity. FXa inhibitory activity was further enhanced by replacing the pyrrolidinone in compound **(47)** by piperidinone and morpholinone yielding compound (**48**, IC_{50} = 0.79 µM) and compound (**49**, IC_{50} = 0.35 µM), respectively. Further substitution of piperidinone ring in compound (**48**) with caprolactam resulted in compound (**51**) leading to loss of some potency (IC_{50} = 2.56 µM). Aromatization of piperidinone ring of compound (**48**), led to development of the most potent compound (**50**) of the series. This novel compound (**50**, IC_{50} = 0.22 µM) revealed improved FXa inhibitory activity than standard drug, apixaban (IC_{50} = 0.32 µM). The compound (**52**) was synthesized by the addition of fluorine atom at ortho position of phenylpyridinone ring in compound (**50**) which resulted in 2-fold decrease in FXa blockage.

Series VI: FXa inhibition, PT and aPTT time measurement of 1,3,4 thiadiazole derivatives (Heterocyclic Substitutions)

Table 5.27: IC_{50} values, PT and aPTT time of compounds (53-66)

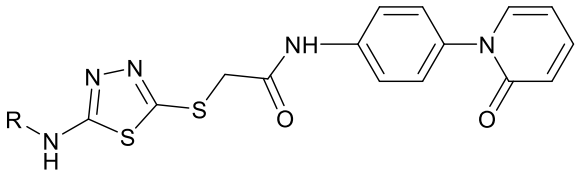

Compound	Where -*R* is	IC_{50} ± SEM (µM)	PT (sec)	aPTT (sec)
53	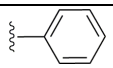	57 ± 4.8	29.106	82.68
54	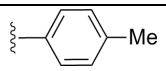	**3.11 ± 1.6**	27.027	59.28
55	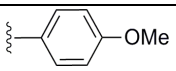	71.96 ± 4.1	23.436	52.26
56	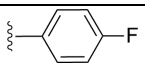	10.43 ± 1.2	39.312	89.31
57	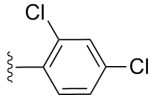	16.53 ± 2.1	28.539	63.18
58	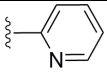	28.14 ± 3.8	33.642	73.71
59	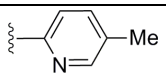	20.72 ± 2.9	36.099	64.74

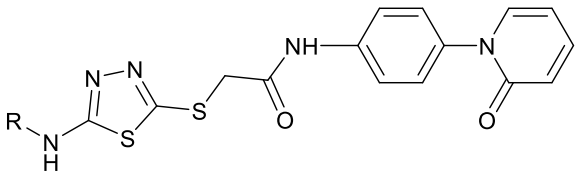

Compound	Where -*R* is	IC_{50} ± SEM (µM)	PT (sec)	aPTT (sec)
60	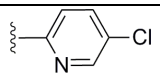	**1.72 ± 1.0**	43.281	109.98
61	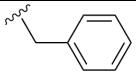	> 100	23.814	50.7
62	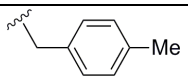	23.92 ± 3.1	24.759	63.18
63	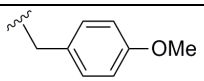	15.70 ± 2.1	29.862	65.91
64	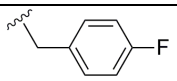	22.64 ± 3.6	38.367	69.42
65	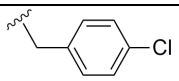	27.12 ± 2.4	28.917	54.21
66	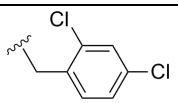	25.60 ± 2.1	26.649	53.04

Further substitutions were carried out to explore favorable P1 motifs with pyridinone as the optimal P4 substituent, but all attempts proved unsuccessful (table 5.27). The replacement of chlorine atom of *p*-chlorophenyl group in compound (**50**) with methyl, methoxy and fluoro groups resulted in compounds (**53-56**) which exhibited notable loss of FXa inhibitory activity. Compound (**57**) containing additional chlorine atom at ortho position of *p*-chlorophenyl group showed a significant loss of activity (**57** vs **50**). Better blockage of FXa was expected with 5-Chloro-2-pyridyl group as P1 motif. Inhibition offered by compound **(61)** (IC_{50} = 1.72 µM) supports the above notion, however, it was found to be inferior than compound **(50)**. To gauge the distance between -Cl and Tyr228 within the active site of FXa, compounds (**61-66)** with substituted benzyl groups as P1 motifs were developed. None of the compounds (**61-66**) from these series displayed significant improvement in FXa inhibition over compound (**50**).

Series VII: FXa inhibition, PT and aPTT time measurement of carbazole derivatives

Table 5.28: IC_{50} values, PT and aPTT time of compounds (67-78)

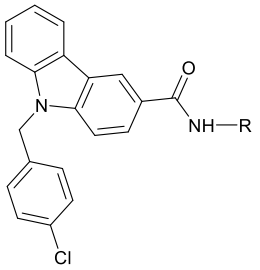

Compound	Where -*R* is	IC_{50} ± SEM (µM)	PT (sec)	aPTT (sec)
67	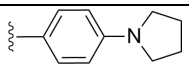	>100	22.1	40.8
68	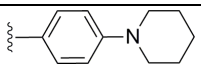	>100	20.7	41.1
69	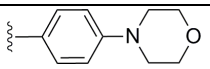	>100	21.5	43.1
70	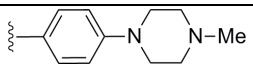	>100	20.02	44.2
71	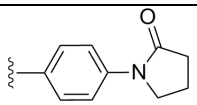	63.15 ± 3.6	23.4	42.7
72	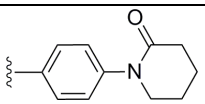	15.87 ± 1.8	**33.5**	**66.1**
73	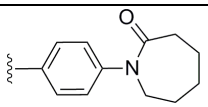	ND	21.76	41.0
74	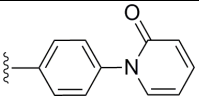	7.49 ± 0.9	**39.9**	**69.6**
75	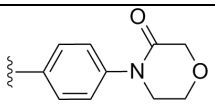	47.20 ± 4.2	29.7	62.6
76	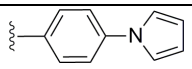	29.40 ± 2.2	22.6	42.8
77	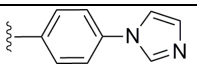	16.60 ± 1.4	24.1	47.7
78	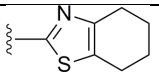	33.10 ± 2.6	29.7	49.8
	Apixaban	**0.35±0.1**	**>180**	**>180**
	Blank	-	18.9	39

The anticoagulation potential of the newly synthesized FXa inhibitors on extrinsic and intrinsic pathways was evaluated by prothrombin time (PT) and activated partial thromboplastin time (aPTT), respectively. Significant prolongation in PT and aPTT displayed the efficacy of novel compounds on both pathways of blood coagulation. All the novel FXa inhibitors were subjected at 1 mM concentration in human plasma for the determination of PT and aPTT.

The table 5.28 shows the *in-vitro* anticoagulant activities of compounds (**67-78**). All the compounds displayed moderate anticoagulant activity. Among the tested compounds, compound (**74**) having 2-oxopyridine moiety displayed good activity with PT (39.9 sec) and aPTT (69.6 sec) time. Compound (**72**) having 2-piperidinone moiety revealed noteworthy prolongation in PT (33.5 sec) and aPTT (66.1 sec) time.

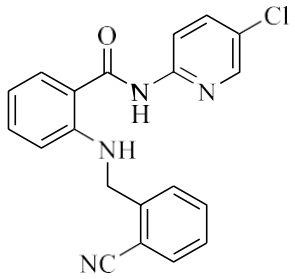

Compound (14)

N-(5-chloropyridin-2-yl)-2-((2-cyanobenzyl)amino)benzamide

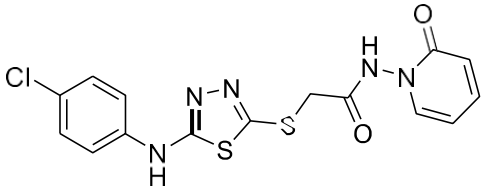

Compound (50)

2-((5-((4-chlorophenyl)amino)-1,3,4-thiadiazol-2-yl)thio)-N-(2-oxopyridin-1(2H)-yl)acetamide

From the extensive *in-vitro* evaluation, it was concluded that Compound **(14),** IC_{50} = **0.7 ± 0.2** and Compound **(50)**, IC_{50} = **0.22 ± 0.08** have excellent interactions at P1 and P4 motif and possess excellent IC_{50} values. They are further explored for their selectivity over thrombin and other serine proteases and *in-vivo* activity.

5.12.2 Molecular docking studies of compound (14) and (50) for FXa enzyme

Molecular docking provides insight interactions ligand with the enzyme, docking studies were performed with FXa. Compound **(14)** offered the highest docking score which indicated its high binding interactions with the enzyme. The intermolecular interactions of the highest binding of compound **(14)** are displayed in figure 5.44 (A). The chloro group of pyridine in compound **(14)** was observed to be stabilized at 3.82 Å from the centroid of Tyr228 aromatic ring which indicated high stability of the ligand-enzyme complex. Compound **(14)**, the –C=O and -NH of the amide interacted with -NH of Gln192 (2.12 Å) and –C=O of Gly219 (1.92 Å), respectively by hydrogen bonding to form a stable complex. The aromatic ring of 2-aminobenzamide displayed π-cation interactions with Arg222. Generally, the π-cation interaction is considered stronger than hydrogen bond or any other physical interactions which impart ligand receptor stability (408). Further, the *ortho* substituted biphenyl group in compound **(14)** exhibited excellent π-π interaction with Tyr99, Phe174 and Trp215 triad in the S4 pocket. From the obtained results, we clearly get an idea that occupying S1 and S4 sites by specific lipophilic moieties is essential for improved binding affinity of the ligands within the ligand binding domain of enzyme (409).

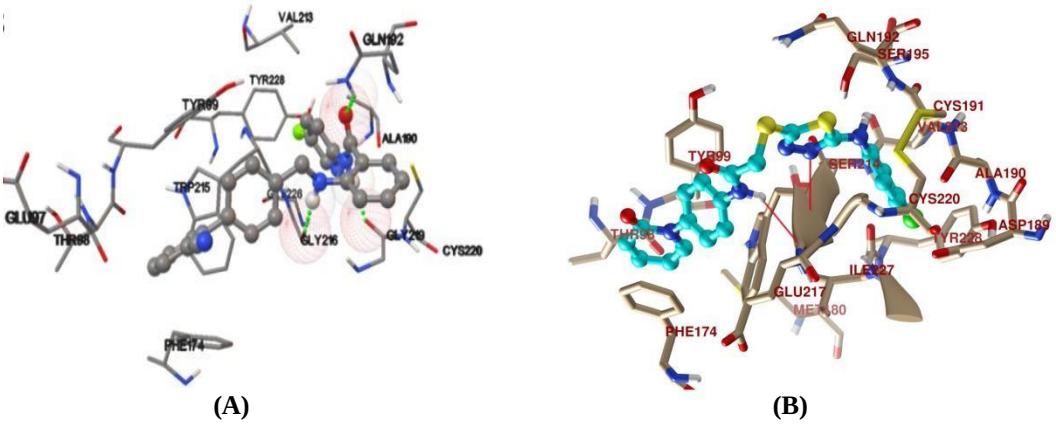

(A) **(B)**

Figure 5.44: Docking pose and representation of interactions between compounds **(A) (14)** and **(B) (50)** and the active site of FXa enzyme.

The most active compound **(50)** offered the highest docking score which indicated its high affinity with the enzyme. The molecular interactions of the compound **(50)** are shown in figure 5.44 (B). The *p*-chlorophenyl group occupied the S1 binding site with promising hydrophobic interactions. Also, the choro was observed in establishing non-covalent interactions with Tyr228. Further –NH- of acetamide and one of the =N- of thiadiazole ring of compound **(50)** interacted with Gly216 by forming hydrogen bonds that imparted

stability to the ligand receptor complex. The phenylpyridinone system was observed to occupy S4 binding site, wherein the pyridinone ring of phenylpyridinone formed strong pi-pi interactions with Phe174 and Trp215.

5.12.3 Selectivity of compound (14) and (50) for FXa

5.12.3.1 Thrombin (FIIa) inhibition assay

Selectivity is a significant issue in the development of factor Xa inhibitors. Factor Xa and other enzymes in the coagulation cascade belong to the trypsin-like serine protease family, the various members of which are involved in numerous physiological functions in the body. Hence, to avoid toxicity and adverse side effects, it is important to selectively inhibit the target enzyme (410). Achieving the needed selectivity has proved challenging due to the high degree of structural homology around the active site of this class of enzymes (411). Among many serine proteases, inhibition of thrombin has been vigorously investigated as an approach to identifying novel anticoagulants. As the generator of fibrin monomers, thrombin is vital for thrombosis and hemostasis. Thrombin, unlike factor Xa, is a multifunctional protein (412). It has been implicated in atherosclerosis, inflammation and neurodegenerative diseases. It is also involved in inhibition of platelet function thus poses high risk of bleeding. These off-target effects are mainly responsible for toxicity and side effects.

After screening of developed NCEs for their FXa inhibitor potential and *ex-vivo* activity, compounds which showed IC_{50} > 5µM were screened for their thrombin inhibition to evaluate their specificity and selectivity. Compounds **(11, 12, 14, 46-52, 54, 60,** apixaban**)** were selected for the study. All the compounds showed high IC_{50} values, while apixaban showed IC_{50}= 12.8 ± 2.2 µM for thrombin. 2-Aminobenzamide derivatives **(11, 12 and 14)** showed IC_{50}> 100 µM. Compounds from 1,3,4-thiadiazolederivatives **(46-52, 54,60)** also exhibited poor selectivity for thrombin as IC_{50} were more than >80µM. These compounds showed high potency for FXa (IC_{50}= 5.4 to 0.22µM for FXa) suggesting excellent candidates for development of novel FXa inhibitors.

5.12.4 Cytotoxicity assay of compounds (14) and (50) in H9C2 cardiac myocytes cells

After confirming FXa inhibitory activity and selectivity over other serine proteases, compounds were subjected to cytotoxic potential by MTT assay. H9C2 cardiac myocytes were selected for the study, and it was found that at different concentrations (0.001 µM-1000 µM) compound **(14)** and **(50)** did not exhibit cytotoxicity as evident in figure 5.45. Hence, it is safe to study these compounds for toxicology and *in-vivo* model of thrombusformation.

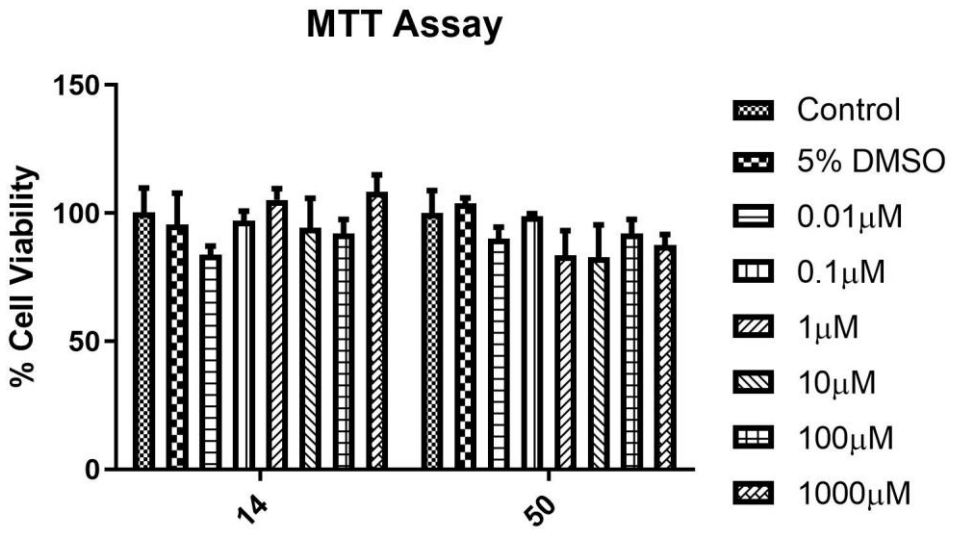

Figure 5.45: Survival of cells post-incubation with different concentrations of compounds **(14), (50)**, 5% DMSO (vehicle) and control cells in H9C2 cells (n=3). Statistical analysis did not find any significant difference between the groups.

5.12.5 Physicochemical properties of compound (14) and (50)

Table 5.29 depicts the physicochemical properties of newly synthesized FXa inhibitor compound (14) and (50). Importance of physicochemical properties in drug discovery, its effect on pharmacokinetic profile and ultimate effect on efficacy outcome have been already explained in earlier section.

Both compounds respect the Lipinski rule of five to satisfy the need of lead or druggable molecule. Molecular weight of compound (14) and (50) were 438.91 and 469.97, respectively, following the general rule of thumb (≤ 500Da) for oral drugs. H-bond interactions are critical descriptors for oral bioavailability. Both the compounds match the criteria for Hba (≤10) and Hbd (≤5).

Table 5.29: Physicochemical properties of compound (14) and (50)

Parameters	Compound (14)	Compound (50)	Apixaban	Rivaroxaban
(A) Lipinski's Parameters				
Mol. Wt. (≤500)	438.91	469.97	460.52	435.88
Hbd (≤5)	2	2	1	1
Hba (≤10)	3	4	5	5
iLogP	2.66	3.27	2.63	2.66
Average LogP	4.69	3.98	2.39	2.23
Lipinski violations	0	0	0	0
(B) Veber's Parameters				
Nrb (≤10)	7	8	5	6
TPSA (≤140 $Å^2$)	77.81	142.45	105.3	116.42
MR	127.4	125.61	138.94	114.09
Veber's violations	0	1	0	0
(C) Solubility				
ESOL solubility (mg/ml)	0.00016	0.00094	0.019	0.044
ESOL solubility class	Poorly soluble	Moderately soluble	Moderately soluble	Soluble
Ali solubility (mg/ml)	0.00002	0.00002	0.0101	0.0115
Ali solubility class	Poorly soluble	Poorly soluble	Moderately soluble	Moderately soluble

Partition coefficient provides the measure of lipophilicity andcontributes to the ADMET characteristics of drugs, contributing to their solubility and permeability through membranes ilogP value indicates the partition coefficient in classical octanol/water system. ilogp value of compound **(14)** was 2.66 and while for compound **(50)**, it was estimated to be 3.27 by SWISS ADME tool. However, SWISS ADME utilizes five algorithms to predict the most accurate estimation of logP. SWISS ADME predicts the consensus logP (cLogP) of 4.69 and 3.98 for compound **(14)** and **(50),** respectively. It is predicted to be at the higher limit for compound **(50)** which correspond to its poor solubility.

Veber's parameters provide the platform for evaluation of druggable physicochemical properties independent from molecular weight. It includes number of rotatable bonds and TPSA which are descriptor of molecular flexibility associated with oral absorption. The set

limit for Nrb should not be more than 10 and TPSA for sufficient oral absorption should be between 60 $Å^2$ to 140 $Å^2$. Both newly synthesized FXa inhibitors obey the Veber's parameters except compound **(50)** is estimated to have 142.45 $Å^2$ which violated the limit of 140 $Å^2$.

5.12.5.1 Radar chart and Brain Or IntestinaL EstimateD permeation method (Boiled-Egg) diagram of compound (14) and (50)

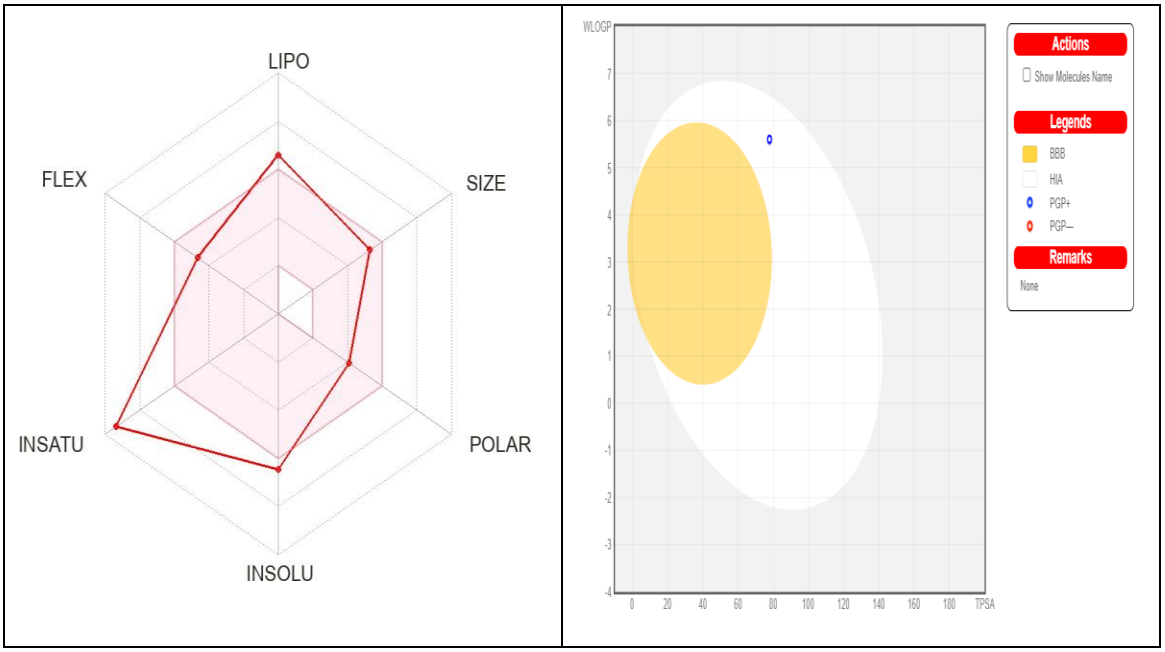

Figure 5.46: Radar chart and Boiled Egg diagram of compound **(14)**

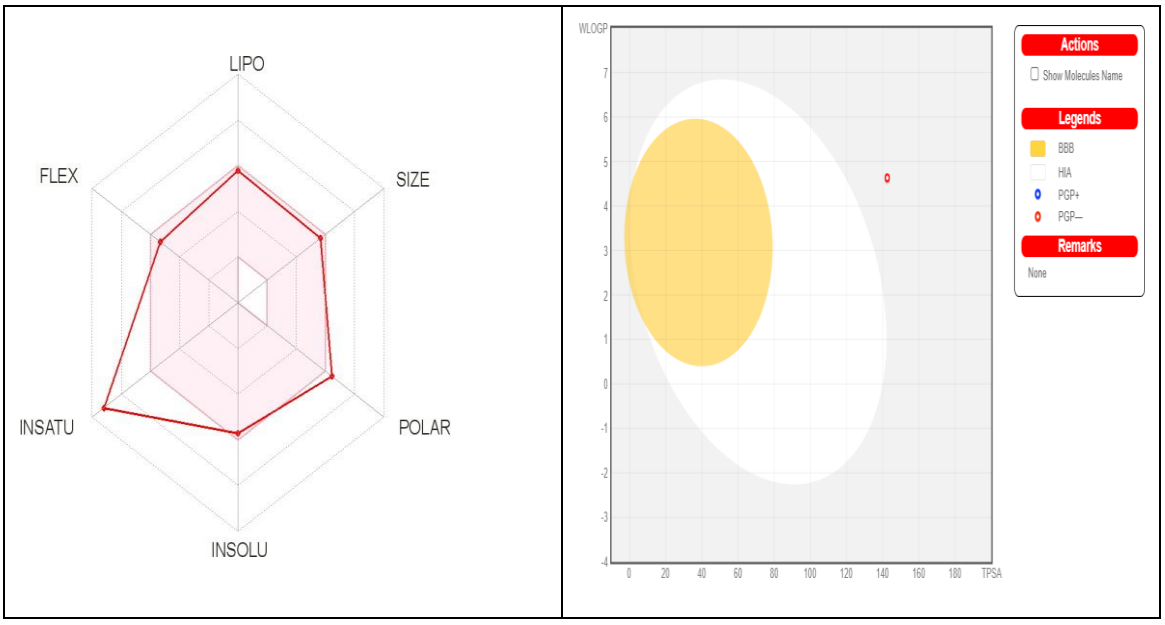

Figure 5.47: Radar chart and Boiled Egg diagram of compound **(50)**

As depicted in figure 5.46 and 5.47, the BOILED-Egg model helps in the computation of polarity and lipophilicity of derivatives as it gives datasets with accuracy and clear graphical outputs. In the BOILED-Egg model, the high probability of passive absorption of the GI tract is represented by the white region, whereas the yellow region (yolk) represents the high probability of BBB penetration. In addition, the blue color indicatesthe active efflux of molecule by P-glycoprotein, represented as (PGP+), whereas the red color indicator shows the non-substrate of Pgp, represented as (PGP−) (279). Compound **(14)** is depicted as a blue dot and compound **(50)** as a red dot in figure 5.46 and 5.47. Both the compounds lie within intestinal absorption area and devoid of BBB permeation.

5.12.6 ADME analysis and toxicity prediction

ADME and toxicity parameters for newly synthesized compounds are summarized in table 5.30. Both compounds are predicted to have excellent absorption profile of more than 90% absorption. Reference drugs also estimated to have similar absorption predicted by pkCSM tool. Caco2 permeability assesses the ability of molecules to penetrate the intestinal cell. Compound **(50)** exhibited the permeability index of 0.65 which was comparable with apixaban (0.652). Rivaroxaban is predicted to show excellent permeation through Caco2 cells compared to other molecules.

Distribution panel showed all the considered molecules were impermeable to BBB which is desired the characters as they were designed for non-CNS ailments.

Cytochrome P450 is an important enzyme system for drug metabolism in liver. The two main subtypes of cytochrome P450 are CYP2D6 and CYP3A4. Almost all the drugs have influential effect of CYP enzyme either by act as a substrate or inhibition of the enzyme system. The compound under evaluation showed negative results for CYP2D6 substrate while all the molecules were found to be substrate for CYP3A4. While both the newly synthesized compounds were found to be inhibit considered CYP subunit except CYP2D6.

Excretion was evaluated using total renal clearance and renal OCT substrate. The OCT2 is a protein transporter that has a vital contribution in the renal uptake, disposition, and clearance of drugs compounds. Evaluating the transfer of a candidate compound by OCT2 offers useful information regarding not only its clearance but also its potential contraindications. All the compounds under investigation were found to be non-substrate for OCT2.

Table 5.30: ADME and toxicity prediction of compound (14) and (50)

	Parameter	Compound (14)	Compound (50)	Apixaban	Rivaroxaban
Absorption	GI absorption (%)	91.92	90.56	88.96	92.80
	Caco2permeability	0.53	0.65	0.652	1.28
	p-glycoprotein substrate	Yes	Yes	Yes	No
Distribution	VD_{ss} (human) (log L/kg)	-0.292	0.1	-0.14	-0.987
	BBB permeability	No	No	No	No
	Fraction unbound	0.039	0.05	0.027	0
Metabolism	CYP 2D6 sub	No	No	No	No
	CYP 3A4 sub	Yes	Yes	Yes	Yes
	CYP 2C19 inh	Yes	Yes	Yes	Yes
	CYP2C9 inh	Yes	Yes	Yes	No
	CYP 3A4 inh	Yes	Yes	Yes	Yes
	CYP 2D6 inh	No	No	No	No
	CYP 1A2 inh	Yes	Yes	No	No
Excretion	Total clearance (log ml/min/kg)	-0.021	-0.413	0.247	0.296
	Renal OCT2substrate	No	No	No	No
Toxicity	AMES	Yes	No	No	Yes
	Carcinogenicity	No	No	No	No
	Skin sensitization	No	No	No	No
	LD_{50} (log mol/kg)	2.642	3.069	2.559	2.707
	LOAEL (Log mg/kg_bw/day)	1.771	1.547	1.276	1.125

Toxicity of compounds were predicted by pkCSM tool by taking LD_{50}, Lowest Oral Dose toxicity (LOAEL), mutagenicity, carcinogenic potential into consideration. Both the compounds **(14)** and **(50)** showed predicted LD_{50} of 2.642 mol/kg and 3.069 which correspond to 1160 mg/kg and 1440 mg/kg. The newly compounds were found to be safe and belong to class IV of Globally Harmonized System, which means they are slightly toxic if swallowed in high amount.

5.12.7 Acute toxicity study of compound (14) and (50) according to OECD guidelines

None of the animals showed the alteration in the muscle activity, reflex activity and secretary activity during the observation period of 14 days after administration of compound **(14)** and **(50)**. Change in body weight is a clear indicative of changes in general health of animals (228), (229). As per the guidelines by OECD, decline in body weight by 20% should be considered as critical (230). The body weights of the animals were recorded on days 0, 7 and 14. All animals showed normal growth behavior with normal food and waterintake.

When awake, periodic observation of animals displayed normal grooming behavior and no alteration of skin or fur, abnormal locomotion or breathing, allergic response in the eye was observed. No untoward observations were made in this regard until end of the study protocol. No macroscopic or microscopic lesions were observed in the vital organs, neither any architecture disruption nor oedema was observed in study animals.

Thus, it was concluded that compound **(14)** and **(50)** possesses LD_{50} >2000 mg/kg and belongs to the category 4 of safety criteria according to the OECD guidelines 423. These results indicate that newly synthesized compounds can be considered to be safe and could be developed in the future for cardiovascular disease.

5.12.8 *In-vivo* antithrombotic activity of compound (14) and (50) against $FeCl_3$ induced arterial thrombosis

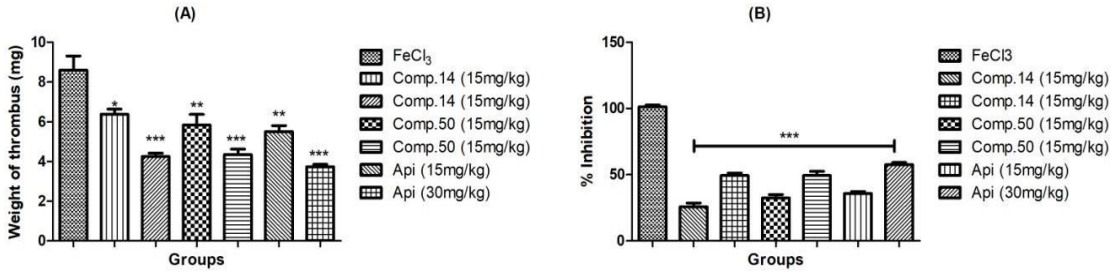

Figure 5.48: Effect of compound **(14), (50)** and apixaban on thrombus weight ($FeCl_3$ induced arterial thrombosis model). Statistical analysis was performed by One way ANOVA using Graph-pad prism 5.0. *= p <0.05, ** =p<0.001, ***=p<0.0001 vs. $FeCl_3$. (n = 5).

The topical application of ferric chloride ($FeCl_3$) to the vasculature is commonly used experimental approach to induce thrombosis in preclinical investigations (413). As depictedin figure 5.48, application of 35% $FeCl_3$ soaked filter paper strip on carotid artery caused thrombus formation. It is proposed that physiochemical effect of $FeCl_3$ on blood cells is themajor trigger of driving blood cell adhesion to the endothelium (414). Vascular endothelialcells (VECs) are extensively involved in blood homeostasis by synthesis and secretion of many active substances to regulate platelet activation, coagulation, and fibrinolysis. Injury to VEC damage is an initial stage of $FeCl_3$ induced thrombus formation. Following this tissue factor is released which causes the conversion of inactive FX to FXa enzyme (415). FXa binds to clots during clot formation and produce pro-coagulant growth of thrombi. VEC destruction set off sequence of events initiated with activation of the extrinsic pathway of coagulation process, leading to fibrin clot and thrombus formation(416),(417).

The "secondary" phase of $FeCl_3$ injury is triggered when red cell aggregates and damaged endothelium causing the exposure a reactive surface for the platelets aggregation and initiation of blood coagulation, necessary for stable thrombus formation (418), (416), (419). Administration of compounds **(14)** and **(50)** at both doses significantly reduce thrombus formation against $FeCl_3$ challenge. Compound **(14)** exhibited 25% and 49% of inhibition at 15 mg/kg and 30 mg/kg respectively while Compound **(50)** displayed excellent anti-thrombotic activity by 33% and 51% inhibition at 15 mg/kg and 30 mg/kg respectively. Apixaban also showed significant inhibition against $FeCl_3$ insult by showing significant reduction in thrombus weight. Antithrombotic activity of compound **(14)** and **(50)** were comparable to standard drug.

5.12.9 *In-vivo* antithrombotic activity of compound (14) and (50) in arteriovenous shunt induced thrombosis

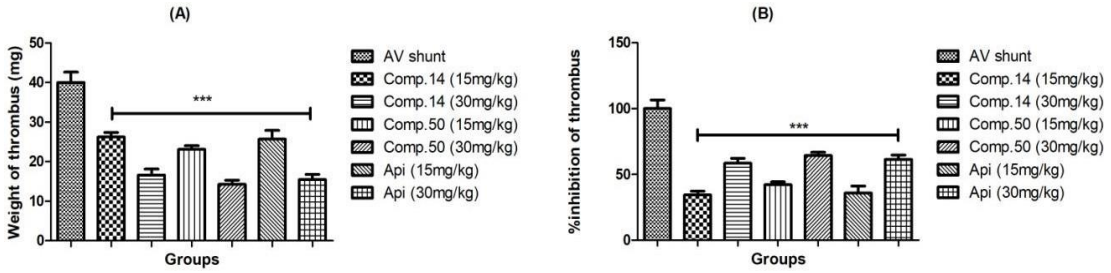

Figure 5.49: Effect of compound **(14)**, **(50)** and apixaban on thrombus weight (AV shunt induced thrombosis model). Statistical analysis was performed by One way ANOVA using Graph-pad prism 5.0 $^{***}p<0.0001$ vs. $FeCl_3$. (n = 5).

Arteriovenous shunt induced thrombosis is frequently utilised model to evaluate antithrombotic potential of existing and novel therapeutic agents and considered to be an optimal model for study of novel thrombotic agents prior to advancing them in further studies (420),(421). Treatment with compound **(14)** resulted into significant inhibition of thrombus weight at 15 mg/kg (40.00±2.64 mg vs. 26.23±1.16 mg, $p<0.0001$) and 30 mg/kg (16.56±1.51 mg vs. 40.00±2.64 mg) compared to positive control animals. Treatment with compound **(50)** at 15 mg/kg produced (23.11±0.90 mg vs. 40.00±2.64 mg, $p<0.0001$) while at the dose of 30 mg/kg (14.28±1.02 mg vs. 40.00±2.64 mg, $p<0.0001$) excellent reduction in thrombus weight compared to AV shunt animals.

5.12.10 Tail bleeding risk of compound (14) and (50) in tail bleeding model

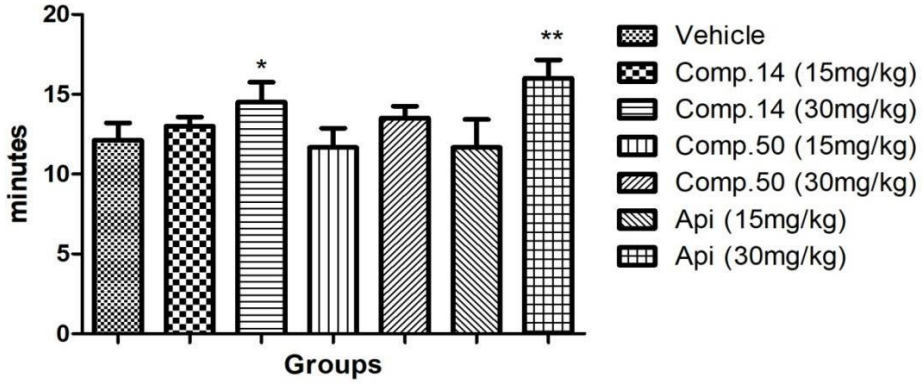

Figure 5.50: Effect of compound **(14)**, **(50)** and apixaban on bleeding time. Statistical analysis was performed by One way ANOVA using Graph-pad prism 5.0, $^{*}p< 0.05$, $^{**}p<0.001$ vs. vehicle (n = 5).

Tail bleeding is utilised to assess possible side effect of anti-thrombotic drugs (422),(423). Administration of compounds **(14)** and **(50)** at therapeutic doses exhibited non-significant difference compared to vehicle control group in tail bleeding model in rats. Compound **(14)** ($p< 0.05$) and apixaban ($p<0.001$) at the dose of 30 mg/kg showed significant bleeding time prolongation. These results demonstrate the safety profile of novel factor Xa inhibitors with standard drug.